UNIVERSITY OF OKLAHOMA

GRADUATE COLLEGE

THE ROLE OF DIVERGENT GENITAL MORPHOLOGIES IN REPRODUCTIVE ISOLATION

A DISSERTATION

SUBMITTED TO THE GRADUATE FACULTY

in partial fulfillment of the requirements for the

Degree of

DOCTOR OF PHILOSOPHY

By

ALEXANDRA ALBERTA BARNARD
Norman, Oklahoma
2018

THE ROLE OF DIVERGENT GENITAL MORPHOLOGIES IN REPRODUCTIVE ISOLATION

A DISSERTATION APPROVED FOR THE
DEPARTMENT OF BIOLOGY

BY

_____
Dr. John P. Masly, Chair

_____
Dr. Ola Fincke

_____
Dr. Rosemary Knapp

_____
Dr. Gary Wellborn

_____
Dr. Stephen Westrop

Acknowledgements

There are many people whose encouragement and support helped me reach this point in my scientific training. First, thanks to my co-advisors JP Masly and Ola Fincke. JP let me elbow my way into his lab and generously shared his time and resources. He made himself readily available to answer questions and provide advice, and did his best to make sure I had the funds to do the research that interested me. His high standards pushed me to do my best, and he believed in my abilities even when I was unsure of myself. Ola Fincke introduced me to the intriguing biology of damselflies and gave me the space and freedom to pursue interesting questions, even when they were outside her area of expertise. Her critical eye helped me to clarify my writing and make compelling arguments. Both JP and Ola gave constructive feedback on my writing, and I appreciate their patience and guidance in helping me develop into the scientist I am today.

I appreciate the assistance and advice of my committee members. Gary Wellborn shared equipment, encouraged me to view my work within a broader ecological, evolutionary, and societal context, and introduced me to a collaborator who greatly aided in my research. Rosemary Knapp was always available to listen to my concerns, and she reviewed each dissertation chapter with a fine-toothed comb, noticing small errors and suggesting ways to make my figures tell their stories more effectively. Steve Westrop offered a broad evolutionary perspective on my research

and inspired me to think beyond the narrow temporal focus of my research and consider the evolution of my study species over geographical timespans.

I am grateful to my collaborator and co-author Mark McPeek at Dartmouth College, who welcomed me into his lab and provided equipment that made my experiments much richer. Big thanks to two of OU's talented microscopists, Ben Smith and Preston Larson, for helping me obtain amazing high-resolution images of damselfly genitalia. Thanks to additional faculty in OU's Department of Biology for kindly offering advice and/or space and materials for my damselfly rearing project: Ken Hobson, Michael Markham, Edie Marsh-Matthews, Bill Matthews, David McCauley, Tarren Shaw, and Larry Weider. Special thanks to Doug Gaffin for pointing out how interesting my scanning electron microscope images were, which took my research down an interesting and unexpected avenue.

My research would not have succeeded without the support of the wonderful staff in the Department of Biology: Liz Cooley made sure I had the right supplies; George Davis solved my tech issues; George Martin built custom devices for rearing damselfly larvae; Kyle Baker, Dianna Crissman, and Robbie Stinchcombe helped me negotiate administrative paperwork; Kay Carter ensured that I got paid on time. Carol Baylor provided comic relief, furniture, food, and companionship from day one.

I am eternally grateful to my former roommates at the Hardin House, Emily Khazan and Jelena Bujan, for friendships that began when I first arrived in Norman seven years ago and will hopefully last for years to come. Their love and support

helped me cope during the unavoidable rough patches that crop up during the PhD experience. I thank my current Hardin House roommates, Steve Bittner, and Michelle Busch, for all the silliness we've shared. I thank Brad Brayfield for all lunches and conversations we've shared, and his supernatural ability to know when to stop by my office with cookies. I thank Anuj Guruacharya, Andrea Contina, and Josh Cooper for their assistance in navigating millions of genomic sequencing reads. Big thanks to my lab mates Mehrnaz Afkhami, Angel Harper, and Michelle Wood, for their support and camaraderie and for putting up with me in the tiny office we all shared.

I thank Tom Buckman: friend, roommate, and the best undergraduate research assistant I could have asked for. Without his dedication and tireless assistance in rearing damselfly larvae, the project in Chapter 1 would not have been as successful as it was. I am indebted to Aaron Geheber and Laura Bergeron, my first non-scientist friend in Norman, for reminding me that there is life outside the lab and I shouldn't feel guilty for escaping sometimes. Of course, eternal thanks to my friend and fiancé Walter Albrecht for his unconditional love and support over the past couple of years. Thanks for being compassionate when I was hungry and cranky, and thanks for all the home cooked meals. Finally, thanks to my parents for believing in me and supporting my decision to pursue what I love, and for letting me store all those bugs in their freezer.

Table of Contents

List of Tables

List of Figures

Abstract

How a single ancestral species can give rise to new, separate species remains a major outstanding question in evolutionary biology. Understanding speciation requires identifying how reproductive isolation (RI) is initiated and maintained in the early stages of population divergence. External male reproductive structures have received considerable attention as an early-acting cause of RI, because the morphology of these structures often evolves rapidly between populations. My dissertation research used a pair of recently diverged damselfly species in the genus *Enallagma* (Odonata: Coenagrionidae) to understand the role of divergent genital morphologies in causing RI at early stages of the speciation process. Specifically, I investigated the mechanisms by which species-specific morphologies limit gene flow between species, and then explored the relationships between morphological differentiation and overall genomic differentiation between species. My research focused on *Enallagma anna* and *E. carunculatum*, two damselfly species that diverged within the past ~250,000 years and differ conspicuously in their reproductive structure morphology, yet currently hybridize in at least one sympatric region. In chapter 1, I tested the importance of mechanical and tactile incompatibilities in RI between *E. anna* and *E. carunculatum* by quantifying 19 potential prezygotic and postzygotic RI barriers, using both naturally occurring and lab-reared damselflies. I found that mechanical incompatibilities between heterospecific male and female reproductive structures limit but do not completely prevent heterospecific mating attempts.

However, females were significantly less likely to mate with hybrid or heterospecific males compared to conspecific males, which suggests that tactile incompatibility between male and female morphologies forms an additional mechanism to limits gene flow between these species. Postmating RI barriers appeared weak or nonexistent, which indicates that premating isolation, mediated by divergence in genital morphologies, was the first type of reproductive barrier to evolve in this group. These results highlight the potential for rapidly evolving genitalia to cause RI via tactile mechanisms, which may be a more widespread RI mechanism than we are currently aware of. In chapter 2, I more closely examined the female structures presumed to be important in evaluating male tactile signals during premating contact and influencing *Enallagma* female mating decisions. I quantified and compared several mechanosensory sensilla phenotypes on the female thorax among multiple sympatric and allopatric populations to test for evidence of reproductive character displacement, which would indicate that sensilla phenotypes are important in species recognition. My results suggest that species-specific placement of female mechanoreceptors is sufficient for species recognition, but mechanosensor variation among females within species may be important for mate choice within species. This hypothesis requires additional study to test the relationships between female sensilla phenotypes and behavior. This experiment reveals *Enallagma*'s potential as a study system for elucidating the neurobiological basis of female mating decisions. In chapter 3, I explored the relationships between morphological divergence and genomic

differentiation during speciation. Persistent gene flow between species as they diverge can homogenize some regions of the genome and make differentiated regions stand out in comparison. Some of these highly divergent loci are predicted to harbor genes responsible for reproductive isolation. However, patterns of genome diversification at this stage remain poorly understood, such as how such loci are arranged across the genome and whether such loci commonly contribute to reproductive isolation or are simply less subject to recombination. I generated a set of genome-wide variant loci in a large collection of samples from multiple populations, including both natural and lab-reared hybrids. I used these loci to quantify introgression patterns in nature, identify divergent loci, and test for associations between genomic ancestry and species-specific phenotypic variation. The results suggest ongoing gene flow between *E. anna* and *E. carunculatum* in nature, but also demonstrate the challenge of differentiating shared ancestral polymorphism from recent admixture when studying young species. Additionally, the results revealed that estimated ancestry proportions in hybrids were a reliable predictor of hybrid reproductive structure phenotype in most cases – but some individuals appeared to have a genome that mostly resembled one parental species, yet morphology more similar to that of the other parental species. Clarifying the relationships between genotypes and phenotypes will likely require more fine-scale genomic sequencing efforts than this study obtained. My dissertation research integrated behavioral studies in the field and lab with quantitative trait comparisons and genomics to

investigate the importance of rapid evolution of reproductive structures in reproductive isolation. This work enhances our understanding of how morphological divergence affects mating behavior to cause RI, and in turn how RI and behavior shape differentiation of genomes. Together, these experiments contribute to our understanding of how biodiversity is generated and strengthen the role of damselflies as models for understanding evolution.

Introduction

How a single ancestral species can give rise to new, separate species remains a major outstanding question in evolutionary biology. Charles Darwin (1859) raised the question of how new species originate, but, as multiple scholars have pointed out, *The Origin of Species* focused on how individual species change over time, but not how new species emerge (Huxley 1958; Coyne and Orr 2004).

The approaches researchers use to understand the origin of new species how they choose to define species. Although various criteria exist for delineating species, one of the most commonly used is the Biological Species Concept (BSC; Mayr 1942). Mayr defined separate species as "groups of interbreeding natural populations that are reproductively isolated from other such groups." Under this definition, separate species cannot interbreed to produce viable, fertile offspring. Like all species concepts, the BSC has limitations – it does not apply, for example, to asexual organisms – but it nonetheless provides a practical framework for studying the process of speciation in sexual organisms as the study of how RI evolves (Coyne and Orr 2004).

The progression from divergent lineages to completely isolated, separate species involves the evolution of phenotypic differences that ultimately reduce gene flow. As multiple reproductive barriers build up over time, lineages progress through intermediate stages in the speciation process, during which reproductive barriers are permeable despite the existence of some reduction in gene flow between populations (Coyne and Orr 2004). These intermediate stages provide the possibility to distinguish

the reproductive barrier(s) that initiated speciation from those that evolved after speciation was complete. Hybridization and speciation in the face of gene flow is more widespread than originally thought (reviewed in Abbott et al. 2013; Harrison 1990; Via 2012; Nadeau et al. 2011; Martin et al. 2013; Larson et al. 2014). To accommodate this knowledge and the utility of studying divergent but incompletely reproductively isolated groups, Coyne and Orr (2004) broadened Mayr's (1942) species definition slightly, allowing for "substantial but not necessarily complete" reproductive isolation (RI).

Reproductive isolating barriers take many forms that act at various times throughout an individual's life history, beginning with the initial encounter between a male and female. From this point, many possibilities exist that can facilitate or prohibit genetic exchange. For example, do separate species encounter one another in the same habitats or at the same times of the day or year? If so, do they recognize one another as potential mates? Can they copulate successfully? Does the male inseminate the female, and do his sperm successfully fertilize her eggs? If the female remates with a conspecific male, does this reduce the fertilization success of the heterospecific male's sperm? If a heterospecific mating produces offspring, do the hybrids survive to reproduce themselves? Breaking down RI into its various mechanisms in this manner demonstrates the myriad ways that species can become reproductively isolated and provides a starting point for asking questions about the process of speciation: How does the process begin? Does one type of RI typically

evolve earlier in the process than others? Is one type of RI particularly important or common (Coyne and Orr 2004; Butlin et al. 2012)? Once one form of RI has developed, how do additional barriers accumulate between two species? Do certain types of RI share similar underlying genetic causes? When two species begin to diverge in isolation and then come into contact, does RI between them become stronger or weaker? (Abbott et al. 2013).

Over the past several decades, evidence has accumulated in support of some broad trends in speciation. Prezygotic RI (e.g., ecological and sexual isolation) tends to evolve earlier than postzygotic RI (hybrid sterility and inviability (e.g., Grant 1992; McMillan et al. 1997; Price and Bouvier 2002; Mendelson and Wallis 2003; Ramsey et al. 2003; Husband and Sabara 2004; Kay 2006; Dopman et al. 2010; Sánchez-Guillén et al. 2012; Williams and Mendelson 2014; Castillo et al. 2015). Hybrid sterility typically evolves faster than hybrid inviability (Coyne and Orr 1997; Sasa et al. 1998; Jiggins et al. 2001; Presgraves 2002; Price and Bouvier 2002; Mendelson 2003; Russell 2003), and multiple genetic mechanisms for postzygotic RI accumulate over time (Orr 1995). The heterogametic sex is typically more susceptible to hybrid sterility or infertility, and sex chromosomes tend to accumulate disproportionate numbers of loci that cause RI (Haldane's rule; Haldane 1922; Coyne and Orr 1989; Coyne 1992; Wu and Davis 1993; Laurie 1997; Naisbit et al. 2002; Price and Bouvier 2002; Payseur et al. 2004; Masly and Presgraves 2007; Delph and Demuth 2016). Despite these advances, much remains to

be learned about how divergence within lineages gives rise to new lineages. One major goal of speciation research is identifying traits that diverge to cause RI.

Because sexual/behavioral barriers act early in the mating sequence, they have more opportunity to prevent interbreeding than later-acting barriers and are therefore often considered more important causes of RI (e.g., Jiggins et al. 2001; Kirkpatrick and Ravigne 2002). Animal genitalia are one set of sexual traits that have been scrutinized for a potential role in RI. Genitalia are among the fastest evolving external morphological traits and it has been suggested that divergent genital morphologies can prevent heterospecific matings and cause RI (Eberhard 1985). Dufour (1844) proposed that mechanical incompatibilities between the genitalia of different species caused RI, based on his observations that many closely related insect species were distinguishable only by their genitalia. However, empirical studies have largely discredited this idea, because few studies have demonstrated mechanical incompatibilities between male and female genitalia resulting in RI. However, genital divergence may cause a sensory RI mechanism in which male genitalia stimulate the female in a species-specific manner, and RI results from female behavioral or physiological responses to the male stimulation (Eberhard 1985; Masly 2012). These observations raise several questions that will help us understand how new species form:

1. How important is divergence of genital morphologies in causing RI at early stages of the speciation process?

2. Does between-species divergence in male genitalia and the threat of hybridizing cause divergence in female sensory traits when two species co-occur?

3. What is the relationship between rapid divergence in genital traits and overall genomic differentiation?

My dissertation research uses a pair of closely-related *Enallagma* damselfly species (Odonata: Coenagrionidae) to address each of these questions.

The study system

Enallagma, the most speciose damselfly genus in North America contains 17 species that radiated within the past 250,000 years. Many of these species differ primarily in their reproductive structures while remaining similar in overall external morphology and ecology, and many *Enallagma* species have overlapping distributions (Turgeon et al. 2005; McPeek et al. 2011). Both sexes possess evolutionarily correlated, species-specific reproductive structures (McPeek et al. 2009) that are considered secondary genitalia: they are not involved in sperm transfer but are integral in mating, and show the same pattern of rapid and divergent evolution as primary genitalia (Eberhard 1985). When a male damselfly attempts copulation, his terminal abdominal claspers grasp the female thorax to form a "tandem" position. Most heterospecific tandems are prevented due to structural incompatibilities of male cerci and female plates among species, creating prezygotic RI among most species. However, some heterospecific pairs can form tandems (e.g., Paulson 1974; Bick and

Bick 1981). In these cases, females typically refuse to mate with heterospecific males. Females are also unlikely to mate with conspecific males whose cerci have been surgically altered (Robertson and Paterson 1982). These two observations suggest that a tactile component influences females' decisions about which males are appropriate mates.

Two species, *E. anna* and *E. carunculatum*, appear to hybridize in nature despite possessing striking differences in the size and shapes of both the mesostigmal plates on the female thorax and the superior male claspers, the cerci (Miller and Ivie 1995; Donnelly 2008; Johnson 2009). Because these species can produce viable hybrids, they are an ideal study system for (1) identifying which forms of RI arose in the early stages of speciation and (2) dissecting the genetic basis of species-specific morphological variation. My dissertation research integrates behavioral and morphological experiments with genomic study of multiple populations of these species to understand the role of rapidly diverging genitalia in speciation.

Is reproductive structure divergence an important cause of RI at early stages of speciation?

Measuring the relative strengths of different reproductive isolating barriers can help identify which barriers were important early in divergence. One common approach to revealing the barriers that initiated the speciation process is to quantify

current pre- and postzygotic reproductive barriers in taxa with incomplete RI (e.g. Ramsey et al. 2003; Kay 2006; Dopman et al. 2010; Sánchez-Guillén et al. 2012). Determining which barriers do and do not currently exist between a species pair indicates which barriers likely evolved first – if a barrier is weak or nonexistent, it cannot have contributed to speciation (Coyne and Orr 2004).

In Chapter 1, I quantified 19 potential barriers to gene flow between *E. anna* and *E. carunculatum*. I found that divergent genitalia are a major cause of reproductive isolation, via both mechanical and tactile mechanisms. Heterospecific tandems were possible in both directions, although the strength of mechanical incompatibility was asymmetric. However, when females were taken in tandem by a heterospecific or a hybrid male, they displayed greater resistance and refusal to mate with hybrid or heterospecific males compared to conspecific males. This finding suggests that tactile incompatibilities involving male reproductive structures can influence female mating decisions and form a strong isolating barrier between species.

Characterizing female phenotypes involved in tactile differentiation of males

One of the major findings from Chapter 1 is that male tactile signals appear to mediate species recognition in *Enallagma* damselflies. Chapter 2 builds on this finding by characterizing a female phenotype that is presumed to facilitate female evaluation of tactile signals from the male genitalia. Although visual, auditory, and chemical communication between the sexes have are well-studied, we know relatively little

about the importance of tactile signals in mating decisions (Coleman 2008). In this study, I quantified the number and distribution patterns of mechanoreceptors (sensilla) on the female mesosgtigmal plates in multiple sympatric and allopatric populations of *E. anna* and *E. carunculatum*. I predicted that selection to avoid hybridization when both species co-occur would lead to increased divergence in these traits between the species when they are sympatric compared to allopatric (reproductive character displacement; Brown and Wilson 1956; Howard 1993; Pfennig and Pfennig 2009). Contrary to this prediction, I did not find strong evidence of reproductive character displacement among the sensilla traits I measured. I did, however, identify species-specific differences in sensilla locations within the thoracic plates, which suggests that sensilla phenotypes may be sufficiently different between species that species recognition is strong enough to preclude selection on further divergence. Additionally, I observed substantial variation of sensilla phenotypes within populations of both species. This intriguing result suggests that intraspecific female variation in sensilla traits may play a role mate choice and sexual selection.

Investigating the relationships between morphological divergence, gene flow, and genomic divergence

Dissecting the genetic basis of reproductive barriers is also important in determining how genetic changes can give rise to new species, (e.g., Coyne 1993; Price and Bouvier 2002; Presgraves et al. 2003; Chamberlain et al. 2009; Ellison et al. 2011).

Whereas Chapters 1 and 2 address external phenotypes such as morphology, behavior, and life history traits, Chapter 3 examines how whole genomes diverge during speciation with gene flow. The incomplete RI between *E. anna* and *E. carunculatum* allows analysis of gene flow in sympatry, plus creation of hybrid genotypes for dissecting the genetic basis of morphological differences between species. I used a restriction enzyme-based reduced-representation genomic approach to genotype a collection of both field-caught and lab-reared hybrid damselflies to identify regions of the genome that are (1) associated with variation in male and female reproductive structure morphologies (2), highly divergent between species, and (3) less subject to gene flow than other regions. Because we know that divergent genitalia are a primary cause of RI between *E. anna* and *E. carunculatum*, loci responsible for variation in genitalia are predicted to be less freely exchanged between species than other genomic regions unrelated to RI. Therefore, they are also expected to be more highly divergent than the surrounding regions.

In the beginning stages of speciation, divergent regions are expected to be small, and ongoing gene flow can result in these infrequently exchanged genomic regions standing out like "islands" against the majority of the genome, which remains undifferentiated (Barton and Bengtsson 1986; Noor and Bennett 2009; Payseur 2010; Yeaman and Whitlock 2011).Understanding the direction and extent of gene flow between these species and how ongoing gene flow affects genome-wide divergence patterns sheds light on the genetic basis of speciation with gene flow, such as how loci

related to RI are distributed throughout the genome and which selective forces act on those loci (Via 2009; Feder and Nosil 2010; Feder et al. 2012; Nosil and Feder 2012). In this final chapter, I characterized patterns of gene flow and genomic divergence between *E. anna* and *E. carunculatum*, quantified introgression patterns in natural populations of the parental species, and demonstrated asymmetric gene flow between the species, with wild hybrids appearing to possess an excess of alleles inherited from *E. anna*. I identified several unmapped loci that show elevated levels of divergence between phenotypic extremes in both sexes of *E. anna* and *E. carunculatum*. The results of this study also illustrate the difficulty of studying the genomes of young species, due to the challenge of discerning patterns left by recent gene flow from patterns due to incomplete lineage sorting and ancestral polymorphisms.

My dissertation research has approached the study of speciation from several directions, by investigating the evolutionary interplay between males and females and how behavior, morphology, genetics, and gene flow interact to strengthen or weaken species boundaries. Together, these projects enhance our understanding of speciation in several ways. The study of speciation in *Enallagma* damselflies occurs within a well-understood ecological context, and studying species that hybridize in nature augment what we have learned from laboratory studies of speciation (e.g., Coyne and Orr 1989, 1997). Damselflies have benefited from decades of ecological, behavioral, and

phylogenetic studies (Córdoba-Aguilar 2008), and this work strengthens *Enallagma*'s role as an emerging system for evolutionary and ecological studies.

CHAPTER 1: Mechanical and tactile incompatibilities cause reproductive isolation between two young damselfly species

This chapter is published, with minor modifications, as Barnard, A. A., O. M. Fincke, M. A. McPeek, and J. P. Masly. 2017. Mechanical and tactile incompatibilities cause reproductive isolation between two young damselfly species. *Evolution* 71(10):2410–2427.

Abstract

External male reproductive structures have received considerable attention as a cause of reproductive isolation (RI), because the morphology of these structures often evolves rapidly between populations. This rapid evolution presents the potential for mechanical incompatibilities with heterospecific female structures during mating and could thus prevent interbreeding between nascent species. Although such mechanical incompatibilities have received little empirical support as a common cause of RI, the potential for mismatch of reproductive structures to cause RI due to incompatible species-specific tactile cues has not been tested. We tested the importance of mechanical and tactile incompatibilities in RI between *Enallagma anna* and *E. carunculatum*, two damselfly species that diverged within the past ~250,000 years and currently hybridize in a sympatric region. We quantified 19 prezygotic and postzygotic RI barriers using both naturally occurring and laboratory-reared damselflies. We found incomplete mechanical isolation between the two pure species and between hybrid males and pure species females. Interestingly, in mating pairs for which mechanical isolation was incomplete, females showed greater resistance and refusal to mate with hybrid or heterospecific males compared to conspecific males. This observation suggests that tactile incompatibilities involving male reproductive structures can influence female mating decisions and form a strong barrier to gene flow in early stages of speciation.

Introduction

Understanding speciation requires identifying how reproductive isolation (RI) is initiated and maintained in the early stages of population divergence (Coyne and Orr 2004; Butlin et al. 2012). Over the past century, speciation researchers have used a variety of experimental and comparative approaches to identify which barriers appear most important in causing RI early in the speciation process. These efforts have revealed that sexual isolation and ecological divergence tend to evolve earlier than hybrid sterility and inviability in both plants (*e.g.,* Grant 1992; Ramsey et al. 2003; Husband and Sabara 2004; Kay 2006) and in animals (*e.g*., McMillan et al. 1997; Price and Bouvier 2002; Mendelson and Wallis 2003; Dopman et al. 2010; Sánchez-Guillén et al. 2012; Williams and Mendelson 2014; Castillo et al. 2015). Prezygotic isolation also typically evolves faster in sympatry than in allopatry, and hybrid sterility typically evolves faster than hybrid inviability (Coyne and Orr 1997; Presgraves 2002; Price and Bouvier 2002; Russell 2003). Identifying the traits that diverge to cause RI underlying these broad patterns is a major goal of speciation research.

One set of traits that has received much attention because of their rapid rates of evolutionary change is external reproductive structures. In internally fertilizing animals, male intromittent genitalia are among the fastest-evolving external morphological traits, and genital morphological variation can affect reproductive fitness within species (Eberhard 1985; Otronen 1998; Danielsson and Askenmo 1999; House and Simmons 2003; Rodriguez et al. 2004; Bertin and Fairbairn 2005; Simmons

et al. 2009). Likewise, non-intromittent contact or grasping structures often show similar patterns of rapid, divergent evolution, and divergence in these structures can also affect reproductive success within species (Arnqvist 1989; Bergsten et al. 2001; Wojcieszek and Simmons 2012).

Rapid divergence of reproductive structures between populations has been hypothesized to cause RI via two different mechanisms. The first is mechanical incompatibility (Dufour 1844), in which structural incompatibilities between male and female genitalia of different species prevent successful copulation and reproduction. Mechanical incompatibilities have been documented in some animal species pairs (Jordan 1896; Standfuss 1896; Federley 1932; Schick 1965; Paulson 1974; Sota and Kubota 1998; Tanabe and Sota 2008; Kamimura and Mitsumoto 2012; Sánchez-Guillén et al. 2012; Wojcieszek and Simmons 2013; Sánchez-Guillén et al. 2014; Anderson and Langerhans 2015), although this mechanism of RI has not received broad support as a common mechanism of RI between young species (Shapiro and Porter 1989; Masly 2012; Simmons 2014).

The second proposed mechanism is tactile incompatibility (de Wilde 1964; Eberhard 1992), in which mismatch between male and female genitalia of different species prevents or reduces the success of mating and reproduction because one or both sexes fail to stimulate the other in the proper species-specific manner. The essence of this idea is that female reproductive decisions are based on the pattern of tactile stimuli transmitted by the male, and improper stimulation can result in female

refusal to mate, early termination of mating, or lowered postcopulatory fitness, including reduced reproductive fitness in hybrid offspring (Eberhard 2010). Tactile isolation likely operates in a similar manner as other sensory modalities involved in mate choice and species recognition such as auditory or chemical signals, in which quantitative variation exists in male traits and female preferences (Ryan and Wilczynski 1991; Shaw 1996; Tregenza and Wedell 1997; Singer 1998; Johansson and Jones 2007). If females discriminate among the mating structures of conspecific mates, female discrimination against heterospecific males can arise as a byproduct of sexual selection within species (reviewed in Panhuis et al. 2001; Turelli et al. 2001; Simmons 2014). Thus, any mismatch between male morphology and female response to stimulation from a particular morphology could result in reduced reproductive success when females mate with a heterospecific male or an interspecific hybrid male. The importance of tactile incompatibilities remains unknown, although there is good reason to expect that these incompatibilities may occur frequently (Simmons 2014), and therefore have the potential to play a significant role in the evolution of RI.

Because identifying the effects of tactile incompatibilities requires carefully quantifying mating behavior and physiology, these incompatibilities have often been overlooked in tests of RI involving divergence of reproductive structures (Masly 2012). Nonetheless, some evidence for tactile incompatibility in the absence of mechanical incompatibilities exists in butterflies (Lorkovic 1953, 1958), scarab beetles (Eberhard 1992), *Drosophila* (Coyne 1993; Price et al. 2001; Frazee and Masly 2015 – but see

LeVasseur-Viens et al. 2015), and sepsid flies (Eberhard 2001). Notably, damselflies (Odonata, suborder Zygoptera) are often touted as a prime example of the importance of both mechanical and tactile incompatibilities in RI among closely related species. The potential for either mechanism to cause RI has been particularly well described in the families Lestidae and Coenagrionidae, whose males do not engage in premating courtship or visual displays (Williamson 1906; Krieger and Krieger-Loibl 1958; Loibl 1958; Paulson 1974; Tennessen 1975; Robertson and Paterson 1982; Hilton 1983; Battin 1993; Sánchez-Guillén et al. 2012; Sánchez-Guillén et al. 2014). Male damselflies have two sets of paired grasping organs at the end of their abdomen (Fig 1). A male initiates the mating sequence by grasping the female's thorax with these appendages to form the "tandem" position. The species-specific male appendages and female thoracic structures engage such that structural mismatch appears to prevent many heterospecific tandems from forming (Paulson 1974). Mechanical isolation appears to be a major cause of RI in *Ischnura* (Krieger and Krieger-Loibl 1958; Sánchez-Guillén et al. 2014). For *Ischnura* species pairs with incomplete mechanical isolation, tactile isolation has been suggested to contribute to RI (Sánchez-Guillén et al. 2012; Wellenreuther and Sánchez-Guillén 2016), although this idea has not been tested quantitatively.

Mechanical isolation also appears to prevent many heterospecific tandems in *Enallagma,* the most speciose North American genus (Paulson 1974; Miller and Fincke 2004; Fincke et al. 2007). Divergence in reproductive structure morphology is

associated with a relatively recent *Enallagma* radiation (250,000-15,000 years ago; McPeek et al. 2008). Importantly, the rapid morphological diversification was not accompanied by marked ecological divergence among many *Enallagma* species (Siepielski et al. 2010). Although male cerci (superior terminal appendages) and female thoracic plates show a pattern of correlated evolution within *Enallagma* species (McPeek et al. 2009), species-specific divergence in these structures does not always cause strong mechanical incompatibilities, and interspecific tandems are occasionally observed (Paulson 1974; Tennessen 1975; Bick and Bick 1981; Forbes 1991; Miller and Fincke 2004; Fincke et al. 2007). After tandem formation, female *Enallagma* control whether or not copulation occurs and they typically refuse to mate with heterospecifics or males whose cercus morphology has been manipulated (Robertson and Paterson 1982). *Enallagma* mesostigmal plates contain mechanoreceptors in species-specific locations that appear to be contacted by the male cerci during tandem, which may allow female assessment of a male's cercus morphology (Robertson and Paterson 1982).

Although prezygotic isolating barriers appear to evolve earlier than postzygotic barriers in damselflies (Sánchez-Guillén et al. 2012; Sánchez-Guillén et al. 2014), the relative importance of mechanical and sensory mechanisms of prezygotic RI remains unclear for two reasons. First, it can be difficult to distinguish between mechanical and tactile mechanisms experimentally: if a male-female pair fails to form a tandem, it is often unclear whether the incompatibility is purely mechanical or whether it

involves tactile or behavioral cues that cause one sex to reject the other (Tennessen 1975; Robertson and Paterson 1982; Shapiro and Porter 1989). Second, mechanical isolation or male-female "fit" is not always defined in a way that makes quantifying variation in these phenotypes straightforward (Masly 2012). This lack of clarity over what constitutes mechanical incompatibility has led to conflation of mechanical RI (*i.e.*, failure of male and female parts to engage) in damselflies with mechanisms that might be better described as tactile (Tennessen 1982).

Distinguishing mechanical from tactile mechanisms requires performing detailed mating observations among males and females that possess interspecific variation in reproductive structures and identifying specific features of reproductive morphology that prevent mating or reduce mating success using high-resolution phenotypic data. Here, we take advantage of a large collection of naturally occurring interspecific hybrids and lab-generated hybrids to test the hypothesis that divergence in reproductive structural morphology causes RI at the early stages of speciation in damselflies. We measure 19 potential pre- and postzygotic isolating barriers between *Enallagma anna* and *E. carunculatum*, two species that diverged from a common ancestor sometime in the last ~250,000 generations (McPeek et al. 2008; Callahan and McPeek 2016) and co-occur over much of the western United States (Westfall and May 2006). Both species have identical ecologies and overall morphologies (Turgeon et al. 2005; McPeek et al. 2009), but display conspicuous differences in the size and shape of the male cerci and female mesostigmal plates (Fig 1). We quantify variation in male

and female reproductive structure morphologies, distinguish mechanical and tactile premating incompatibilities, estimate the cumulative strengths of multiple reproductive barriers, and independently test predictions of mechanical and tactile isolation hypotheses (Richards and Robson 1926; Shapiro and Porter 1989). If mechanical incompatibilities occur, male *E. anna* × *E. carunculatum* hybrids that possess intermediate cercus morphologies will have less success at forming tandems compared to conspecific males. If tactile incompatibilities occur, males will be able to achieve tandem regardless of their cercus morphology, but females will refuse to mate with males whose morphologies deviate significantly from the conspecific mean phenotype.

Materials and Methods

Damselfly cerci and mesostigmal plates are non-intromittent sexual structures that are not directly involved in the transfer of gametes from male to female. However, terminal appendages of male insects and the female structures they contact during mating are often referred to as secondary genital structures. We thus include them as genital traits, consistent with previous definitions (Eberhard 1985; Arnqvist and Rowe 2005; Eberhard 2010; Simmons 2014; Brennan 2016) and refer to them generally as "genitalia" in the presentation of our results.

Natural population sampling

We studied wild populations of *E. anna* and *E. carunculatum* in July and August 2013 at a site on the Whitefish River (Montana, U.S.A.; 48°22'15"N 114°18'09"W), where putative interspecific hybrids have been reported (Miller and Ivie 1995; Westfall and May 2006). To estimate relative frequencies of each species, we collected solitary males and tandem/copulating male-female pairs during peak activity between 1030-1600 hr. We initially assigned species identity after inspecting cercus and mesostigmal plate morphology with a hand lens or dissecting microscope, respectively. Males and females with morphologies that appeared intermediate were initially designated as hybrids. We reassessed these assignments in the lab after 3-D morphometric analysis (see below). We calculated the proportions of *E. anna*, *E. carunculatum* and hybrid males from all sampling bouts and used these male frequencies to estimate the expected frequencies of each type of male-female pair under random mating.

We attempted to cross virgin *E. anna* and *E. carunculatum* to measure postzygotic RI between pure species, but we did not obtain heterospecific copulations in either cross direction. Instead, we established laboratory populations of hybrids and parental species by collecting eggs from mated pairs captured in the field. Offspring of field-caught pairs are hereafter referred to as "lab generation 1." Mated females oviposited on moist filter paper, which was kept submerged in 2-4 cm of water until larvae hatched. We obtained embryos from 24 *E. anna* pure species crosses, 32 *E. carunculatum* pure species crosses, and 8 mixed crosses: 1 *E. carunculatum* female × *E. anna* male, 1 *E. anna* female × *E. carunculatum* male, 1 *E.*

carunculatum female × hybrid male, and 5 hybrid female × *E. anna* male ("hybrid" refers to damselflies with intermediate cercus or mesostigmal plate morphologies). After sampling, egg collection, and behavioral observation, we stored adult damselflies in 95% ethanol for subsequent morphometric analyses.

Laboratory rearing

We transported embryos from the field site to the University of Oklahoma Aquatic Research Facility where the larvae hatched and were reared to adulthood in individual 140 ml cups. These lab generation 1 larvae were provided with *Artemia*, *Daphnia*, or *Lumbriculus* as food sources and experienced a natural photoperiod and daily water temperatures that averaged 20.0 $\pm$ 0.19 °C. We housed adults in mesh cages (30.5 cm^3; BioQuip), segregated by sex until sexual maturity and provided with adult *Drosophila* as a food source *ad libitum*. We used lab generation 1 virgin adults to quantify prezygotic barriers, plus additional postzygotic barriers that we could not measure in the field. We mated 24 adult pairs from this first lab generation: 11 *E. anna*, 2 *E. anna* female × hybrid male, 2 *E. carunculatum* female × hybrid male, 6 hybrid female × *E. anna* male and 4 hybrid female × hybrid male and raised them under the conditions described above. Embryos from these crosses (hereafter, "lab generation 2") contributed fecundity, fertility, and hatch rate data but were not raised to adulthood due to difficulties with rearing them. Mated adults were stored in 95%

ethanol after mating (males) or after oviposition (females). Unmated damselflies were maintained to calculate captive lifespan, then preserved in 95% ethanol.

Morphometric analysis

We photographed ethanol-preserved adults using a Nikon D5100 camera (16.2 MP; Nikon Corporation, Tokyo, Japan) and measured abdomen length (abdominal segments 1-10, excluding terminal appendages) as a proxy for body size using ImageJ (Abramoff et al. 2004) for 175 males and 171 females. To reduce measurement error, we measured each abdomen twice, then used the mean length in subsequent analyses after confirming that repeatability was high for the separate measurements (r = 0.97). We obtained 3-D digital reconstructions of male cerci and female mesostigmal plates by scanning 140 male terminal segments and 162 female thoraces in a SkyScan 1172 micro-computed tomography scanner (Bruker microCT, Kontich, Belgium). Male structures were scanned at a voxel resolution of 2.36 or 2.53 um, and female thoraces at 2.78 or 3.88 um, and the scan data were converted to image stacks using NRecon version 1.4.4 (Bruker microCT).

To quantify cercus shape, we digitally segmented the right cercus from each male's image stack and converted it to a solid surface object using Avizo Fire software (FEI Software; Hillsboro, Oregon) as described in McPeek et al. (2008). We measured the volume of each cercus object as a proxy for cercus size, using Avizo's volume measurement tool. To quantify and compare their shapes, each cercus was

represented by a mesh of 20,000 triangles with 10,002 vertices, each defined by distinct (*x*, *y*, *z*) coordinates (Fig S1). We placed 7 landmarks on common points on each cercus, then used these landmarks to register all digitized cerci in identical orientations within the coordinate plane. To ensure that only shape and not size was compared in the analysis, all objects were standardized to have the same centroid size. Next, we performed spherical harmonic analysis (Shen et al. 2009), which represents the shape of a closed surface in terms of the sum of 3-D sines and cosines on a sphere. We performed the analysis using 18 degrees of spherical harmonic representation, which captures relevant surface detail without introducing excess noise (Shen et al. 2009). The analysis generated 1,083 coefficients to describe the shape of each cercus, which we reduced into the primary axes of shape differentiation using principal component analysis.

Because female mesostigmal plates are relatively flat structures, we represented plate morphology using 3-D geometric morphometrics. For each female plate we assigned 11 fixed landmarks and 248 sliding semi-landmarks to the right anterior thorax of each female (Fig S2) using Landmark software (Wiley et al. 2005). We imported landmark coordinates into R and used the Geomorph package (version 2.1.7; Adams and Otarola-Castillo 2013) to assign 79 landmarks as “curve sliders” on the medial thorax and around the plate periphery, and 169 “surface sliders” evenly spaced across the plate. We obtained 3-D shape variables for these representations using general Procrustes analysis superimposition (Rohlf 1999), then obtained a

smaller set of plate shape variables from the Procrustes-superimposed coordinates using principal component analysis.

Measuring pre- and postzygotic reproductive isolating barriers

To measure the strength of RI barriers between *E. anna* and *E. carunculatum*, we quantified 19 potential pre- and postzygotic isolating mechanisms that act from the beginning of the mating sequence through an individual's life history. Table 1 summarizes these RI measures and describes the equations used to estimate the absolute strength of each (Sobel and Chen 2014). Although it is often preferable to quantify RI using only reciprocal F_1 hybrids, the rarity of heterospecific crosses and our small sample of F_1 individuals made this impractical for estimating the strength of postzygotic RI barriers. Thus, to measure postzygotic barriers, we pooled all hybrid damselflies, including presumed F_1s from both cross directions and offspring from field-caught hybrids for which the exact genotypes were unknown.

Mate discrimination

We measured males' visual discrimination of potential mates by restraining individual field-caught *E. anna* and *E. carunculatum* females on wooden dowels near the water at the Whitefish River site and measuring the frequencies of each type of male that attempted tandem with them. We attached live females of each species by their legs to wooden dowels using Duco cement (ITW Devcon, Glenview, IL, USA; Miller

and Fincke 1999) and placed individual dowels level with surrounding vegetation within 5 m of the water's edge. Over 20-minute intervals, we captured each male that either attempted or achieved tandem with a restrained female and assigned them to species by examining the cerci with a hand lens. Males were held in paper envelopes until the end of the observation period to prevent the possibility of a second encounter with the restrained female and were then released.

Mating assays

We measured several premating RI barriers using mating experiments in which females were placed in mesh cages with either heterospecific, hybrid, or conspecific males. We used both field-caught and lab-reared damselflies, and used only virgin females in each mating assay. To obtain virgins in the field, we captured newly emerged females, identified by their pale teneral coloration. We assigned species identity as described above, then housed virgin females in cages until they reached sexual maturity (~10 days post-emergence). We placed 2-5 individuals of each sex in a cage under partial shade in the grass and observed behaviors between 1000-1600 hr.

We quantified precopulatory mechanical RI by measuring the frequency of tandem attempts in which the male was unable to securely grasp a female for longer than five seconds. A secure hold was confirmed by observing the male flying while engaged with the female, or attempting to fly without losing contact while the female remained perched. We measured copulatory mechanical RI as the proportion of

copulation attempts in which the male and female failed to achieve genital coupling. This estimates mechanical incompatibility between male grasping appendages and female thoracic plates and excludes the possibility of male loss of interest, because males were often observed repeatedly attempting tandem on the same female despite being unable to grasp her.

We quantified two types of precopulatory tactile incompatibilities using pairs that formed tandems. First, we recorded whether each female showed resistance behaviors during tandem (*e.g.*, head shaking, wing flapping, dorsal abdominal extension, or body repositioning) (Tennessen 1975; Xu and Fincke 2011). Second, we recorded whether females in tandem cooperated in copulation or refused to mate.

Postzygotic isolation

We quantified several postmating RI barriers using both lab generations. We measured oviposition success as the proportion of females from each cross type that oviposited. When females failed to oviposit within three days post-mating, we checked their male partners for motile sperm by anesthetizing them with CO_2, immediately dissecting out the seminal vesicle, gently squashing it under a coverslip, and examining the contents under a Zeiss Axio Imager 2 stereomicroscope (100$\times$ total magnification). We dissected females that failed to oviposit to check the oviduct for mature eggs and the bursa copulatrix for sperm.

We calculated fecundity by counting all eggs laid by each mated female within three days of mating. The date of egg hatch was recorded as the first day that larvae were observed. We calculated the proportion of eggs that hatched from each clutch by counting the number of unhatched eggs that remained in the filter paper seven days after first hatch. We calculated fertility of lab-reared matings by counting the number of fertilized eggs, as indicated by a dark spot that develops on the apical end of the egg (Corbet 1999). We calculated embryo development time as days from oviposition to egg hatch, larval maturation as days from egg hatch to adult emergence, larval survivorship as the proportion of hatched larvae that emerged as adults, and adult sex ratio and total adult lifespan.

Strength of RI barriers

We estimated the absolute strength of each individual RI barrier using the following general equation (Sobel and Chen 2014):

$$RI = 1 - 2 \times \left(\frac{H}{H+C}\right)$$

where *H* and *C* denote the frequency of heterospecific and conspecific interactions, respectively (prezygotic barriers), or fitness of hybrid or conspecific matings or offspring, respectively (postzygotic barriers; Table 1). This equation yields values between -1 and 1 in which 0 indicates no barrier to gene flow, 1 indicates complete RI,

and -1 indicates complete hybrid advantage. In essence, the term $\frac{H}{H+C}$ describes the probability of gene flow between species. Larger values of the parameters *H* and *C* are typically associated with higher fitness in this equation. However, for duration of copulation interruptions, a larger value represents lower fitness. We therefore modified this equation by using the inverse of *H* and *C* values when calculating the contribution of copulation interruptions to RI. We estimated total RI between *E. anna* and *E. carunculatum* as described in Sobel and Chen (2014) for sympatric populations as:

$$RI_{total} = 1 - 2 \times \left(\frac{\prod_{i=1}^{n} P(H)_i}{\prod_{i=1}^{n} P(H)_i + \prod_{i=1}^{n} P(C)_i} \right)$$

We also used this same general equation to calculate cumulative RI for each barrier in the sequence, which yields each barrier's absolute contribution (*AC*). Finally, we used both of these values to calculate each barrier's relative contribution (*RC*) to total RI (AC_i / RI_{total}).

Statistical analyses

We compared males' sexual approaches toward con- and heterospecific females, observed vs. expected frequency of heterospecific pairs, and adult sex ratios using binomial tests. We compared presence or absence of female resistance behaviors, female mating refusal or cooperation, frequency of copulation

interruptions, and oviposition success among parental species and hybrid pairs using Fisher Exact tests. We examined the relationship between male abdomen length and cercus size using linear regression. We compared copulation and copulation interruption durations between conspecific and non-conspecific matings using *t*-tests. We compared abdomen length, fecundity, fertility, proportion eggs hatched, developmental timing, and adult lifespan among *E. anna*, *E. carunculatum*, and hybrids using analysis of variance (ANOVA), after arcsin-transformation of proportion data. When an ANOVA indicated a significant difference existed among the three groups for any measure, we conducted Tukey post-hoc tests to identify the differences among groups. For both forms of premating tactile isolation data, we omitted all cross types with sample size < 6 from statistical analyses. When possible, we combined data (field and lab, or lab generations 1 and 2) to increase statistical power, after confirming with ANOVA that measurements not differ significantly between the two groups. All analyses were conducted in R version 3.1.1 (R Core Team 2015). Means are reported as $\pm$ 1 SEM.

Results and Discussion

Males mate indiscriminately and hybridization occurs at low frequency in nature

At the Whitefish River site, *E. anna* males outnumbered *E. carunculatum* males by a factor of ~1.5. This was observed for both solitary males (*E. anna*: n = 165, *E. carunculatum*: n = 108, over 8 sampling days) and male-female pairs (*E. anna*: n = 44,

E. carunculatum: n = 28, over 9 sampling days). *E. anna* males attempted tandem with *E. carunculatum* females (46.3%, 19 of 41) as frequently as they did with *E. anna* females (53.7%, 22 of 41; $\mathcal{X}_1^2$= 0.010, *P* = 0.76; Fig 2). *E. carunculatum* males also attempted tandem with females of both species equally (50.0%, 8 of 16 each; $\mathcal{X}_1^2$ = 0.00, *P* = 1.0; Fig 2). These results show that premating interactions between *E. anna* and *E. carunculatum* are random, similar to observations from other *Enallagma* (Paulson 1974; Fincke et al. 2007; Xu and Fincke 2011) and *Ischnura* species (Sánchez-Guillén et al. 2012; Sánchez-Guillén et al. 2014).

Despite this lack of habitat and visual isolation in sympatry, heterospecific pairs were rarely captured in the field. In more than one month at the field site, we captured only two heterospecific male-female pairs, one in each cross direction. Based on the relative frequencies of each pure species, heterospecific pairs occur significantly less often than expected under random mating between *E. anna* and *E. carunculatum* ($\mathcal{X}_3^2$ = 65.40, $P < 1 \times 10^{-5}$). This suggests that although males may frequently initiate tandems with heterospecific females, such pairs likely remain in tandem only briefly. However, even the rare occurrence of both types of heterospecific tandems suggests that pure species may interbreed at low frequencies in the wild, and our collection of field-caught individuals supports this notion: 41 of 630 males and 7 of 547 females we collected possessed intermediate reproductive structure morphologies that were visibly different from either pure species.

Hybrids are morphologically distinct from either parental species

Among males, the first 5 principal component (PC) scores explained >77% of the cercus shape variance. PC1 (60.05%) distinguished pure species and represented differences in overall cercus length, from short (*E. carunculatum*) to long (*E. anna*), with hybrids showing a range of intermediate scores (Fig 3A). PC2 (7.50%) represented a difference in the relative angles of the upper and lower projections of the cercus, with many hybrids occupying a different space along this axis than parental species. Most field-caught males we identified as hybrids had distinctly intermediate cercus morphologies, whereas the lab-reared males from heterospecific or backcross pairs possessed morphologies that spanned the entire range of variation between *E. anna* and *E. carunculatum* males (Fig 3A).

Among females, the first 6 principal components scores accounted for >42% of the variance in mesostigmal plate shape. *E. anna* and *E. carunculatum* specimens formed separate clusters along PC1 (17.9%), but there was considerable overlap between hybrids and *E. anna* on PC1 (Fig 3B). This overlap might reflect limitations of the resolving power of our morphometric approach to distinguish intraspecific variation from intermediate hybrid morphology of these complex female structures. Additional PC axes indicated that parental species and hybrid plate shapes showed similar levels of variation in several features, including the angle of the plate's anterior edge relative to the thorax (PC2; 6.0%), curvatures of the plate's lateral edge (PC3; 5.5%) and plate surface (PC5; 4.6%), and dimensions of the space between the

bilateral plates (PC4; 5.3%). Because slight variation in the manual placement of the fixed landmarks on each female has the potential to contribute to this apparent overlap between *E. anna* and the hybrid females, we repeated the entire analysis beginning with placement of landmarks on a subset of 157 plates selected at random. Repeatability was high among landmark coordinates in both sets ($r > 0.99$) and both replicate analyses produced similar results (Fig S3).

Our behavioral, rearing, and morphometric data confirm that individuals with intermediate reproductive structure morphologies are hybrids between *E. anna* and *E. carunculatum* and not a separate species as originally suggested (Miller and Ivie 1995). Interestingly, the collection of lab-reared hybrids (both F_1 and backcross) included cercus and plate phenotypes not observed in the field-caught samples (Fig 3). Some lab-reared hybrid morphologies were even indistinguishable from those of the parental species, which could be the result of collecting eggs in the field from mated females that may have been storing sperm from previous conspecific matings. Alternatively, some field-caught adult damselflies that we designated as pure species may in fact have been hybrids that maintained "phenotypic integrity" with one parental species despite having highly admixed genomes (Poelstra et al. 2014). Despite this possibility of occasional misidentification, the majority of field-caught individuals we identified as hybrid possess morphologies that fall well outside of the distributions of either pure species. This is particularly true for cercus shape, which has pronounced differences between *E. anna* and *E. carunculatum*.

The distributions of the field-caught versus lab-reared hybrids also suggest that hybrid genital morphology may be under selection in the wild. In particular, the distribution of male morphologies shows that some lab-reared backcross hybrid males possess cercus morphologies rarely observed among field-caught males. This result suggests that although interspecific mating occurs in the field, F_1 hybrids either rarely backcross with parental species or backcross hybrids rarely survive to reproductive age. Our lab-rearing data show that hybrids can in fact backcross with parental species and advanced backcross individuals are viable and fertile (see below). However, future genomic studies will be needed to reveal the direction and genomic extent of introgression and the frequency of F_1 versus advanced-generation hybrids in the wild.

Mechanical incompatibilities cause substantial, asymmetric reproductive isolation

Between pure species, precopulatory mechanical RI was incomplete in both directions of interspecific cross, and RI appears asymmetric: 25% (7/28) of *E. anna* males achieved tandems with *E. carunculatum* females, whereas 66.7% (6/9) of *E. carunculatum* males achieved tandems with *E. anna* females (Fig 4A). These data show that mechanical isolation is relatively weak between *E. carunculatum* males and *E. anna* females, which presents the opportunity for interspecific matings. Mechanical isolation due to males' inability to grasp heterospecific females is frequently evoked as the major contributor to RI in coenagrionid damselflies (Paulson 1974; Robertson and Paterson 1982; Fincke et al. 2007; Bourret et al. 2012; Wellenreuther and Sánchez-

Guillén 2016), although several exceptions exist (Paulson 1974; Tennessen 1975; Bick and Bick 1981; Forbes 1991; Miller and Fincke 2004). Our results suggest that mechanical incompatibilities are not sufficiently strong enough to completely exclude the possibility of hybridization in *Enallagma*. Additionally, it has been suggested that species with longer cerci are better at grasping females of other species (Paulson 1974), but our data show that *E. anna* males, whose cerci are roughly twice as long as *E. carunculatum* cerci, were less capable of grasping heterospecific females compared to *E. carunculatum* males.

The existence of incomplete precopulatory mechanical incompatibilities between *E. anna* and *E. carunculatum* suggests that the intermediate cercus morphology of hybrid males might reduce their ability to form tandems with pure species females. Eighty-six percent (30/35) of hybrid males we tested achieved tandem with *E. anna* females, and 63.6% (7/11) achieved tandem with *E. carunculatum* females (Fig 4A). Thus, male hybrids achieved tandem with both pure species more frequently than males of either pure species achieved tandem with heterospecific females. These results show that although hybrid males were less successful at forming tandems with females than conspecific males, they were more successful than heterospecific males.

Mechanical incompatibility involving the primary genitalia (intromittent organs) may also cause RI. No heterospecific matings occurred during our behavioral observations, so we could not directly measure copulatory mechanical RI between *E.*

anna and *E. carunculatum*. However, among the tandem pairs involving hybrids in which the female initiated copulation (2 *E. anna*, 2 *E. carunculatum*, and 3 hybrid females), all 7 pairs achieved genital coupling. Although this sample size is modest, this result suggests that no copulatory mechanical incompatibility exists between hybrids and parental species. This is not unexpected, as *E. anna* and *E. carunculatum* penes have similar morphologies (Kennedy 1919). Taken together, the results from these mating assays show that as the morphological mismatch between interacting male and female mating structures increases, the possibility of forming tandem and mating decreases.

Tactile incompatibilities cause substantial RI when mechanical isolation is incomplete

A significantly greater proportion of lab-reared *E. anna* females (12/22) engaged in resistance behaviors during conspecific tandems than did field-caught *E. anna* females (1/13, Fisher exact test, $P = 0.01$). For this reason, we analyzed presence/absence of female resistance during tandem separately for field-caught and lab-reared populations. In the field, *E. anna* females were significantly more likely to resist during tandems with heterospecific males (67%; 4 of 6) or hybrid males (50%; 9 of 18) than with conspecific males (7.7%; 1 of 13; Fisher exact tests, $P_{heterospecific} = 0.02$, $P_{hybrid} = 0.02$; Fig 4B). Additionally, 71.4% (5/7) of *E. carunculatum* females displayed

resistance behaviors during tandem with *E. anna* males in the field, which was significantly greater than 7.7% of *E. anna* females ($P = 0.007$; Fig 4B).

Surprisingly, lab-reared *E. anna* females resisted during tandems with conspecific males as frequently as they resisted during tandems with hybrid males (54.5%, 12 of 22 vs. 81.8%, 9 of 11, respectively; $P = 0.25$; Fig S4). *E. anna* and hybrid females also showed similar levels of resistance during tandem with *E. anna* males (14.3%, 1 of 7 of hybrid females resisted; $P = 0.09$; Fig S4). A comparison of the two reciprocal *E. anna* $\times$ hybrid crosses, however, showed that *E. anna* females were significantly more likely to resist during tandem with hybrid males (81.8%) than were hybrid females (14.3%; $P = 0.01$; Fig S4). Female resistance during tandem with a conspecific male is not unusual (Tennessen 1975; Fincke 2015), but because the field-caught and lab-reared *E. anna* populations behaved so differently, and the field data reflects behavior in a natural setting, we used the field-caught female data to calculate this form of tactile isolation (Table 1).

Field-caught and lab-reared females showed similar copulatory refusal rates: 94.7% (18/19) field-caught and 81.8% (9/11) lab-reared *E. anna* females refused hybrid males (Fisher exact test, $P = 0.54$), and 69.2% (9/13) field-caught and 51.9% (12/25) lab-reared *E. anna* females refused conspecific males ($P = 0.31$). We therefore pooled field-caught and lab-reared data to analyze female copulation refusal or acceptance. Ninety percent (27/30) of *E. anna* females taken in tandem by hybrid males refused to copulate, which was significantly greater than the 55.3% (21/38) of *E. anna* females

that refused conspecific males (P = 0.003; Fig 4C). All six *E. anna* females observed in tandem with *E. carunculatum* males refused to copulate, although this level of refusal was not statistically different from the conspecific refusal rate (P = 0.07; Fig 4C). This is likely due to the low number of heterospecific pairs we could observe. *E. carunculatum* females, in contrast, were significantly more likely to refuse an *E. anna* male (100%, 7 of 7) than a conspecific male (16.7%, 1 of 6; P = 0.005; Fig 4C). *E. anna* females also refused to mate with *E. carunculatum* males more frequently than did *E. carunculatum* females (P = 0.015). We obtained a similar result for the reciprocal cross, where more female *E. carunculatum* females refused *E. anna* males than did *E. anna* females (P = 0.03; Fig 4C).

Females' behavioral responses to different types of males reveal strong assortative mating between *E. anna* and *E. carunculatum* when premating mechanical isolation fails. Tactile isolation also predicts that pure species females should refuse to mate with hybrid males because intermediate cerci fail to relay the proper tactile species recognition signal to the female. Our behavioral data support this prediction for *E. anna* females, which mated with hybrid males less frequently than with conspecific males. The finding that some *E. anna* females mated with hybrid males, but none mated with *E. carunculatum* males suggests that females display some latitude in their preferences and are more likely to refuse males whose cercus morphology greatly deviates from a conspecific phenotype. Although incomplete mechanical isolation has been documented in several *Enallagma* species pairs, few

cases of hybridization are known, based on morphological or genetic evidence (Catling 2001; Turgeon et al. 2005; Donnelly 2008). This suggests that even with incomplete mechanical isolation, tactile isolation might prevent interbreeding among most *Enallagma* species. A full understanding of tactile isolation will require quantitative study of the mechanoreceptors on female plates to understand how patterns of phenotypic variation might contribute to RI.

The relative sizes of male and female reproductive structures may influence both mechanical and tactile mechanisms of RI. Larger males tended to have larger cerci, as indicated by regressing cercus volume on abdomen length (*E. anna*: $F_{1, 26}$ = 18.80, R^2 = 0.397, P = 0.0002; *E. carunculatum*: $F_{1, 17}$ = 7.744, R^2 = 0.273, P = 0.013). Hybrids, however, showed a weaker relationship between body size and cercus size, because hybrids display more variation in cercus morphology than either parental species ($F_{1,55}$ = 6.70, R^2 = 0.092, P = 0.01). A size mismatch in male and female structures either within or between species may contribute to mechanical incompatibilities, although our current data do not allow us to examine that relationship robustly.

Postmating barriers contribute little to reproductive isolation

Compared to the strong premating RI caused by mechanical and tactile incompatibilities of male and female reproductive structures, we found relatively weak RI from postmating barriers. Copulation duration was similar among conspecific

mating pairs and pairs including at least one hybrid partner (t_{25} = -0.028, P = 0.98; Fig 5A). Sixty percent (6/10) of *E. anna* matings experienced interruptions, which was not significantly different from the hybrid matings (61.5%, 8 of 13; Fisher exact test, P = 1.0; no data on *E. carunculatum* interruptions). The total duration of these interruptions was also not significantly different between *E. anna* or hybrid pairs ($t_{13.26}$= -1.51, P = 0.15; Fig 5B). Although it has been suggested that Lepidoptera (Lorkovic 1958) and *Ischnura* (Córdoba-Aguilar and Cordero-Rivera 2008) use copulatory morphology or stimulation to identify conspecifics, our results indicate that this type of tactile discrimination during copula does not occur in *Enallagma*.

Similar proportions of *E. anna* (94.3%; 33 of 35) and hybrid females (76.9%, 10 of 13) oviposited after mating with *E. anna* males (Fisher exact test, P = 0.81). Two *E. anna* females mated with hybrid males, but neither laid any eggs. In contrast, two *E. carunculatum* females mated with hybrid males and both oviposited. Two of the three hybrid females that mated with hybrid males also oviposited. Dissections of females that failed to oviposit confirmed that they had been inseminated and possessed mature eggs, and dissections of hybrid males in these matings confirmed that hybrid males produce motile sperm. *E. anna, E. carunculatum*, and hybrid parings also produced comparable numbers of eggs ($F_{2,80}$ = 0.79, P = 0.46; Fig 5C). Although there appears to be a trend towards smaller clutches or complete failure to oviposit in females mated to hybrids, small samples prevent us from drawing strong conclusions

about whether tactile incompatibilities might contribute to postcopulatory isolating mechanisms.

Lab generation 2 consisted solely of *E. anna* and advanced generation hybrid clutches, because in generation 1, *E. carunculatum* adults emerged earliest and few were available for crosses with *E. anna* or hybrids. In generation 2, *E. anna* and hybrid clutches had similar fertilization rates ($F_{1, 17}$ = 0.51, P = 0.49). In generation 1, *E. anna*, *E. carunculatum*, and hybrid clutches had similar proportions of hatched eggs (Kruskal-Wallis $\mathcal{X}_2^2$= 1.3385, P = 0.51; Fig 5C). In generation 2, *E. anna*, and hybrid clutches had similar proportions of hatched eggs ($t_{17.97}$= 0.49404, P = 0.63, Fig S6). Oviposition date had a significant effect on hatch timing in generation 1 ($F_{1,41}$ = 49.1, $P = 1.6 \times 10^{-8}$), but not in generation 2 ($F_{1,41}$ = 2.96, P = 0.11). We therefore analyzed hatch timing separately for each generation. In generation 1, *E. carunculatum* larvae hatched earlier (15.4 $\pm$ 0.9 days, n =19 families) than *E. anna* (19.2 $\pm$ 0.7 days, n =17 families) and hybrid larvae (20.0 $\pm$ 1.3 days, n =7 families; ANCOVA with oviposition date as covariate, $F_{2, 39}$ = 10.8, $P = 2 \times 10^{-4}$). In generation 2, *E. anna* and hybrid hatch rates did not differ significantly ($t_{11.92}$= -1.22, P = 0.25; Fig 5D). If *E. carunculatum* larvae develop at a faster rate in the wild as they did in the lab, this could contribute to RI via seasonal temporal isolation, in which early-emerging *E. carunculatum* adults are less likely to encounter, and thus potentially interbreed with, *E. anna* adults. Detecting and measuring this potential temporal barrier will require regular sampling throughout the breeding season.

An anomalous water quality problem at the Aquatic Research Facility where larvae were housed caused substantial larval mortality of generation 2, so we analyzed larval development timing for generation 1 only (Fig 5F). An ANCOVA with oviposition date as a covariate and Tukey post-hoc tests indicated that hybrids and parental species spent significantly different lengths of time in the larval stage ($F_{2, 29} = 97.3$, $P < 1.4 \times 10^{-13}$). *E. carunculatum* (n =13 families) larvae reached adulthood an average of 58.6 $\pm$ 2.5 days earlier than *E. anna* (n =14 families; $P < 1 \times 10^{-5}$) and 18.2 $\pm$ 7.3 days earlier than hybrids (n =6 families; $P = 0.056$). Hybrid larvae also developed significantly faster than *E. anna* ($P = 3 \times 10^{-5}$). Although *E. carunculatum* larvae developed faster than *E. anna* and hybrid larvae in the lab, mean adult abdomen length was similar among all three groups for both males ($F_{2, 19} = 0.334$, $P = 0.72$) and females ($F_{2, 21} = 3.30$, $P = 0.57$; Fig S5). These results suggest that hybrid development was not affected by intrinsic genetic incompatibilities.

Larval survivorship in the lab was similar for both parental species' and hybrid clutches (Kruskal-Wallis $\mathcal{X}_2^2 = 4.4$, $P = 0.1$; Fig 5G). Of those individuals that reached adulthood, adult lifespans under laboratory conditions did not differ significantly (ANCOVA with emergence date as covariate, $F_{2, 48} = 1.35$, $P = 0.29$; Fig 5H). Finally, adult sex ratios were not significantly different from the expected 1:1 ratio for any group (Fig 5I), which shows that among pure species and hybrids, both sexes had similar viability. The combination of our postmating isolation results demonstrate that

neither strong intrinsic nor extrinsic (*e.g.*, ecological selection against hybrids in the field) postzygotic barriers exist between *E. anna* and *E. carunculatum*.

Because heterospecific and hybrid matings were rare, we pooled the data obtained from reciprocal F_1s and advanced generation hybrid individuals to calculate postzygotic isolation. Although pooling these data could weaken the estimate of F_1 fitness loss, our field collection, behavior, and rearing data together suggest that the strength of intrinsic postzygotic RI between *E. anna* and *E. carunculatum* is minor compared to the strength of RI caused by intermediate reproductive structure morphologies.

Divergent reproductive structures cause reproductive isolation early during speciation

Figure 6 shows the cumulative strength of RI barriers measured for each reciprocal cross. Premating mechanical and tactile incompatibilities form the most substantial barriers to gene flow between *E. anna* and *E. carunculatum*, whereas later-acting barriers contribute little to total RI. Our results thus unequivocally demonstrate the potential of divergent mating structures to cause RI in the early stages of speciation via mechanical and tactile mechanisms. These incompatibilities also appear to provide particularly strong barriers to gene flow, as they act as both a premating barrier between pure species and also as a postzygotic barrier that reduces hybrid male mating success. Such incompatibilities represent a potent barrier to gene flow

and may be a common characteristic of traits that are under sexual selection within species (Stratton and Uetz 1986; Naisbit et al. 2001; Höbel et al. 2003; Svedin et al. 2008; Van Der Sluijs et al. 2008).

Our results also show that premating barriers appear to have evolved first in *Enallagma*. Because *E. anna* × *E. carunculatum* hybrids appear to survive as well as parental species and suffer no intrinsic fertility deficits, the primary factor likely to affect their fitness is with whom they can mate. We observed that *E. anna* females often refuse to mate with conspecific males, indicating strong intraspecific discrimination. If the male cerci are under sexual selection similar to non-intromittent mating structures in other taxa (reviewed in Simmons 2014), and if females rely on the same tactile cues for both intraspecific mate choice and species discrimination, then female discrimination among conspecific males could extend to discrimination of heterospecific males. Prezygotic RI has been shown to evolve rapidly under laboratory settings due to assortative mating, independent of local adaptation (Castillo et al. 2015), which supports the plausibility of rapid evolution of RI driven by sexual selection in the wild. Female discrimination against males with intermediate cerci also provides an opportunity for reinforcement to strengthen premating isolation between *E. anna* and *E. carunculatum*— a potential example of sexual selection rather than natural selection driving reinforcement (Naisbit et al. 2001). Reinforcement could result in shifting or narrowing of female preferences (Ritchie 1996) or an increase in female discrimination in regions of sympatry (Noor 1999), two ideas that deserve

further study in these species. Alternatively, evolution of cercus morphology may be driven by sexual conflict over mating rate, in which selection favors females that are less easily grasped by males (Fincke et al. 2007).

Many researchers have dismissed genital mechanical incompatibilities as having an important role in RI and speciation (reviewed in Shapiro and Porter 1989; Eberhard 2010), primarily because of the small number of convincing cases that show strict support for it. We might be better equipped to investigate the reproductive consequences of the widespread pattern of rapid, divergent evolution of male genitalia if we broaden our scope to include explicitly tactile mechanisms. This may require dropping the genital "lock-and-key" imagery – which often evokes an "all or nothing" scenario in causing RI – in favor of a framework that allows for more variation, similar to our understanding of auditory, visual, and chemical communication signals. Indeed, our data show that mechanical isolation can be strong yet incomplete, and that tactile isolation can form a strong subsequent mating barrier. A full understanding of the contribution of mechanical incompatibilities in RI will require detailed morphological study to understand how male and female structures interact (*e*.g., Willkommen et al. 2015) and which features cause morphological mismatch. A deeper understanding of tactile RI mechanisms will require detailed studies of sensory mechanisms and the neurobiological basis of female reproductive decisions, all of which are admittedly challenging to investigate. Where females discriminate against heterospecific reproductive structures (*e.g.*, Bath et al. 2012), the

female nervous system poses a potentially more complex spectrum of incompatibilities compared to genitalia. Taxa such as damselflies or stick insects (Myers et al. 2016) provide ideal systems to begin to tease apart mechanical and tactile contributions to RI. Neural circuits that integrate olfactory and auditory cues with internal physiological processes to influence female mating decisions are being mapped in *Drosophila* (Bussell et al. 2014; Feng et al. 2014; Zhou et al. 2014), paving the way for similar mechanistic understanding of sensory modalities in emerging model systems. Although odonates have a unique mode of mating that presents multiple opportunities for both mechanical and tactile mismatch, our results highlight the potential contribution of tactile signals involving the genitalia to RI among internally fertilizing animals.

Chapter 1 – Tables

Table 1. Reproductive isolation formulas

Barrier	RI formula
Prezygotic	
Visual	1 – (number heterospecific tandem attempts / conspecific tandem attempts)
Precopulatory mechanical	1 – (number heterospecific tandems / number heterospecific tandem attempts)
Tactile I (female resistance)	1 – (proportion heterospecific tandems without resistance / proportion conspecific tandems without resistance)
Tactile II (female refusal)	1 – (proportion heterospecific matings / proportion conspecific matings)
Postzygotic	
Hybrid mechanical I (tandem)	1 – (number hybrid tandems / number hybrid tandem attempts)
Hybrid mechanical II (intromission)	1 – (number hybrid copulations / number hybrid intromission attempts)
Hybrid tactile I (female resistance)	1 – (proportion hybrid tandems without resistance / proportion conspecific tandems without resistance)
Hybrid tactile II (female refusal)	1 – (proportion hybrid matings / proportion conspecific matings)
Hybrid copulation duration	1 – (mean hybrid copulation duration / mean conspecific copulation duration)
Hybrid copulation interruption duration	1 – (mean conspecific copulation interruption duration / mean hybrid copulation interruption duration)
Hybrid oviposition	1 – (proportion females oviposited, hybrid matings / proportion females oviposited, conspecific matings)
Fecundity	1 – (mean number eggs, hybrid clutch / mean number eggs, conspecific clutch)

Formulas for the absolute strength of each reproductive isolating barrier measured, listed in the order in which they act during the mating sequence and subsequent life history of an individual. In the postzygotic barrier formulas, "heterospecific" includes male-female pairs composed of both pure species and any male-female pair involving at least one hybrid partner.

Table 2. Contributions of individual barriers to total reproductive isolation

	A♀C♂			C♀A♂		
Barrier	AS	SS	RC	AS	SS	RC
Prezygotic						
Visual	0.000	0.000	0.000	0.000	0.000	0.000
Tandem	0.333	0.333	0.334	0.750	0.750	0.752
Resistance	0.639	0.426	0.427	0.643	0.161	0.161
Refusal	0.721	0.173	0.174	0.829	0.074	0.074
Postzygotic (hybrid vs conspecific)						
Hybrid Tandem	0.098	0.007	0.007	0.364	0.006	0.006
Hybrid resistance	0.458	0.028	0.028	0.583	0.006	0.006
Hybrid refusal	0.776	0.026	0.026	0.520	0.002	0.002
Hybrid Intromission	0.000	0.000	0.000	0.000	0.000	0.000
Hybrid copulation duration	-0.101	-0.001	-0.001	-0.126	0.000	0.000
Hybrid copulation interruption	0.542	0.004	0.004	na	na	na
Hybrid oviposition	0.222	0.001	0.001	na	na	na
Hybrid fecundity	0.180	0.001	0.001	0.230	0.001	0.001
Hybrid fertility	0.033	0.000	0.000	na	na	na
Egg hatching	-0.065	0.000	0.000	-0.065	0.000	0.000
Embryo development	0.041	0.000	0.000	0.206	0.000	0.000
Larval maturation	-0.176	0.000	0.000	0.079	0.000	0.000
Larval survivorship	-0.053	0.000	0.000	-0.714	-0.001	-0.001
Adult sex ratio	0.004	0.000	0.000	-0.067	0.000	0.000
Prezygotic RI total		0.933			0.985	
Postzygotic RI total		0.064			0.013	
Total RI		**0.997**			**0.998**	

Estimated absolute strength (AS), sequential strength (SS), and relative contribution (RC) to total reproductive isolation of each potential barrier in sympatric populations of *Enallagma anna* and *E. carunculatum*. Equations for AS, SS, and RC are described in Dopman et al. (2010). "na" indicates values that could not be calculated due to a lack of data for *E. carunculatum* conspecific crosses. A = *E. anna*, C = *E. carunculatum*.

Chapter 1 – Figure legends

Figure1. Male grasping appendages and female mesostigmal plate morphology. The right cercus on each male is shaded yellow.

Figure 2. Overview of spherical harmonic (SPHARM) analysis of male cercus shape. **(A)** Digital volume rendering of right male cercus after CT scanning and digital segmentation from surrounding tissue. **(B)** Cercus represention as a solid surface comprised of 20,000 triangles; SPHARM produces coeffients that describe the shape of the triangular mesh. **(C)** Spherical harmonic model constructed using the coefficients recreates the shape of original model.

Figure 3. Female geometric morphometric landmarks. (A) Locations of single landmarks (points), curves (lines), and patch (closed outline and dotted lines) on a digitized 3-D surface of the right female mesostigmal plate and nearby thoracic structures. **(B)** Fixed and sliding semilandmark locations within the XYZ coordinate system. Red points indicate fixed landmarks, blue points indicate sliding semilandmarks designated as “curve sliders” in Geomorph, yellow points indicate sliding semilandmarks designed as “surface sliders” in Geomorph. Note that although not all semilandmarks appear evenly spaced when shown in two dimensions, they are spaced evenly across the 3-D surface.

Figure 4. Male visual isolation. Number of male tandem attempts on conspecific and heterospecific females at the Whitefish River site.

Figure 5. Variation in *E. anna*, *E. carunculatum*, and hybrid male and female reproductive structure morphologies. (A) Distribution of the first two principal components (PC) that represent variation in male cercus shape. Cercus representations above the plot show the range of hybrid male variation across the PC1 axis and representations below the plot show parental species morphologies. **(B)** Distribution of the first two principal components (PC) that represent variation in female mesostigmal plate shape. Examples of representative parental species and hybrid morphologies are shown below the plot (left: *E. anna*, middle: hybrid, right: *E. carunculatum*). The percentage of variation explained by each PC axis is shown in parentheses. Open symbols represent lab-reared individuals, filled symbols represent field-caught individuals.

Figure 6. PCA results of replicate 3-D geometric morphometric analysis of female mesostigmal plate shape. The percentage of variation explained by each PC axis is shown in parentheses. Open symbols represent lab-reared females, filled symbols represent field-caught females.

Figure 7. Sequentially-acting mechanisms of prezygotic reproductive isolation. (A) Mechanical isolation. **(B)** Proportion of tandems in which females displayed resistance behaviors (field-caught only). **(C)** Proportion of tandems in which females refused to copulate (field-caught and lab-reared data). Crosses shown on the x-axis list female first. A: *E. anna*, C: *E. carunculatum*, H: hybrid. Numbers at the base of the bars in panels A-C show the numbers of female-male pairs that were measured. "nd" refers to cross types for which no data were collected. Error bars represent the upper and lower bounds of 95% binomial confidence intervals. For proportions of 0 or 1, bars represent one-sided 97.5% confidence intervals.

Figure 8. Presence/absence of female resistance behaviors during mating observations with lab-reared damselflies. A = *E. anna*, C = *E. carunculatum*, and H = hybrid.

Figure 9. Sequentially-acting mechanisms of postmating reproductive isolation. (A) Copulation duration. **(B)** Length of copulation interruptions. **(C)** Fecundity (field-caught and lab-reared data). **(D)** Proportion hatched eggs per clutch. **(E)** Embryonic development timing. **(F)** Larval maturation timing. **(G)** Larval survivorship. **(H)** Adult lifespan. **(I)** Adult sex ratios. In panels A and B, each point represents one male-female pair. "nd" denotes no data. In panels C-G, each point represents one clutch. Within each panel, letters indicate homogeneous groups assigned at the statistical

cutoff at α = 0.05. Boxplots show the interquartile range. The line within the box shows the median and whiskers extend to the most extreme observation within ±1.5 times the interquartile range. Each open circle represents one mating pair (A, B), one clutch (C-E, G), or the clutch mean (F, H).

Figure 10. Adult *Enallagma* abdomen length measurements. Within each panel, letters indicate homogeneous groups as indicated by Tukey post-hoc tests at the statistical cutoff α = 0.05. Boxplots show the interquartile range. The line within the box shows the median and whiskers extend to the most extreme observation within 1.5 times the interquartile range. Each open circle represents one individual damselfly and each closed circle represents the mean for individuals within a lab-reared family.

Figure 11. Proportion of hatched eggs in lab generation 2. Boxplots show the interquartile range. The line within the box shows the median and whiskers extend to the most extreme observation within ±1.5 times the interquartile range. Each open circle represents one clutch.

Figure 12. Sequential strength of reproductive isolating barriers, beginning with male-female encounter and proceeding through the reproductive sequence and life history. Estimates of the strength of the first four barriers were obtained from conspecific and heterospecific crosses only, and estimates of the remaining barriers

also include crosses involving hybrid individuals. Estimates for the values of the strength of two barriers from the *E. carunculatum* female × hybrid male cross (copulation interruption duration and fertility) are represented by the best-fit line at these barriers.

Figure 1. Male grasping appendages and female mesostigmal plate morphology

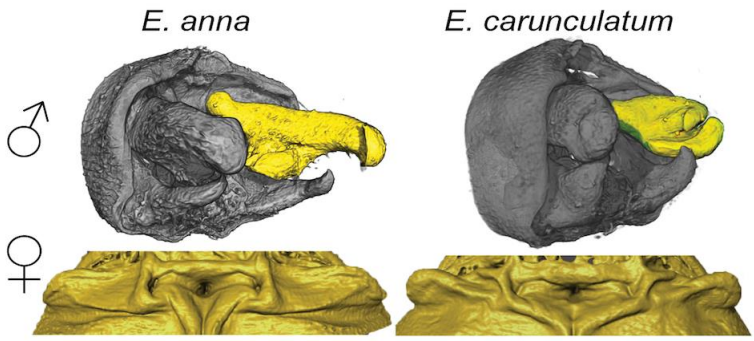

Figure 2. Overview of spherical harmonic analysis of male cercus shape

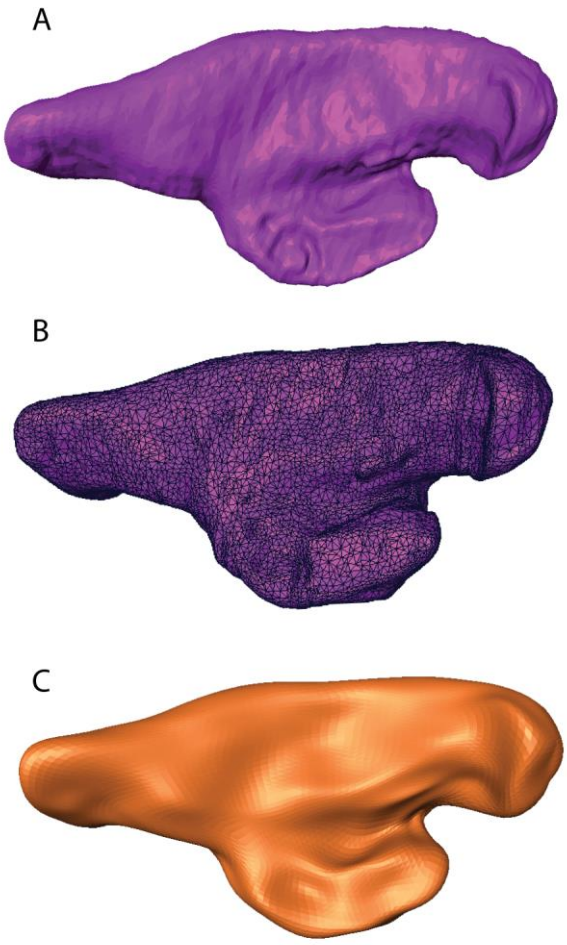

Figure 3. Female geometric morphometric landmarks

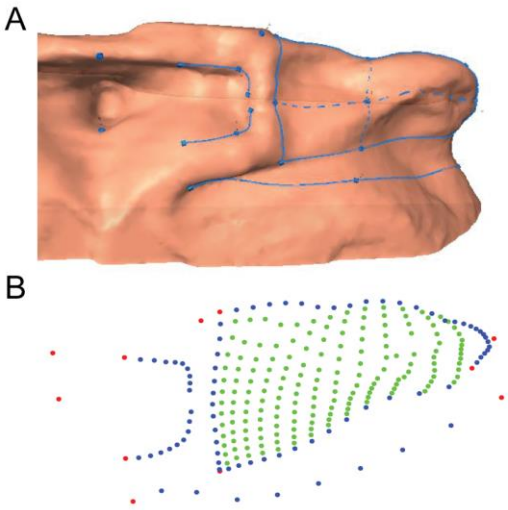

Figure 4. Male visual isolation

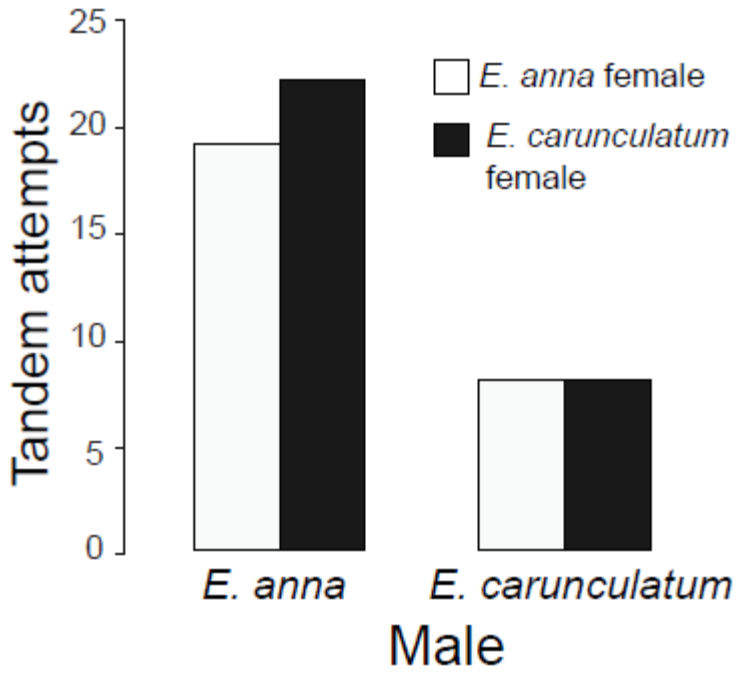

Figure 5. Variation reproductive structure morphologies

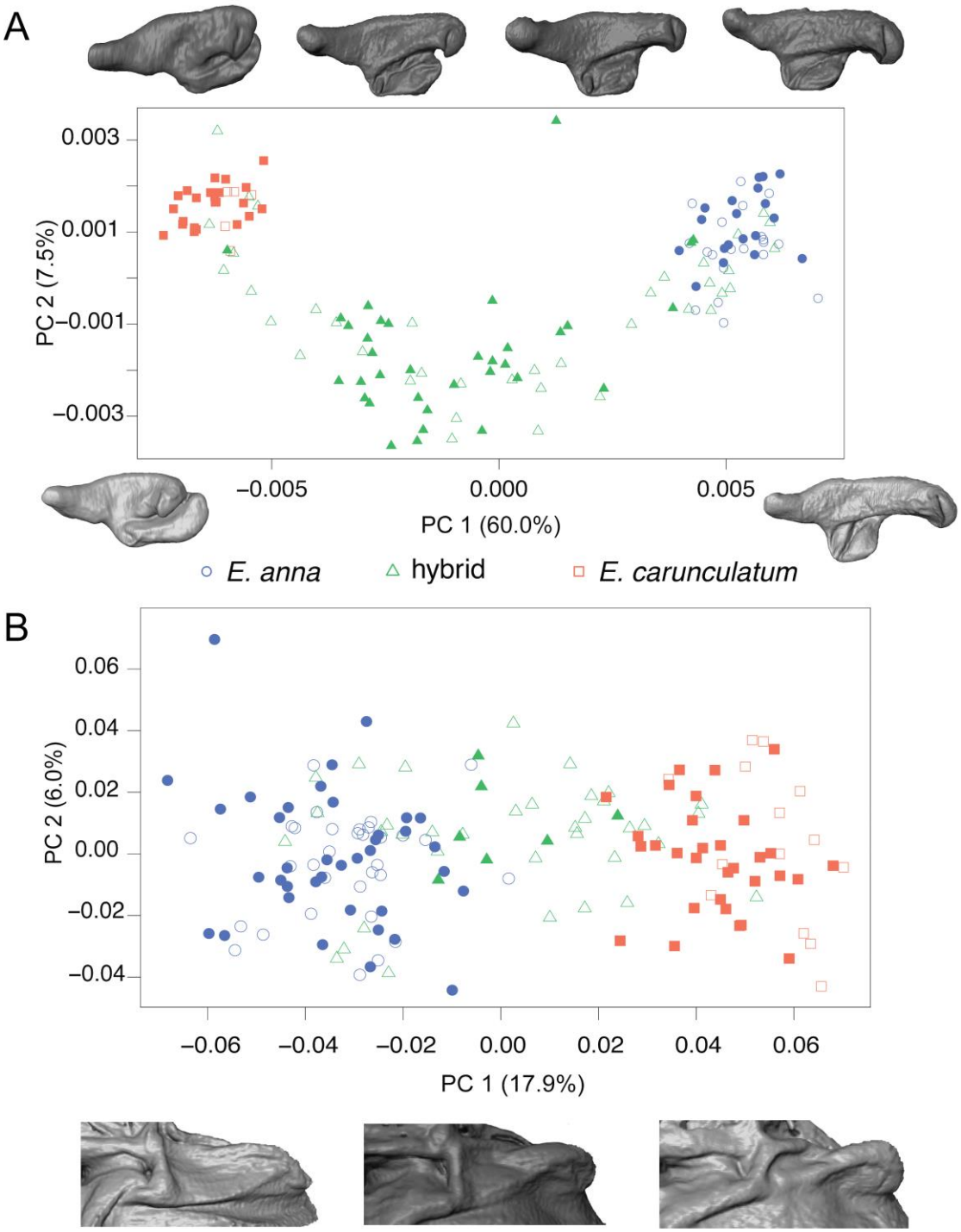

Figure 6. PCA results of replicate 3-D geometric morphometric analysis of female

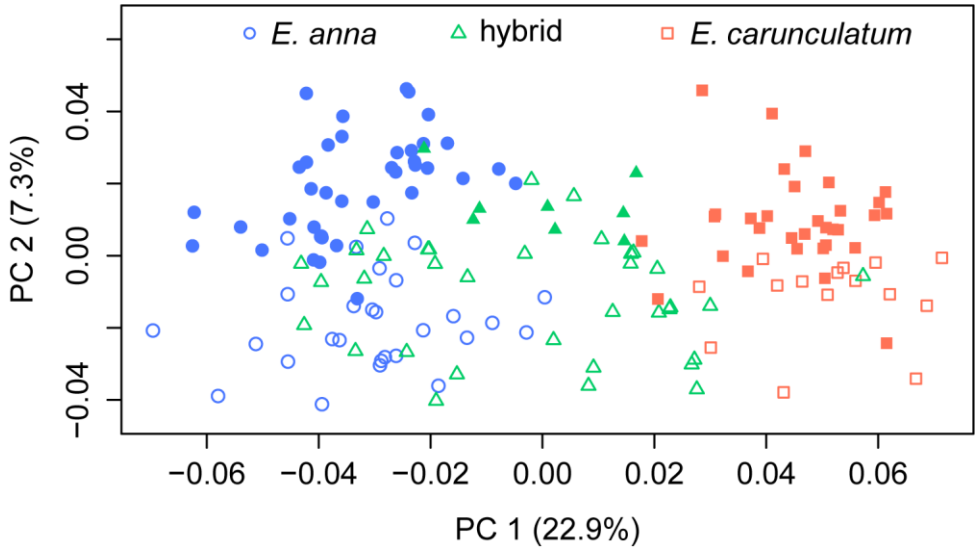

Figure 7. Sequentially-acting mechanisms of prezygotic reproductive isolation

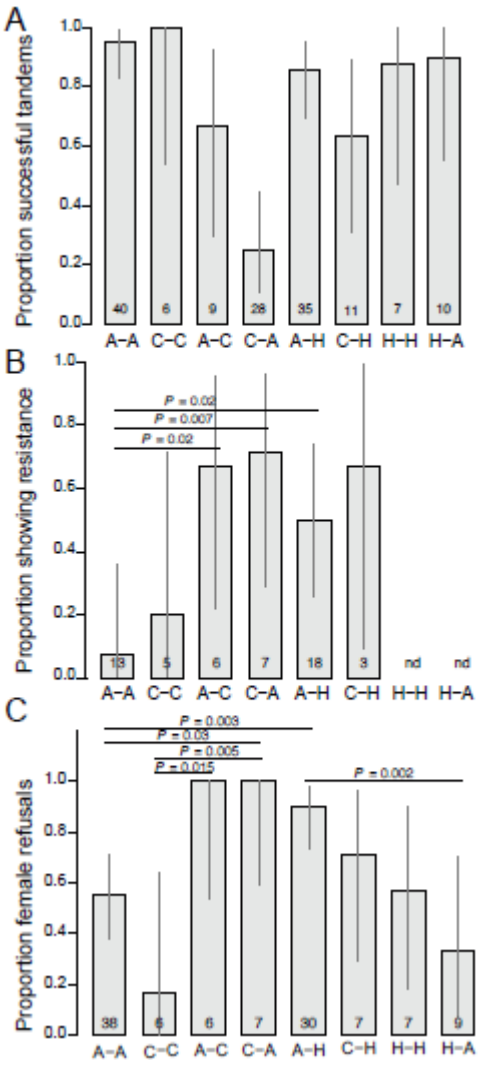

Figure 8 Female resistance behaviors during mating observations

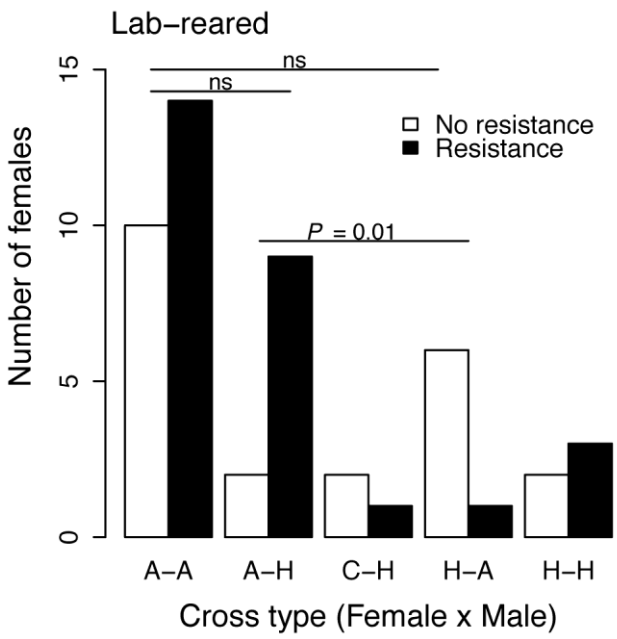

Figure 9. Sequentially-acting mechanisms of postmating reproductive isolation

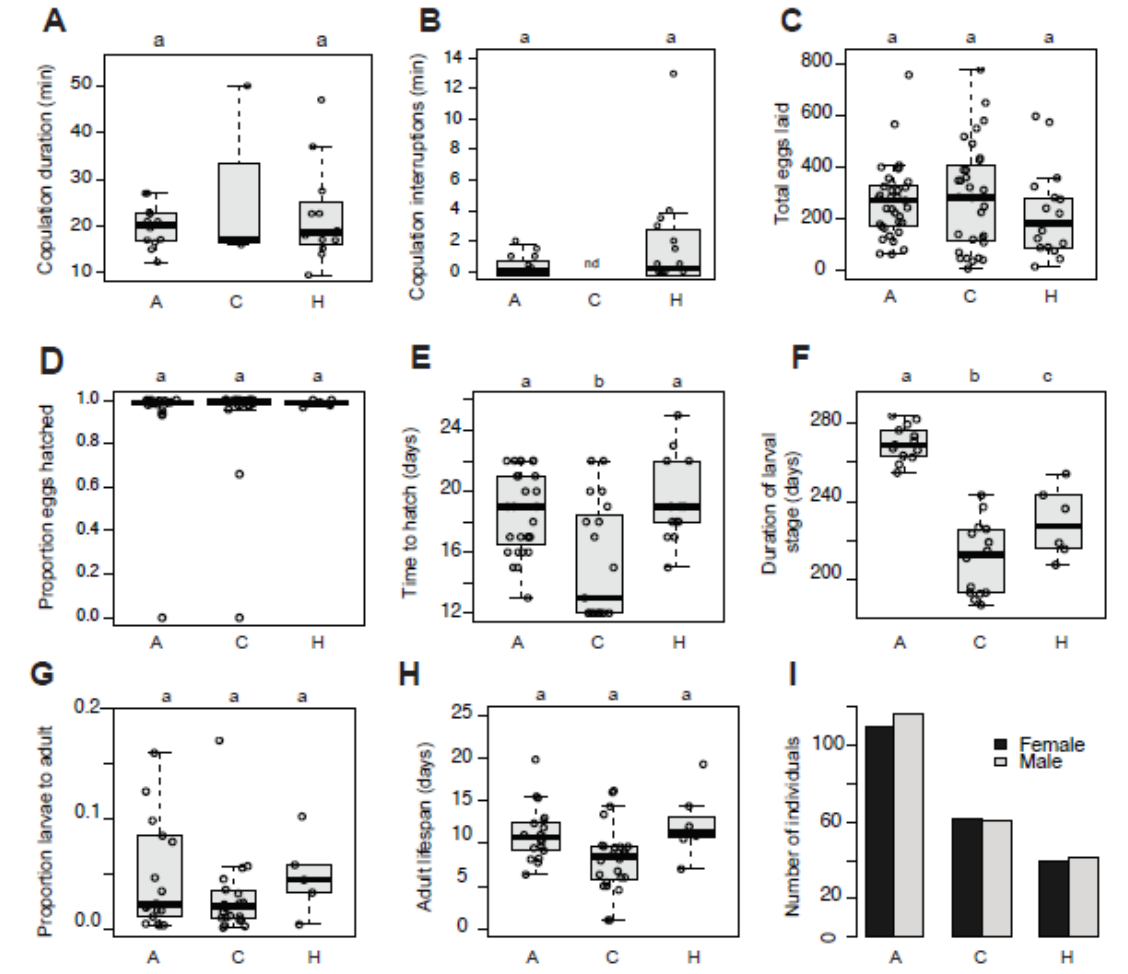

Figure 10. Adult *Enallagma* abdomen length measurements

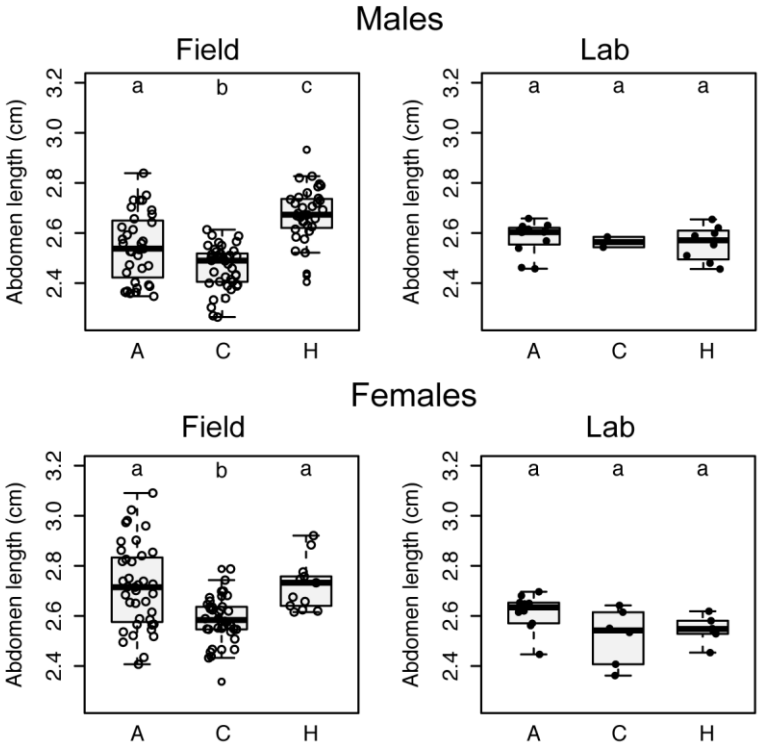

Figure 11. Proportion of hatched eggs in lab generation 2

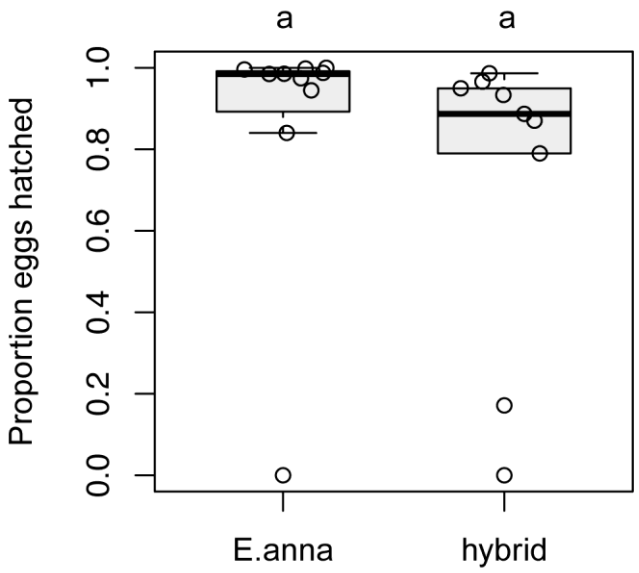

Figure 12. Sequential strength of reproductive isolating barriers

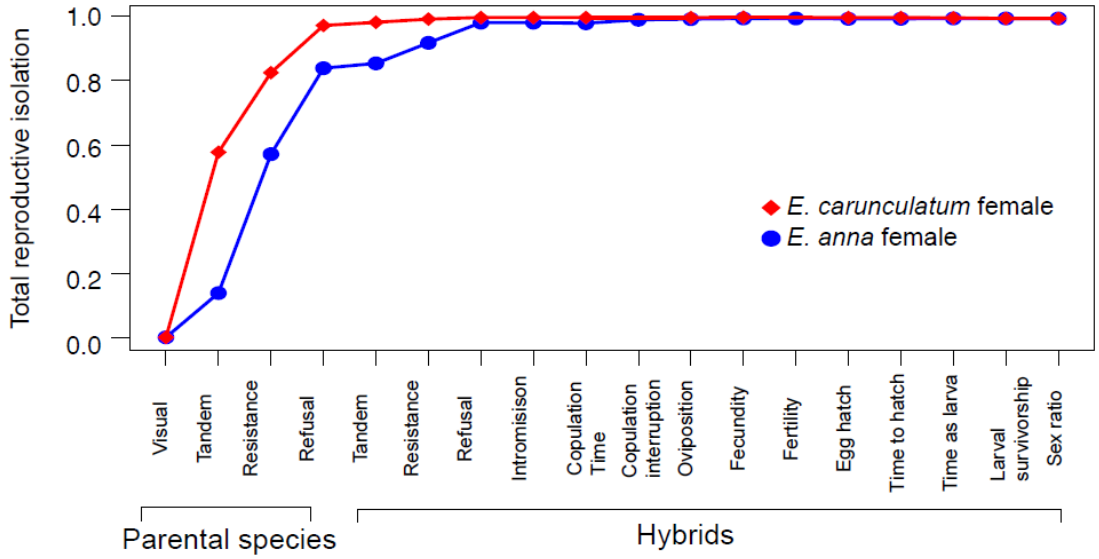

CHAPTER 2: Quantitative variation in female sensory structures supports species recognition and intraspecific mate choice functions in damselflies

Submitted for publication and currently under review. Co-author: J.P. Masly

Abstract

Males and females exchange signals prior to mating that convey information such as sex, species identity, or individual condition. Tactile signals relayed during physical contact between males and females before and during mating appear to be important for mate choice and reproductive isolation in some animals. However, compared to our understanding of visual, auditory, and chemical signals, we know little about the importance of tactile signals in mating decisions. Among North American damselflies in the genus *Enallagma* (Odonata: Coenagrionidae) species-specific tactile stimulation contributes to reproductive isolation between species and may also be important for intraspecific mate choice. We quantified several mechanosensory sensilla phenotypes on the female thorax among multiple sympatric and allopatric populations of two *Enallagma* species that occasionally interbreed in nature. Although each species differed in features of sensilla distribution within the thoracic plates, we found no strong evidence of reproductive character displacement among the sensilla traits we measured in regions of sympatry. However, substantial variation of sensilla traits was observed within populations of both species. Our results suggest that species-specific placement of female mechanoreceptors appears sufficient for species recognition, but mechanosensor variation among females within species may be important for mate choice.

Introduction

For sexual species, maintenance of species boundaries relies on reproductive isolation (RI) between recently diverged species (Mayr 1942). Premating reproductive isolating barriers, including behavioral or sexual isolation, often evolve earlier in the speciation process than postmating barriers in a variety of animal taxa (*e.g.*, McMillan et al. 1997; Price and Bouvier 2002; Mendelson and Wallis 2003; Dopman et al. 2010; Sánchez-Guillén et al. 2012; Williams and Mendelson 2014; Castillo et al. 2015; Barnard et al. 2017). Behavioral isolation requires that mate recognition signals and/or preferences diverge between populations, which ultimately results in the ability for individuals to discriminate conspecifics from heterospecifics. Species recognition signals may rely on a variety of sensory modalities such as color (Wiernasz and Kingsolver 1992; Sætre et al. 1997; Jiggins et al. 2001; Boughman et al. 2005; Kronforst et al. 2006; Williams and Mendelson 2014), courtship behavior (Stratton and Uetz 1986), sound/vibration (Ewing and Bennet-Clark 1968; Wells and Henry 1998; Shaw 2000; Gerhardt and Huber 2002; Arthur et al. 2013), and volatile chemicals (Coyne et al. 1994; Noor and Coyne 1996; Trabalon et al. 1997; Rafferty and Boughman 2006). Often, multiple signals act in concert to affect species recognition (*e.g.*, Costanzo and Monteiro 2007; Girard et al. 2015).

Although much is known about the importance of visual, chemical, and auditory signals and responses in sexual communication and species recognition, we know relatively little about other sensory modalities that may have strong effects on

individual mating decisions. Tactile signals have been hypothesized as a likely contributor to mating decisions (Mendelson and Shaw 2012), but it is unclear whether touch could represent a primary species recognition signal, given that visual and auditory cues usually act earlier during the mating sequence. Research on the prevalence of tactile signals in mating decisions is limited (Coleman 2008) because of the experimental challenge it poses: whereas other sensory modalities present male signals to a focal female from a distance, studying female preference for tactile cues requires contact between males and females, which is not always easily achieved or quantified under controlled conditions.

Despite this challenge, the role of tactile signals along the continuum between intraspecific mate choice and interspecific RI deserves attention because it broadens our understanding of the causes and consequences of a common pattern in nature—the rapid divergence of male genital morphology between species. It has been suggested that rapid genital differentiation can cause RI (Dufour 1844), although mechanical incompatibilities between heterospecific male and female genitalia do not appear to be a common cause of RI (Shapiro and Porter 1989; Masly 2012; Simmons 2014). However, observations both within (Eberhard 1994; Edvardsson and Göran 2000; Briceño and Eberhard 2009a; Briceño and Eberhard 2009b; Frazee and Masly 2015) and between species (Patterson and Thaeler Jr 1982; Robertson and Paterson 1982; Eberhard 1992; Coyne 1993) suggest that male genitalia may convey tactile information to females that affects their subsequent behavior and/or physiology.

Although female genital structures often appear invariant among closely related species (Shapiro and Porter 1989), subtle morphological differences (*e.g.*, Kamimura and Mitsumoto 2011; Yassin and Orgogozo 2013) could enable females to detect variation among males' genital morphology. This variation could occur in signal processing at the level of neurons and neural networks and/or in the distribution and morphology of sensory structures that receive male tactile signals.

Female sensory structures that reside in body regions that contact species-specific male structures during mating have been documented in several arthropods, including flies (Eberhard 2001; Ingram et al. 2008) and damselflies (Cordoba-Aguilar 2005; Robertson and Paterson 1982). Other studies have demonstrated that tactile cues from male grasping organs influence female mating responses, either via experimental manipulation of male structures and/or desensitization of females (Eberhard 2002; Briceño et al. 2007; Briceño and Eberhard 2009a; Eberhard 2010; Myers et al. 2016) or comparison of female behavior when grasped by males with varying genital morphologies (Sánchez-Guillén et al. 2012; Sánchez-Guillén et al. 2014; Barnard et al. 2017). Premating tactile isolation may also be important in vision-limited vertebrates. For example, contact cues via the lateral line system may influence female mate choice in a cavefish (Plath et al. 2004; but see Rüschenbaum and Schlupp 2013).

Tactile signals appear to be a significant cause of RI in Zygoptera, the damselfly suborder of Odonata (Krieger and Krieger-Loibl 1958; Loibl 1958; Robertson and

Paterson 1982; Corbet 1999). Concentrations of cuticular mechanoreceptors (sensilla) on the female thorax have been described in several coenagrionid damselfly genera. These sensilla reside in areas where male grasping appendages contact the female thorax before and during mating, which has led to speculation that they allow females to evaluate male morphologies and identify conspecifics (Jurzitza 1974, 1975; Tennessen 1975; Robertson and Paterson 1982; Battin 1993a,b). Each mechanoreceptor is associated with a single sensory neuron (McIver 1975; Kiel 1997). The thoracic sensilla thus represent a spatial matrix that can transmit signals to the female central nervous system based on the pattern in which the sensilla are stimulated. Greater numbers of these receptors enhance a female's sensory resolution by increasing the combinatorial complexity of tactile signals that a female can perceive. For example, if a female possesses 25 sensilla, and each sensillum has two response states ("on" if contacted and "off" if not contacted), then the number of unique tactile patterns that the female could distinguish is $2^{25} = 3.4 \times 10^7$. A female that possesses just one additional sensillum would be able to distinguish among roughly twice as many patterns ($2^{26} = 6.7 \times 10^7$). Should individual sensilla respond to quantitative variation in touch (rather than a binary response), this would dramatically increase the number of response states and therefore further enhance tactile acuity (Gaffin and Brayfield 2017). Female damselfly thoracic sensilla thus present an external, quantifiable phenotype to investigate the mechanistic basis of tactile stimuli and female mating decisions.

The North American damselfly genus *Enallagma* includes several recently diverged species that often co-occur in the same habitats (Johnson and Crowley 1980; McPeek 1998), and do not engage in premating courtship (Fincke et al. 2007; Barnard et al. 2017) or use chemical cues for mate selection (Rebora et al. 2018). A female's first opportunity to assess a potential mate occurs when the male uses his terminal appendages to grasp the mesostigmal plates on the female's thorax to form tandem, the premating position. The males' superior appendages (cerci) have species-specific morphologies, and differences in genital morphology are the primary cause of RI in this genus (Paulson 1974; Barnard et al. 2017). Two species, *E. anna* and *E. carunculatum*, occasionally hybridize in nature to produce males and females with morphologies that are intermediate to each of the pure species (Donnelly 2008; Johnson 2009; Barnard et al. 2017). Females of both pure species discriminate strongly against both heterospecific and interspecific hybrid males that take them in tandem, which shows that not only can *E. anna* and *E. carunculatum* females detect large differences in male cercus morphologies, but also more subtle differences such as those between conspecific and hybrid males (Barnard et al. 2017).

Because it appears that mesostigmal sensilla are used to mediate species recognition, they might be expected to show signs of reproductive character displacement (RCD) in regions where species co-occur (Brown and Wilson 1956; Howard 1993; Pfennig and Pfennig 2009). RCD can evolve via direct selection on adult prezygotic phenotypes or via reinforcement, in which direct selection against

interspecific hybrids gives rise to selection for enhanced premating isolation between species (Dobzhansky 1937). *Enallagma anna* and *E. carunculatum* can interbreed, but these species produce hybrids with significantly reduced fitness (Barnard et al. 2017). This suggests that species-specific sensilla phenotypes might show patterns consistent with RCD in regions of sympatry, where females are known to experience frequent mating attempts from heterospecific males (Paulson 1974; Fincke et al. 2007; Barnard et al. 2017). Here, we test the hypothesis that variation in female sensilla phenotypes supports a function in species recognition. We test this hypothesis by quantifying sensilla number, density, and location phenotypes on the mesostigmal plates of a large set of *E. anna* and *E. carunculatum* females from multiple populations across the western United States and comparing phenotypes of each pure species from sympatric and allopatric populations to identify patterns consistent with RCD.

Methods

Population sampling

We measured the sensilla traits of 29 *E. anna* females across 13 populations, and 74 *E. carunculatum* females across 19 populations (Figure 13, Table 3). We classified each population as either allopatric, locally allopatric, or sympatric. Sympatric populations are those where *E. anna* and *E. carunculatum* co-occur temporally as well as spatially. Because *E. anna*'s geographic range falls completely within *E. carunculatum*'s range, only *E. carunculatum* has completely allopatric

populations. We designated populations that exist at sites within the area of range overlap, but where only one species is known to occur, as locally allopatric. Some specimens were collected as early as 1945, but the majority of samples (82 of 103) we studied were collected between 2012 and 2016.

Trait imaging and quantification

We photographed each damselfly using a Nikon D5100 camera (16.2 MP; Nikon Corporation, Tokyo, Japan). We dissected the ventral thoracic cuticle from each female using forceps and imaged the mesostigmal plates using scanning electron microscopy. Specimens were mounted on aluminum stubs with carbon tape, sputter-coated with gold-palladium, and imaged at 200X magnification and 3kV using a Zeiss NEON scanning electron microscope.

To avoid any potential bias during measurements, we blind-coded image files before measuring traits. We measured abdomen length (abdominal segments 1-10, excluding terminal appendages) on the full-body photos as a proxy for body size using the segmented line tool in ImageJ (Abramoff et al. 2004). We quantified sensilla traits on the right mesostigmal plate of each female damselfly unless the right plate was dirty or damaged, in which case we quantified the left plate. Sensilla counts on a subset of 57 females showed that left plate and right plate sensilla counts are highly correlated (r = 0.85). In cases where we quantified the left plate, we flipped the image horizontally, so it was in the same orientation as a right plate. We standardized the

position of the mesostigmal plate in each image by cropping and rotating so that the lower medial corner of the plate was in line with the lower left corner of each image. We counted sensilla and obtained their *x* and *y* coordinates in ImageJ using the multi-point selection tool. We traced an outline around the plate image, excluding the lateral carina (Figure 14), using a Wacom Cintiq 12WX tablet and stylus (Wacom, Saitama, Japan) and the freehand selection tool in ImageJ. This procedure provided *x* and *y* coordinates that describe the plate outline. We performed all measurements twice for each specimen. Measurements across the two technical replicates were highly correlated ($r_{abdomen}$ = 0.96, n = 155; r_{count} = 0.97, n = 183; $r_{plate\ area}$ = 0.98, n = 157), so we used the mean trait values of the two replicates in subsequent analyses.

Sensilla trait analyses

We conducted all morphometric and statistical analyses using R v. 3.4.1 (R Core Team 2015). We used the plate outline coordinates to calculate each plate's two-dimensional area.

To calculate the area of the sensilla-covered region of each plate, we generated a polygon connecting the coordinates of the outermost sensilla and calculated the area within this outline. We determined the proportion of each plate that is covered by sensilla by dividing the sensilla area by total plate area. We calculated sensilla density in two ways. First, we divided sensilla number by the area of the sensilla-covered region. This measures the number of sensilla that occur in a particular area but does

not capture the relative arrangement of sensilla within that area. Second, we computed the nearest neighbor distances among all sensilla within each plate based on their *x* and *y* coordinates and then calculated the mean and median nearest neighbor distances between the sensilla for each female. Nearest neighbor mean and median distances were highly correlated ($r_{E.\ carunculatum}$ = 0.83; $r_{E.\ anna}$ = 0.88), so we report only the analyses using the mean values.

To determine whether larger females possess more sensilla, we regressed sensilla number against abdomen length. We found no significant relationship between these traits in either species (*E. anna*: R^2_{adj} = -0.02, $F_{1,43}$ = 0.13, P = 0.73; *E. carunculatum*: R^2_{adj} = 0.005, $F_{1,65}$ = 1.35, P = 0.25). We thus present the results that compare sensilla counts without correcting for differences in body size.

Sensilla spatial analyses

To quantify sensilla distributions within each plate, we generated kernel density estimates (KDEs) for populations with at least four sampled individuals (two *E. anna* and six *E. carunculatum* populations) using the R package ks (Duong 2016). First, we randomly selected one of the two replicate sets of sensilla and plate outline coordinates for each female. To prepare the coordinate data for KDE analyses, we concatenated the sensilla and plate coordinates for each female and adjusted all plate outlines to have an area of one. This standardized each set of sensilla coordinates for size while maintaining their relative positions within each plate. Next, we translated

each set of coordinates to place the origin of the coordinate system at the plate outline's centroid. We concatenated sensilla coordinates for all females sampled within each population to compute a representative KDE for each population.

Within each species, we conducted pairwise tests to compare each population's KDE against every other population using the function kde.test() with the default settings. This test returns a *P*-value that reflects the probability of generating the two sets of from the same distribution of points. Because we performed multiple pairwise tests among *E. carunculatum* populations, we adjusted the resulting *P*-values using the false discovery rate (Benjamini and Hochberg 1995).

We generated an average plate outline for each population on which to visualize the KDEs. The total number of coordinates that describe each plate outline varied among females, ranging from 647-1078 for *E. anna* and 688-1028 for *E. carunculatum*. We standardized the number of coordinates representing each plate by retaining the points for each of the upper and lower medial corners and randomly sampled 198 points in between. We then treated each of these 200 points as landmarks (the corners represented fixed landmarks and the remaining points were designated as sliding semilandmarks) and used the R package geomorph (Adams and Otarola-Castillo 2013) to perform general Procrustes analysis (Rohlf 1999) and obtain an average two-dimensional plate shape for each population.

Statistical analyses

Some populations were well-sampled and other populations were represented by a single female (Table 3). To avoid psedoreplication, for each population with N > 1, our analyses used population means of trait values, so that each population was represented by a single measurement. We arcsin transformed proportion data prior to analysis. We pooled data for locally allopatric and fully allopatric *E. carunculatum* after *t*-tests showed that these groups did not significantly differ with respect to sensilla number ($t_{2.7}$ = 0.80, P = 0.49), sensilla density ($t_{9.2}$ = -1.62, P = 0.13), or the proportion of the plate that contained sensilla (t_{10} = 0.06, P = 0.95). To compare traits between sympatric and allopatric populations of each species, we used *t*-tests or Wilcoxon rank sum tests. We combined data for the two locally allopatric *E. carunculatum* populations with the data from completely allopatric populations, after determining that these data were similar enough to pool (sensilla number: $t_{2.1}$ = -0.91, P = 0.46; proportion plate with sensilla: t_{11} = -1.24, P = 0.24; sensilla density: $t_{5.8}$ = 0.51, P = 0.63). To understand the relationships between sensilla number, sensilla density, and the area of the plate occupied by sensilla, we performed linear regressions between pairs of these traits.

Results

E. anna and *E. carunculatum* females possess distinct sensilla traits

Enallagma anna females possessed significantly more sensilla per plate ($\bar{x}$ = 46.2 $\pm$ 1.4) than *E. carunculatum* females ($\bar{x}$ = 28.7 $\pm$ 0.6; $t_{19.4}$ = 7.37, $P = 4.9 \times 10^{-7}$;

Figure 15A). *Enallagma anna* females also had sensilla distributed over a larger proportion of each plate ($W = 240$, $P = 2.6 \times 10^{-7}$; Figure 15B), and larger mean distances between sensilla ($t_{30} = 5.2$, $P = 1.3 \times 10^{-5}$; Figure 15C), which made *E. anna*'s overall sensilla distributions less dense than *E. carunculatum*'s ($W = 239.5$, $P = 9.2.\times 10^{-6}$; Figure 15D). The sensilla occurred in different locations on the mesostigmal plates of each species: they were more medial in *E. anna* and more lateral in *E. carunculatum* (Figures 3, S2).

Both species showed a strong positive relationship between sensilla number and the absolute area of the plate occupied by sensilla (*E. anna*: $R^2_{adj} = 0.33$, $F_{1,27} = 14.71$, $P < 0.0007$; *E. carunculatum*: $R^2_{adj} = 0.33$, $F_{1,72} = 37.68$, $P = 4.1 \times 10^{-8}$). Consistent with this result, linear regressions also revealed that females with more sensilla also had a larger proportion of the plate occupied by sensilla (*E. anna*: $R^2_{adj} = 0.26$, $F_{1, 27} = 10.65$, $P = 0.003$*; E. carunculatum:* $R^2_{adj} = 0.20$, $F_{1, 65} = 18.93$, $P = 4.4 \times 10^{-5}$). Females with more sensilla had smaller mean distances between neighboring sensilla (*E. anna*: $R^2_{adj} = 0.11$, $F_{1, 27}$ 4.34, $P = 0.046$; *E. carunculatum*: $R^2_{adj} = 0.09$, $F_{1,72} = 3.80$, $P = 0.01$). Overall, these results showed that a greater number of sensilla was more strongly associated with a sensilla distribution that covers a larger area of the mesostigmal plate rather a greater concentration sensilla within in a smaller area.

***E. carunculatum* sensilla traits do not show a strong pattern of reproductive character displacement**

We made several non-mutually exclusive predictions expected under RCD for sensilla traits in sympatric populations relative to allopatric populations. In particular, we predicted to observe at least one of the following phenotypic differences in sympatric females relative to allopatric females: (1) more numerous sensilla (2) denser sensilla, (3) sensilla concentrated in different regions of the mesostigmal plates. We did not find significant differences in any of these traits between sympatric and locally allopatric *E. anna* females (Table 4). However, because our *E. anna* samples included only four females from three locally allopatric populations, we could not perform a robust comparison of *E. anna* sensilla traits between populations that do, or do not encounter *E. carunculatum*. We thus focus our analysis on comparisons between sympatric and allopatric *E. carunculatum* populations, for which we had larger sample sizes.

Sympatric *E. carunculatum* populations did not differ significantly from allopatric populations in sensilla number ($t_{16.3} = 0.98$, $P = 0.35$), proportion of the mesostigmal plate covered by sensilla ($t_{16.8} = 1.33$, $P = 0.20$), or sensilla density (overall density: $t_{9.7} = -0.26$, $P = 0.80$; mean distance between sensilla: $t_{18} = -1.31$, $P = 0.21$). In addition to divergence of mean trait values, RCD can also result in reduced trait variance in sympatry without affecting the mean (Pfennig and Pfennig 2009). Sympatric *E. carunculatum* populations displayed less variance in both sensilla number (Figure 15A) and the proportion of the plate covered by sensilla (Figure 15B). However, these trends were not statistically significant (sensilla number with locally

allopatric outlier removed: Bartlett's $K^2_1 = 0.75$, $P = 0.39$; proportion of plate covered by sensilla: Bartlett's $K^2_1 = 2.5$, $P = 0.11$). KDE comparisons also did not reveal significant differences in sensilla distributions between sympatric and allopatric *E. carunculatum* populations (Table 5). However, the analysis revealed significant differences in sensilla distributions between several pairs of populations that are not sympatric with *E. anna* (Figure 16E). This result is consistent with those described above that indicated higher variance in sensilla traits among allopatric populations compared to sympatric populations.

Interestingly, although mean trait values did not differ significantly between sympatric and allopatric populations, sensilla traits displayed considerable variation within the populations we sampled. For example, within a single population, a particular female might have twice as many sensilla than another female (Figure 17). This pattern was also observed in the *E. anna* populations we studied.

Discussion

Enallagma anna and *E. carunculatum* females possessed different numbers of sensilla in species-specific distributions on their mesostigmal plates. This result supports the idea that receptors that receive male stimuli will occur in patterns that correspond to the male organs during contact (Eberhard 2010). An association between male morphology and female sensilla has been described for African *Enallagma* species (Robertson and Paterson 1982), and our results show a similar

pattern. *Enallagma anna* male cerci are considerably larger than *E. carunculatum* cerci, and the observation that *E. anna* females had a larger number of sensilla compared to *E. carunculatum* females is consistent with the difference in species-specific male genital morphology.

When species make secondary contact after initial divergence in allopatry, the possible outcomes are increased species divergence (*e.g*., Sætre et al. 1997; Noor 2000; Naisbit et al. 2001; Yukilevich 2012; Dyer et al. 2014), decreased divergence (*e.g*., Ritchie et al. 1989; Shurtliff et al. 2013; Yang et al. 2016), one species goes locally extinct due to reproductive exclusion (Hochkirch et al. 2007, Groning and Hochkirch 2008), or no change in either direction (Abbott et al. 2013). Because *E. anna* and *E. carunculatum* produce reproductively disadvantaged hybrids (Barnard et al. 2017), selection is expected to favor increased premating isolation. Within each species, we predicted that female sensilla traits would show character displacement in sympatric populations, which could indicate a shift in female preferences to avoid mating with heterospecifics. Contrary to this prediction, *E. carunculatum* sympatric and allopatric populations were not significantly different in mean sensilla trait values (Figure 15) or sensilla density distributions (Figure 16E). Although we observed a trend toward more sensilla in sympatric *E. anna* populations relative to allopatric populations (Figure 15A), it is difficult to conduct a robust comparison for this species because (1) *E. anna*'s entire geographic range overlaps with *E. carunculatum*'s range and (2) *E. anna* are often relatively rare (Acorn 2004; A. Barnard, personal obs.). It was therefore difficult

to collect sufficient *E. anna* samples from populations that do not co-occur with *E. carunculatum*. We do, however, expect a stronger pattern of RCD in sympatric *E. anna* females because *E. carunculatum* males can take them in tandem relatively easily, whereas *E. anna* males are typically unsuccessful at taking *E. carunculatum* females in tandem (Barnard et al. 2017). This means that *E. anna* females may have more opportunities for mating mistakes than *E. carunculatum* females, which can result in stronger asymmetric RCD (Lemmon 2009; Pfennig and Pfennig 2009).

There are at least four potential explanations for the absence of RCD in the form of significant differences in the sensilla traits we measured between sympatric and allopatric populations of *E. carunculatum*. First, species-specific sensilla distributions may be sufficiently different to allow females to recognize when they are taken in tandem by heterospecific or conspecific males. If this is true, small degrees of variation within the overall species pattern among females might not affect females' species-recognition abilities. RCD is most easily facilitated when the trait under selection already differs between species (Pfennig and Pfennig 2009). However, these traits may have already diverged enough sufficiently to preclude strong selection for further divergence.

Second, it is possible that the external sensilla phenotypes we measured are not representative of proximate female sensory traits, and the important variation lies deeper within the female nervous system. For example, individual sensilla might differ in response rate or ability to distinguish different levels of pressure applied by the

cerci, and grasping pressure might differ between males of each species. The direction of mechanosensor deflection is also important for stimulus detection (Keil 1997), and different species' cercus morphologies may contact sensilla from different angles. Female mate preferences may also be influenced by male exposure and sexual experience (Svensson et al. 2014).

Third, the thoracic sensilla may not be a target of strong selection. For example, earlier acting forms of RI may prevent most heterospecific interactions in the sympatric populations we sampled. In one region where *E. anna* and *E. carunculatum* co-occur, habitat and temporal isolation were close to zero (Barnard et al. 2017), but the strength of these isolating barriers may vary geographically.

Finally, although we did not detect a statistically significant difference between group means, the small differences we observed may still have biological relevance. If gaining just one additional mechanosensor can (at least) double a female's tactile discriminatory power (Gaffin and Brayfield 2017), then females in a population with a seemingly minor upward shift in sensilla number could gain a remarkable increase in their ability to detect and avoid mating with heterospecifics. Similarly, it is difficult to determine the features of sensilla density distributions that may influence female preference solely by conducting statistical tests between KDEs. The human eye can visually detect differences in the KDE plots shown in Figure 16, and it is thus possible that these spatial differences reflect salient variation in the way females might receive tactile stimuli.

These possible explanations highlight the interesting avenues that female damselfly sensilla provide for investigating how females evaluate male tactile signals to make mating decisions. The ability to quantify the number and locations of female mechanoreceptors in a region contacted by male reproductive structures complements our understanding of patterns of variation in male morphologies (McPeek et al. 2008; McPeek et al. 2009; McPeek et al. 2011; Barnard et al. 2017). Females of both species display substantial intrapopulation variation in sensilla traits (Figure 17) and this variation may play a role in sexual selection and female preferences within species. Behavioral studies will be crucial to link mechanoreceptor phenotypes to female mating decisions and clarify how sensilla traits influence both species recognition and sexual selection. For example, do females with more sensilla make fewer mating mistakes than females with fewer sensilla (Lemmon 2009)? Another outstanding question of this system is how the cerci stimulate individual sensilla during tandem. This might be determined by flash-freezing male-female tandem pairs and using micro-CT scanning to understand how the male and female structures interact, similar to a recent approach used in seed beetles (Dougherty and Simmons 2017). Once we understand how cerci contact the sensilla, functional tests of sensilla electrophysiology could reveal how individual sensilla respond to stimulation and indicate whether certain sensilla make greater contributions to reproductive decision-making than others.

Female preference can drive sexual selection, promote trait divergence, and cause RI between species (Ritchie 1996). A longstanding presumption in the literature on genital evolution and speciation has been that female reproductive morphologies are less variant or species-specific than male genitalia (Shapiro and Porter 1989). However, recent studies of variation in female reproductive structures suggest that variation does exist among individuals and species (Ah-King et al. 2014), and our data support the need to look beyond the visible external morphologies. When male genital morphologies are obviously divergent, but female morphologies are not, females may possess important variation at neurophysiological levels that affects how they evaluate male tactile signals, similar to the way females evaluate signals in other sensory modalities.

Chapter 2 - Tables

Table 3. Sampling sites for *E. anna* and *E. carunculatum* sensilla analyses

Type	Site (site number)	Species	Year collected	N	Source
Sympatric	Big Spring, UT (1)	*E. anna*	2016	10	AB
		E. carunculatum		4	
	Big Sandy Creek, MT (2)	*E. carunculatum*	2015	1	AB
	Creston, MT (3)	*E. anna*	1972	1	BM
	Dry Sheep Creek, NE (4)	*E. anna*	2012	1	BM
	Fish Springs Run, CA (5)	*E. anna*	1998	2	BM
	Grace Coolidge Creek, SD (6)	*E. anna*	1969	1	BM
	Horseshoe Springs, UT (7)	*E. anna*	2016	1	AB
		E. carunculatum		1	
	Long Valley Creek, CA (8)	*E. anna*	1973	5	DP
	Murray Creek, NV (9)	*E. anna*	2001	1	
	Malad River, UT (10)	*E. carunculatum*	1983	2	BM
	Niwot Ditch, CO (11)	*E. anna*	2015	2	AB
		E. carunculatum		1	
	Pondera Coulee, MT (12)	*E. anna*	2015	1	AB
		E. carunculatum		1	
Locally allopatric	Beaver Creek, WY (13)	*E. anna*	2015	1	AB
	Indian Road Camp, MT (14)	*E. carunculatum*	2015	4	AB
	Jackson, WY (15)	*E. anna*	1971	2	BM
	Muddy Creek, MT (16)	*E. anna*	2015	1	AB
	Strawberry River, UT (17)	*E. carunculatum*	2016	1	AB
	West Greenbelt, CO (18)	*E. carunculatum*	2014	9	AB
Allopatric	Bull Lake, MT (19)	*E. carunculatum*	2015	1	AB
	Crab Creek, WA (20)	*E. carunculatum*	2016	20	DP
	Clear Lake, IN (21)	*E. carunculatum*	1945	1	BM
	Columbia River, WA (22)	*E. carunculatum*	1952	2	BM
	Douglas Lake, MI (23)	*E. carunculatum*	2016	17	OF
	Flathead River, MT (24)	*E. carunculatum*	2015	4	AB
	Home Lake, CO (25)	*E. carunculatum*	2015	1	AB
	Little Lake, CA (26)	*E. carunculatum*	1967	1	DP
	Drumond Island, MI (27)	*E. carunculatum*	2002	1	BM
	Snake River, ID (28)	*E. carunculatum*	1983	2	BM

N refers to the number of females that were imaged and measured for this study.
Sources: A. Barnard (AB), Ola Fincke (OF), Bill Mauffray (BM), and Dennis Paulson (DP).

Table 4. Results of *E. anna* sensilla trait comparisons in allopatry and sympatry

Trait	Mean ± SE		*t*	*P*
	Allopatry (N = 3)	Sympatry (N = 10)		
Sensilla number	39.8 ± 3.8	48.5 ± 2.3	-1.93	0.13
Proportion plate containing sensilla	0.39 ± 0.04	0.41 ± 0.09	-0.25	0.82
Sensilla density (sensilla/mm^2)	1.5 ± 0.2	1.6 ± 0.1	-0.43	0.70
Mean distance (μm) between sensilla pairs	20.0 ± 1.0	19.3 ± 0.5	0.64	0.53

N = number of populations.

Table 5. E. carunculatum sensilla kernel density estimate comparisons

	BS	CC	DL	FR	GB	N	Population type
BS	1					4	sympatric
CC		1				20	allopatric
DL	0.263	**$2.53e^{-10}$**	1			17	allopatric
FR	1	**0.0103**	0.263	1		4	allopatric
GB	1	0.0625	0.384	0.502	1	4	Locally allopatric
IR	1	1	**0.0103**	0.0625	0.3115	4	Locally allopatric

False discovery rate-adjusted *P*-values are reported. Bold values indicate $P < 0.05$. N indicates the number of females whose sensilla coordinates were used to calculate KDE. Population abbreviations: Big Springs, UT (BS), Crab Creek, WA (CC), Douglas Lake, MI (DL), Flathead River, MT (FR), West Greenbelt, CO (GB), Indian River, MT (IR)

Chapter 2 – Figure legends

Figure 13. Sampling sites and species ranges. *Enallagma anna*'s geographic range (red) occurs within *E. carunculatum*'s geographic range (orange). Names of sites associated with each number are described in Table 3. Symbol color indicates the species sampled and symbol shape indicates the population type. (Species ranges adapted from Johnson 2009; Paulson 2009, 2011).

Figure 14. Obtaining XY coordinates of plate outline and individual sensilla from SEM images. The orange line shows how we traced the boundaries of the mesostigmal plate. Yellow dots indicate individual sensilla. The yellow line around them shows the polygon generated by connecting the outermost sensilla.

Figure 15. *E. anna* and *E. carunculatum* sensilla traits by population type. (A) The number of sensilla on one mesostigmal plate. **(B)** Proportion of the plate that contains sensilla. **(C)** Mean nearest neighbor distances between sensilla. **(D)** Sensilla density in the region of the plate that contains sensilla. Within each panel, each open circle represents the mean of one population. Boxplots show the interquartile range. The line within the box shows the median and whiskers extend to the most extreme observation within 1.5 times the interquartile range.

Figure 16. Sensilla locations. (A) White box indicates the location of right mesostigmal

plate on the thorax. **(B)** Ultrastructural details of individual sensilla. Scale bar represents 10 μm. **(C, D)** Scanning electron micrographs show the locations of sensilla (yellow) on the mesostigmal plates of *E. anna* (C) and *E. carunculatum* (D). Scale bars represent 100 μm. **(E, F)** Population kernel density estimates for *E. carunculatum* (E) and *E. anna* (F) sensilla. The shading indicates different regions of sensilla density: red represents the 75-99th percentile, orange represents the 50-74th percentile of sensilla density, and yellow represents the 25th-49th percentile. Each outline represents the average mesostigmal plate shape for the population. Asterisks indicate *E. carunculatum* populations whose KDEs were determined to be significantly different (* indicates $P < 0.05$, *** $P < 0.001$).

Figure 17. Individual trait values for sensilla number (A), sensilla density (B), and proportion of plate containing sensilla (C). Each symbol represents a single female, separated by population along the y-axis. Horizontal lines indicate the mean value for each population type (completely allopatric, locally allopatric, or sympatric), calculated from population means. Populations are described in Table 3.

Figure 13. Sampling sites and species ranges

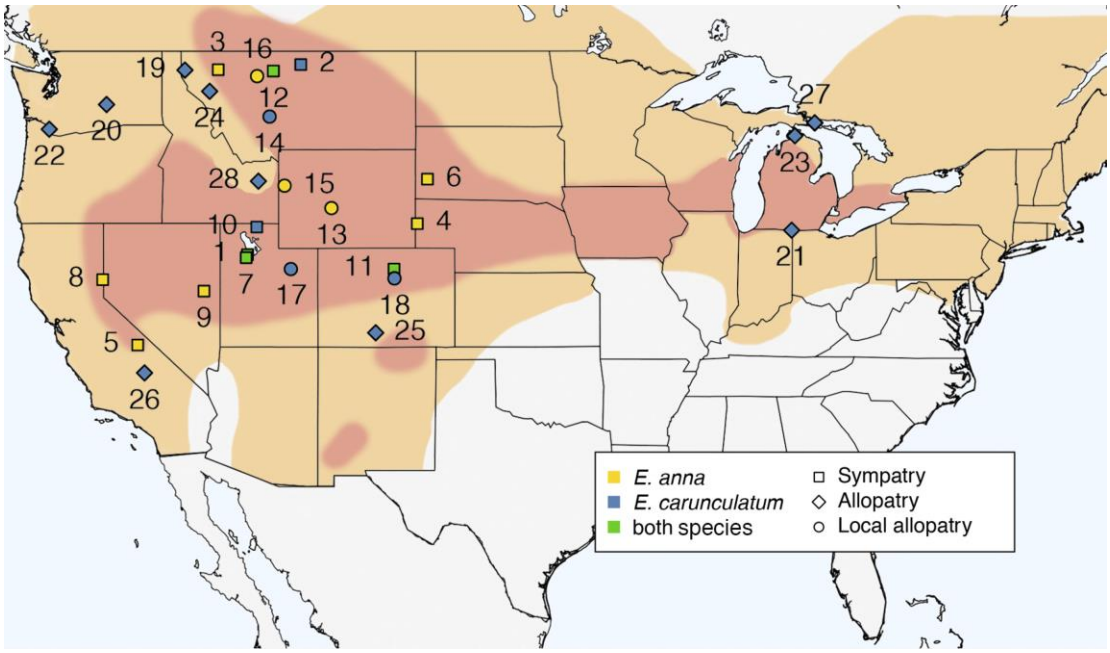

Figure 14. Obtaining XY coordinates of plate outline and individual sensilla from SEM images

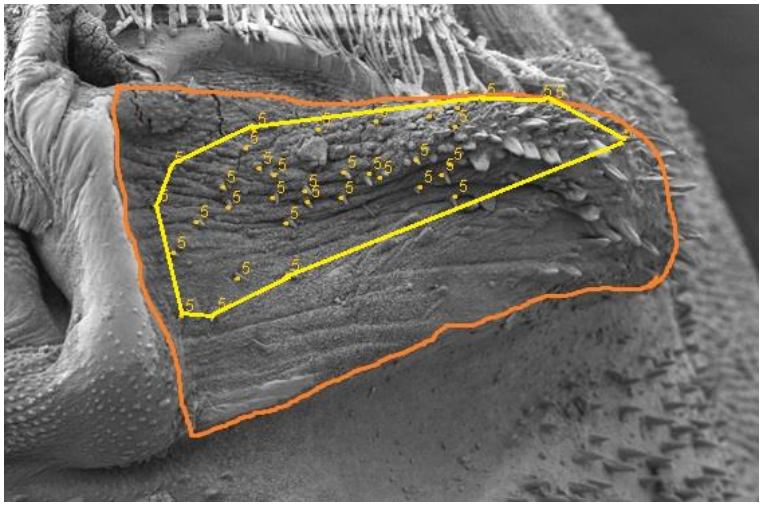

Figure 15. E. anna and E. carunculatum sensilla traits by population type

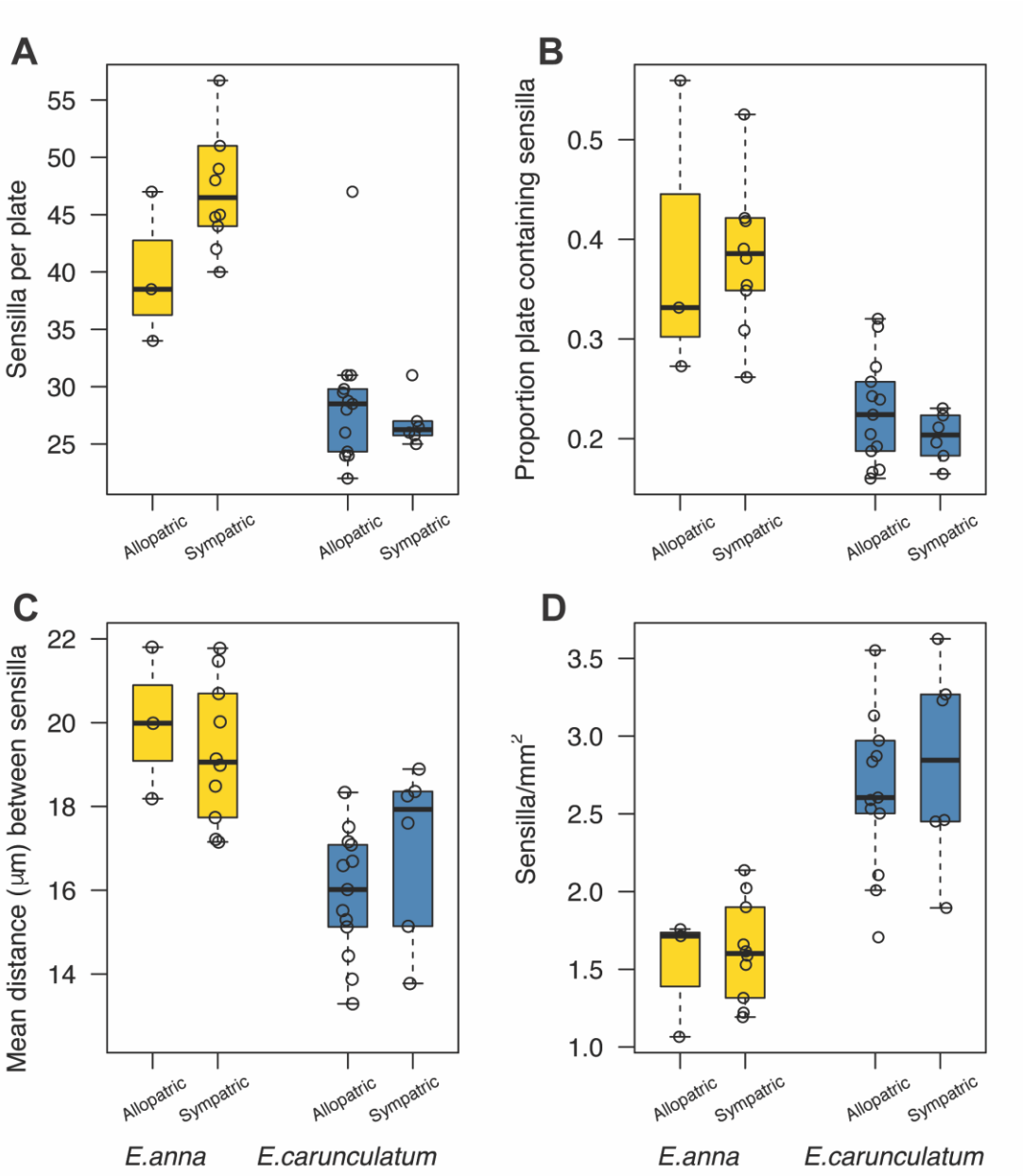

Figure 16. Sensilla locations

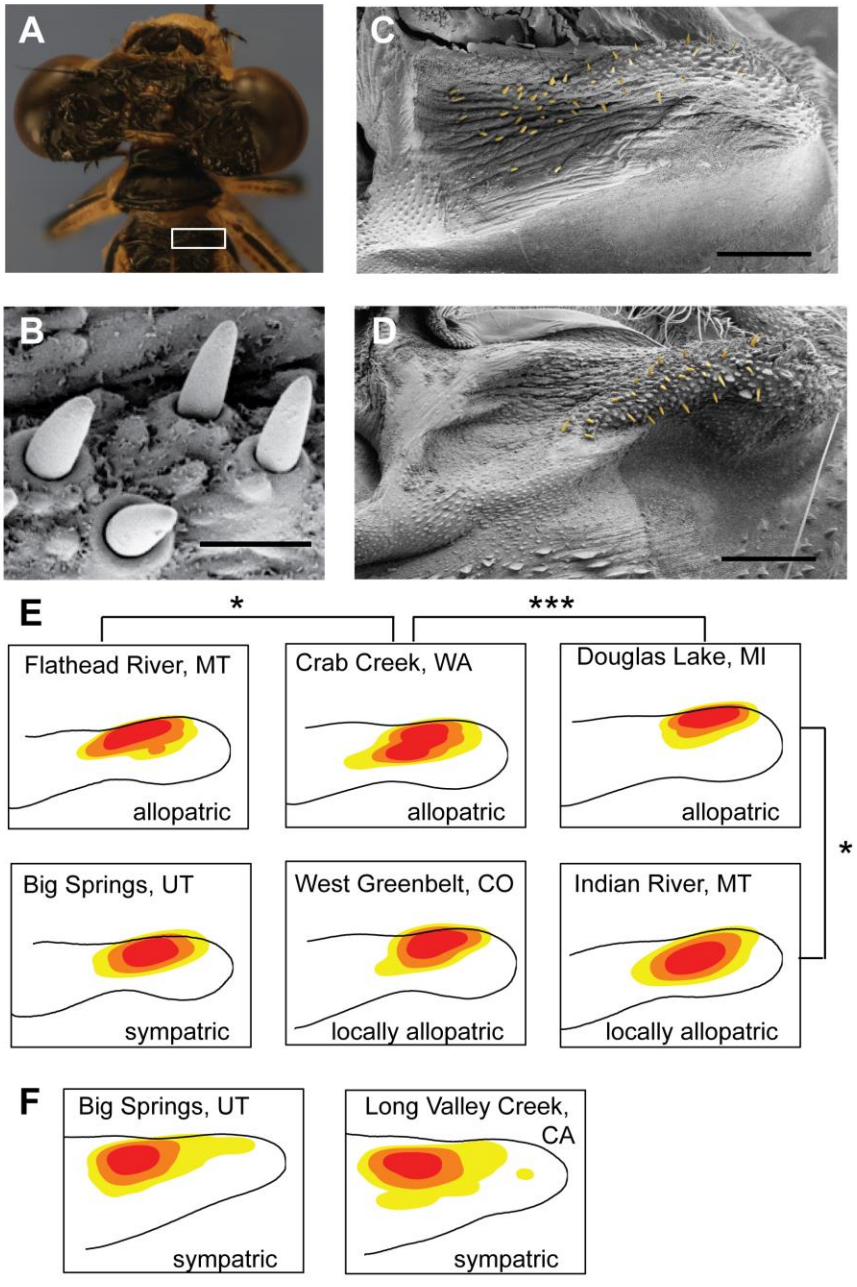

Figure 17. Individual trait values

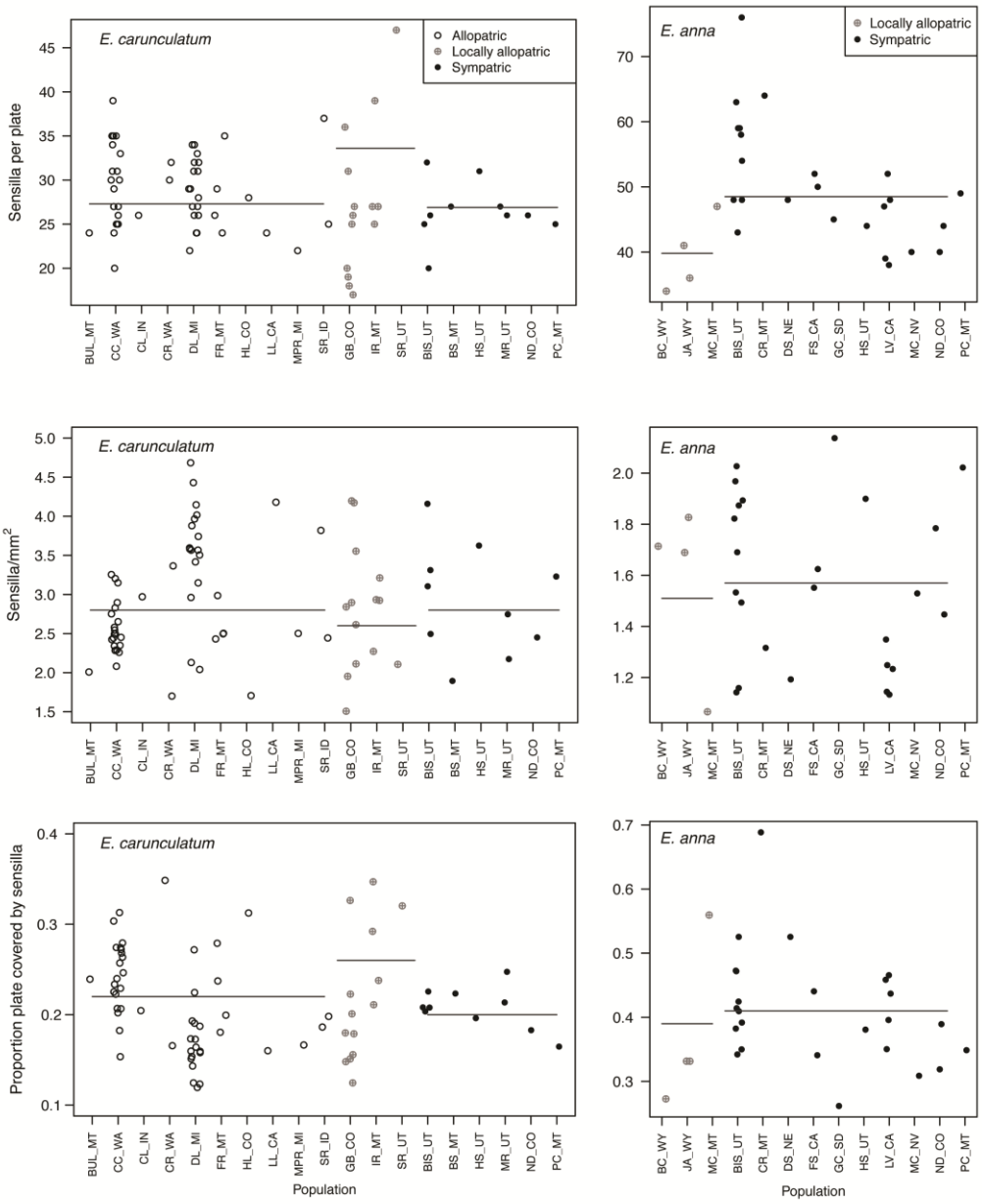

CHAPTER 3: Using RADseq to characterize gene flow and genomic divergence between two hybridizing damselfly species

Abstract

As species diverge, their genomes accumulate differences. Persistent gene flow between species as they diverge can homogenize some regions of the genome and make highly differentiated regions stand out in contrast. Some of these highly divergent loci are predicted to harbor genes responsible for reproductive isolation. However, common patterns of genome diversification at this stage remain poorly understood, such as how these divergent loci are arranged across the genome and whether these loci commonly contribute to reproductive isolation or are simply less subject to recombination. Here, I characterized patterns of gene flow and genomic divergence between *E. anna* and *E. carunculatum*, a pair of hybridizing damselfly species that shared a common ancestor within the past 250,000 years. I performed a *de novo* assembly of a set of genome-wide variant loci in a large collection of samples from 9 populations spanning a hybrid zone. I quantified patterns of introgression between *E. anna* and *E. carunculatum* in nature, identified loci with elevated divergence between the two species, and tested for associations between genomic ancestry and species-specific phenotypic variation in male and female hybrids. My results revealed that *E. anna* and *E. carunculatum* genomes are largely undifferentiated, which is consistent with ongoing gene flow but also with a relatively short divergence time and incomplete lineage sorting of shared ancestral polymorphism. Additionally, the results show that the proportion of the genome inherited from *E. anna* is a strong predictor of quantitative variation in reproductive

structure morphology in most hybrid individuals. Finally, the results demonstrate the need for higher-resolution sequencing to identify loci strongly associated with variation in male and female reproductive structure morphologies.

Introduction

Hybrid zones have historically been studied to understand speciation dynamics (Barton and Hewitt 1989; Harrison 1990; Harrison 1993; Matute 2010; Good et al. 2015; Payseur and Rieseberg 2016). Gene flow between species provides opportunities to dissect the evolution of individual reproductive isolating barriers (e.g., McMillan et al. 1997; Kay 2006; Sánchez-Guillén et al. 2012), understand the ecological and evolutionary forces that shape reproductive isolation (e.g., Rand and Harrison 1989; Via et al. 2000; Nosil et al. 2005; Pfennig et al. 2007), discover genes that are important in local adaptation (e.g., Payseur 2010; Harrison and Larson 2016), and reveal patterns of how whole genomes differentiate during different stages of the speciation process (e.g., Jiggins et al. 2001; Roux et al. 2016).

It is now recognized that speciation can proceed despite ongoing gene flow between diverging lineages and that different regions of the genome diverge between species at different rates (Harrison 1990; Via 2012; Martin et al. 2013; Larson et al. 2014). When two species have diverged relatively recently from a common ancestor, they are likely to share many loci that neither cause reproductive isolation (RI) directly

nor are physically linked to loci that cause RI. These neutral loci are likely to be freely exchanged between species, giving rise to genomes that are largely homogeneous between species. Within this undifferentiated background, genomes of separate species should contain small regions that display high differentiation (Barton and Bengtsson 1986; Payseur 2010; Yeaman and Whitlock 2011). Such divergent sections of the genome may experience lower gene flow relative to other regions, either due to reduced recombination or selection, which may or may not be associated with RI.

Genomic analyses of hybrid zones have revealed certain regions of the genome that commonly play a role in RI and experience reduced levels of introgression. For example, genes associated with hybrid sterility and hybrid inviability are often concentrated on the X (or Z) chromosome (Masly and Presgraves 2007), and genes on these sex chromosomes often experience less gene flow than autosomal genes (e.g., Payseur et al. 2004; Macholán et al. 2007; Garrigan et al. 2012; Carneiro et al. 2013; Maroja et al. 2015). However, although several decades of research have been dedicated to understanding individual traits and genes responsible for RI and the selective forces that act on them (e.g. Wittbrodt et al. 1989; Ting et al. 1998; Presgraves et al. 2003; Orr et al. 2004; Brideau et al. 2006; Masly et al. 2006; Phadnis and Orr 2009), we still lack a comprehensive understanding of how highly differentiated loci are positioned within the genome, how genomes diverge as mechanisms of RI build up over time (Nosil and Feder 2012), or how the relationships

between and placement of divergent loci influence the speciation process (Feder et al. 2012).

One approach to begin to answer these questions is to identify loci associated with traits known to cause RI and determine how resistant to gene flow these loci are compared to other genomic regions. For example, multiple species of interbreeding *Heliconius* butterfly initially diverged primarily in genomic regions associated with wing patterning (Nadeau et al. 2012; Kronforst et al. 2013), a set of traits known to cause premating isolation (e.g., Jiggins et al. 2001; Kronforst et al. 2006; Chamberlain et al. 2009). Similarly, in *Lycaeides* butterflies, a set of loci associated with either male genital morphology or female oviposition preference showed exceptionally high levels of genomic differentiation between *L. idas* and *L. melissa*, which suggests that these traits reduce hybrid fitness and are therefore less subject to gene flow than other regions (Gompert et al. 2012).

Loci associated with divergent genital traits may be expected to show high levels of differentiation between species, especially among insects. Many insects are characterized by striking morphological differences in the male genitalia among closely-related species (Dufour 1844; Eberhard 1985; Shapiro and Porter 1989). Sexual selection is thought to be the primary force driving rapid genital divergence, but how strongly this morphological divergence contributes to speciation is not well understood. To help understand the connections between genital evolution, genome differentiation, and RI, I estimated levels of gene flow between *Enallagma anna* and *E.*

carunculatum, two damselfly species that diverged within the past 250,000 years (McPeek et al. 2008) and possess conspicuously divergent male and female reproductive structures (McPeek et al. 2009; Barnard et al. 2017).

Specifically, the cerci (the upper terminal abdominal appendages on the male) and mesostigmal plates (structures on the female thorax that are clasped during mating by the male appendages) have distinctive species-specific morphologies, while many *Enallagma* species share similar overall morphologies and ecological niche use (Siepielski et al. 2010). *E. anna* and *E. carunculatum* are commonly sympatric (Paulson 2009) and possess divergent genital morphologies that are the primary cause of premating RI. However, these species can interbreed to produce viable, fertile offspring with intermediate cerci and mesostigmal plate morphologies (Miller and Ivie 1993; Donnelly 2008; Johnson 2009; Barnard et al. 2017). This morphological variation in hybrids, which has been quantified and described elsewhere (Barnard et al. 2017), facilitates dissection of the genetic basis of species-specific male and female morphologies.

Intrinsic postzygotic isolating barriers appear negligible between these species, possibly because they have not had sufficient time since divergence to accumulate genetic incompatibilities that would cause hybrid sterility or inviability (Turgeon et al. 2005; Bourret et al. 2012; Barnard et al. 2017). Because these young species also show no obvious divergence in ecology or non-reproductive morphological traits, I predicted that their genomes would possess small differentiated regions within a relatively

homogeneous background. I further predicted that the most differentiated and least introgressed loci would be those associated with genital morphologies.

To characterize the genetic architecture of morphological divergence between *E. anna* and *E. carunculatum*, I generated a set of genome-wide single nucleotide polymorphisms (SNPs) using restriction-site associated DNA sequencing (RADseq; Etter et al. 2012). I then took advantage of interspecific hybrid genomes to search for loci associated with variation in male and female reproductive structure morphologies. I further identified genomic regions of reduced gene flow and regions with elevated sequence divergence; the former are implicated in RI and the latter are likely targets of directional selection (Gompert and Alex Buerkle 2010; Nadeau et al. 2012). My goal was to test whether loci associated with genital morphological variation comprise the majority of highly differentiated and infrequently exchanged regions between the two focal species. If a large number of loci unrelated to genital morphologies also show low introgression, this could implicate either strong RI that prohibits all but very low levels of gene flow, or additional forces besides genital divergence in speciation, such as ecological factors.

Methods

Population sampling

I sampled damselflies from several Montana populations spanning a known hybrid zone. Most samples came from the Whitefish River, Montana, USA, where *E.*

anna and *E. carunculatum* display strong positive assortative mating based on morphology but occasionally interbreed (Barnard et al. 2017), although the directionality of backcrossing is currently unclear. I reared two consecutive generations of *E. anna, E. carunculatum,* and their hybrids in the lab (methods described in Barnard et al. 2017). Because gene flow between *E. anna* and *E. carunculatum* in Whitefish may complicate the identification of species-diagnostic SNPs, I collected each parental species from three additional sites beyond the known hybrid zone to aid in identifying species-specific alleles (Table 6, Figure 18). Samples were placed in ethanol upon capture and stored this way prior to DNA extraction.

Phenotyping

To quantify morphological differences between hybrids and parental species, I produced high-resolution 3-D digital reconstructions of male cerci and female mesostigmal plates using micro-computed tomography (micro-CT) as described in (Barnard et al. 2017). Briefly, I quantified the 3-D surfaces of male cerci using spherical harmonics (SPHARM; Shen et al. 2009, McPeek et al. 2008). SPHARM is an extension of 2-D Fourier techniques that describes a 3-D shape in terms of the sum of 3-D sines and cosines on a sphere, resulting in a large set of coefficients that reconstruct the shape of the original object. The analysis produced 2,883 coefficients to describe each cercus, which I condensed into the major modes of shape difference using principal

component analysis (PCA). I quantified female plate mesostigma plate shape using 3-D geometric morphometrics (Barnard et al. 2017) and reduced the data using PCA.

Genomic library preparation and sequencing

I prepared genomic sequencing libraries for 134 *E. anna* (from 4 populations) 116 *E. carunculatum* (from 4 populations), and 136 presumed hybrids (all from the Whitefish River site; Table 6, Figure 18). I isolated genomic DNA from each damselfly using Qiagen's Gentra Puregene DNA Tissue Kit (Qiagen Inc., Valencia, CA, USA). I generated reduced complexity genomic sequencing libraries for each sample using restriction site associated DNA sequencing (RADseq; Etter et al. 2011). Briefly, I digested ~1ug of genomic DNA from each individual using the restriction enzyme *BbvCI*, then ligated to double-stranded adapters containing a unique 5-nucleotide sequence to barcode each individual. Each barcode contained at least 2 mismatches from all other barcode sequences to ensure the data could be de-multiplexed after sequencing even with low levels of sequencing error. The DNA for up to 48 individuals with different barcodes was equimolarly pooled, then sheared using a Bioruptor (Diagenode, NJ, USA) to produce fragments with the adapter at one end and a randomly sheared site at the other end. A custom adapter containing an index to identify each pool was ligated at this randomly sheared end and fragments were size-selected between 300 and 600 bp using a MinElute Gel Extraction Kit (Qiagen). Sample placement was randomized during library preparation to prevent potential bias from

location in 96-well plates, gels, or sequencing lanes. I pooled ~150 samples per sequencing lane to allow an estimated 30X mean sequencing coverage per sample. Libraries were sequenced to 150 bp read lengths on three separate lanes of an Illumina HiSeq 3000, which generated ~702 million reads.

Genotyping

I processed the raw reads using Stacks (v1.48) software (Catchen et al. 2011; Catchen et al. 2013), following the protocol outlined in Rochette and Catchen (2017). I first filtered out low-quality reads and those without a correct barcode. Of the original 386 samples, 303 passed the initial quality filtering. These samples possessed a total of ~387 million reads with an average of 16x coverage per individual. I aligned the raw forward reads with each other in a *de novo* assembly using the following parameters: minimum stack depth (m) = 5, minimum distance allowed between stacks (M) =6, maximum distance to align secondary reads to primary stacks (n) = 6, and default values for all other parameters. These parameters were selected based on the optimization procedures described in Paris et al. (2017). I used the *populations* module in Stacks to filter out loci found in fewer than 55% of samples within each population and selected 1 SNP per locus. This filtering resulted in a set of 556 SNPs present in all populations as well as a set of 647 SNPs for only the Whitefish samples. Each of these datasets was used in subsequent analyses.

Measuring genome-wide and per-locus F_{ST}

To quantify population-level genetic differentiation, I used Stacks' *populations* module to calculate genome-wide F_{ST} among all possible population pairs. To identify highly differentiated loci between *E. anna* and *E. carunculatum* – which may potentially be associated with species-specific reproductive structure morphologies – I calculated per-locus F_{ST}, pooling all individuals of each field-caught parental species, regardless of locality.

I conducted a similar analysis using only individuals with phenotypic data from Barnard et al. (2017), to identify loci with elevated differentiation between phenotypic extremes. I assigned each hybrid a morphological hybrid index by dividing them into 5 separate bins based on where they fell along PC1 from the morphometric analyses of cercus or mesostigmal plate shape. Males and females with morphology most similar to *E. carunculatum* received a hybrid index of 1, whereas individuals with morphology most similar to *E. anna* received a hybrid index of 5. I calculated F_{ST} between these extreme individuals within each sex and included parental species with morphological data in the analysis to increase the likelihood of capturing genotypes associated with species-specific morphologies. I then identified loci with significantly high F_{ST} values from each group, based on analyses of molecular variance (AMOVA), Bonferroni-corrected for multiple comparisons.

Genetic ancestry and admixture analyses

To investigate populations' genetic structure and admixture between *E. anna* and *E. carunculatum* in Whitefish, I used *STRUCTURE* v2.3.4 (Pritchard et al. 2000; Falush et al. 2003) to cluster individuals based on their likely ancestry at each locus. I conducted three separate analyses in *STRUCTURE* to analyze different groupings of individuals using the same set of model parameters for each. The first analysis included all field-caught damselflies, grouped by sampling location. The second analysis included field-caught damselflies from only the Whitefish River site. The third analysis used all Whitefish damselflies, including those reared in the lab. The goal of the separate analyses of Whitefish individuals was to compare admixture patterns in nature compared to all known hybrid individuals.

I conducted the *STRUCTURE* analysis using the admixture model with independent allele frequencies and sampling location as a prior. I ran 10 iterations with a 10,000 replicate burn-in followed by 20,000 Markov chain Monte Carlo (MCMC) repetitions. Because morphology and previous phylogenetic analyses indicate that *E. anna* and *E. carunculatum* are two distinct lineages (Turgeon et al. 2005, Callahan and McPeek 2017) and damselflies with intermediate morphologies are hybrids (Barnard et al. 2017) – and because my primary goal was to examine admixture between *E. anna* and *E. carunculatum* – I set the number of genetic clusters (*K*) = 2. However, in the analysis of all sampled populations, I also ran iterations with K ranging from 3 to 9 to reflect the full range of possible genetic clusters (4 populations of each parental species and one group of putative hybrids).

I also examined inheritance patterns across loci in hybrid damselflies using the R package *introgress* (Gompert and Buerkle 2010). The program estimates ancestry of alleles in hybrids based on parental species' allele frequencies to calculate a genome-wide hybrid index, or the proportion of an individual's genome that was inherited from one of the parental species (here, *E. anna*). I used all Whitefish samples (lab and field) to estimate hybrid index values. To determine locus-specific levels of introgression and identify loci that were introgressed less frequently than the background level, I used *introgress* to calculate maximum likelihood estimates of hybrid index at each individual locus, then compare these individual locus estimates to the genome-wide hybrid index. To produce a genomic cline for each locus, I plotted the per-locus hybrid index values against allele frequency at each locus. A steep genomic cline for an individual locus indicates that it is exchanged less frequently than other loci. To allow testing for significantly steep clines, the genomic cline for each locus is evaluated for deviations from a neutral distribution. I ran 1000 permutations to estimate this neutral distribution.

Analysis of association between morphology and genotype

For each hybrid, I compared the admixture proportion estimated in *STRUCTURE* with the hybrid index estimated in *introgress*. To determine whether either of these measures showed a relationship between genotype and phenotype, I conducted linear regressions of cercus and mesostigmal plate PC1 values (described in Barnard et al.

2017) against *STRUCTURE* estimates and conducted Kruskal-Wallis tests to examine relationships between the rarely-introgressed loci and either cercus or mesostigmal plate morphology. Additional PCs captured negligible morphological variance and I therefore did not expect them to show a noticeable relationship with allele frequencies. I also tested for associations between cercus and mesostigmal plate phenotype and genotype in 122 males and 123 females for 130 and 132 loci, respectively, identified as divergent by the AMOVA-F_{ST} analysis, adjusting the significance threshold for multiple tests using Bonferroni correction. Unless otherwise noted, analyses were conducted in R version 3.3.1 (R Core Team 2013).

Results

F_{ST} estimates between all population pairs indicated that individual *E. anna* and *E. carunculatum* populations were more differentiated from each other than they were from other conspecific populations (Table 7). F_{ST} values between *E. anna* and *E. carunculatum* in Whitefish were lower than they were between other pairs of *E. anna* and *E. carunculatum* populations, indicating gene flow between the species in Whitefish. Finally, F_{ST} between Whitefish and other populations was relatively low compared to F_{ST} between heterospecific populations.

Heterozygosity was higher in Whitefish than in other populations (Figure 19A), consistent with the expectation for hybrid zones. Nucleotide diversity varied among populations but was overall lower for each species in Whitefish than for other

populations of either parental species (Figure 19B). Similarly, inbreeding coefficient values (F_{IS}) were high across separate *E. anna* and *E. carunculatum* populations, but in Whitefish showed remarkable variation among individuals and covered the entire range of possible values (Figure 19C).

I identified 15 loci with significantly elevated F_{ST} between species (Figure 19D). Three of these loci were also identified as F_{ST} outliers in the analysis of males with long versus short cerci (Figure 19E), and an additional two were identified as F_{ST} outliers in the analysis of females with *E. anna*-type versus *E. carunculatum*-type mesostigmal plate morphologies (Figure 19F). There was no overlap of loci with elevated F_{ST} between males and females with variant morphology.

Admixture analyses suggested high levels of gene flow between *E. anna* and *E. carunculatum*

The admixture analysis of field-caught and lab-reared damselflies originating in Whitefish indicated a high level of admixture between *E. anna* and *E. carunculatum*, with an overall pattern in hybrids indicating roughly similar genomic contributions from each parental species rather than an excess of alleles from one parental species that would indicate asymmetric hybridization (Figure 20A). Patterns for the two parental species show small proportions of each genome assigned to the heterospecific cluster, but overall each species is distinguishable from the other. However, ongoing admixture at the Whitefish River site could complicate the

identification of species-diagnostic alleles. For this reason, I also analyzed admixture using the additional *E. anna* and *E. carunculatum* populations.

Results of this analysis show a lack of distinct clustering by species or by population, with many *E. anna* individuals assigned primarily to the *E. carunculatum* genetic cluster, or vice versa (Figure 20C). Additionally, this analysis indicated higher variability among hybrids in the proportions of their genome associated with each parental species, compared to the Whitefish-only analysis.

Results of the admixture analysis with higher K values yielded similar overall results: high variability in genetic clusters assigned to individuals in several of the separate *E. anna* and *E. carunculatum* populations and shared alleles among Whitefish damselflies, although hybrids were clearly intermediate between the parental species clusters (Figure 21).

Admixture proportion predicted phenotype in each sex

There was little agreement between the *STRUCTURE* and *introgress* estimates of proportion of each hybrid's genome associated with each parental species (R^2_{adj} = -0.005, $F_{1, 108}$ = 0.49, P = 0.48; Figure 23A). Admixture proportion estimated in *STRUCTURE* (Figure 20B) was a strong predictor of trait values in both sexes (males: R^2_{adj} = 0.46, $F_{1,106}$ = 92.2, P = 4.4 x 10^{-16}; females: R^2_{adj} = 0.47, $F_{1,65}$ = 59.2, P = 1.0 x 10^{-10}; Figure 23), but hybrid index estimates from structure showed no relationship with morphology (males: $F_{1,58}$ =2.75, P = 0.10, R^2_{adj} = 0.029; females: $F_{1,29}$ = 2.75, P = 0.19,

R^2_{adj}= 0.026). Accordingly, Kruskal-Wallis tests did not reveal associations of any of the rarely-introgressR^2_{adj}d loci with either with male cercus morphology (PC1 or PC2; 37 males, all $P > 0.01$; Figure 22B) or female mesostigmal plate morphology (PCs 1-4; all $P > 0.01$).

Discussion

This study aimed to identify regions of the genome that are (1) highly divergent between *E. anna* and *E. carunculatum*, (2) less subject to gene flow than other regions, and (3) associated with species-specific variation in male and female reproductive structure morphology. I predicted that the genomes of *E. anna* and *E. carunculatum* would be largely undifferentiated, but punctuated by small, highly divergent regions. I further predicted that these highly differentiated regions would also show relatively low levels of introgression and would primarily be associated with variation in male and female reproductive structure morphologies.

My genotyping results yielded high variation in locus representation across individuals, which resulted in a smaller than anticipated set of variant loci with which to make inferences about genomic divergence as well as lower than expected coverage, which may limit genotyping accuracy. However, I did identify loci that met each of my criteria and gained an overview of gene flow between these species.

Asymmetric gene flow

Both admixture and introgression analyses showed a pattern of hybridization between *E. anna* and *E. carunculatum* in nature and indicated that wild hybrids possessed roughly similar genomic contributions from either parental species. I previously showed that asymmetric premating RI makes matings between *E. anna* females and *E. carunculatum* males more likely than the reciprocal (Barnard et al. 2017), which leads to an expectation of asymmetric gene flow, but the present study's results do not support that prediction. The cause of this apparently symmetric gene flow is still not understood. Most of the hybrids included in the analysis do not appear to be F_1s, based on their morphology and their low heterozygosity at most loci, as revealed by the genomic clines analysis. This finding of low heterozygosity is consistent with a prediction of underdominance and selection against heterozygotes (Payseur 2010). One potential explanation for this observation of low heterozygosity is that intermediate genital morphology puts male hybrids at a reproductive disadvantage (Barnard et al. 2017). More research is needed to identify loci with biased introgression patterns and clarify their effects on RI.

Additionally, the genomic cline analysis results must be interpreted cautiously. A somewhat surprising result is that although *STRUCTURE* and *introgress* both estimated that natural hybrids possessed alleles inherited from both parental species, these relationship between the estimates were inconsistent when examined on an individual basis (Figure 22B). The results of both analyses must be considered carefully, because both included samples categorized as pure species but with

unknown levels of admixture in their own genomes. Additionally, the recent divergence time of these species makes it difficult to distinguish recent admixture from incomplete lineage sorting of shared ancestral polymorphisms. Both processes result in a similar pattern that make it difficult to distinguish either species at many loci (e.g., Mason et al. 2015).

Phenotypic and genotypic divergence

I identified several loci with elevated sequence differentiation between *E. anna* and *E. carunculatum*, several of which were identified in both a species-level analysis and an analysis based on sex- and species-specific morphology). This finding alone does not indicate whether any of these loci are responsible for morphological variation, but it does suggest a starting point for a deeper examination of genes that may specify male or female morphologies. To complement this approach, I also examined whether any of the infrequently introgressed loci I identified were implicated in RI by testing for associations with male and female morphological variation. This analysis did not reveal any significant connections, probably due in large part to the relatively low number of variant loci included in the analyses.

It is highly likely that the loci analyzed in the present study did not cover a sufficient portion of the genome to capture highly divergent areas associated with divergent phenotypes in *E. anna* and *E. carunculatum*. Early in divergence, differentiated regions may be quite small, and the loci I identified in this study may not

be sufficiently dense to detect small regions of genomic divergence (Ellison et al. 2011; Nadeau et al. 2012; Kronforst et al. 2013). *E. anna* and *E. carunculatum* shared a common ancestor within the last 250,000 – 15,000 years (McPeek et al. 2008). Incomplete lineage sorting among *E. anna* and *E. carunculatum* populations within the past 15,000-250,000 generations has likely resulted in many shared ancestral polymorphisms and few species diagnostic markers, similar to findings in the closely related species *E. hageni* and *E. ebrium* (Bourret et al. 2012). Indeed, my admixture analysis suggests high ancestral polymorphism in populations of both species (Figure 19C).

Moreover, RI appears to often be caused by many loci with small individual effects, which are more difficult to detect in the sparser sets of loci obtained by reduced representation genome sequencing (Szymura and Barton 1986; Janoušek et al. 2012; Payseur and Rieseberg 2016). High levels of gene flow can further exacerbate the difficulty of pinpointing divergent areas of the genome, and morphologically distinct groups may not be easily distinguished at a large number of molecular markers (e.g., (Poelstra et al. 2014; Mason and Taylor 2015; Toews et al. 2016). A noteworthy recent example of this phenomenon comes from a whole genome comparison of blue- and golden-winged warblers, which showed that these species' genomes show high differentiation at only six small regions – regions that had gone unnoticed by multiple other genotyping methods that covered less of the genome, including RADseq (Toews et al. 2017).

Conclusion

Divergence in genital morphologies appears to have been a major driving force in *Enallagma* speciation (McPeek et al. 2008, 2009; Barnard et al. 2017). Loci linked to male and female genital morphologies are expected to show reduced levels of introgression relative to other genomic regions, and should also be among loci that display high levels of between-species divergence. Along with a *de novo* transcriptome assembly in *E. hageni* (Shanku et al. 2013), the present study is among the first attempt to characterize the *Enallagma* genome. My results revealed discordance between various methods of investigating patterns of genomic divergence and searching for divergent loci related to morphological divergence and RI. Additional sequencing efforts to cover a higher proportion of the genome in a smaller set of individuals may be necessary to confidently determine whether *E. anna* and *E. carunculatum* genomes show elevated divergence and reduced introgression primarily at loci that specify genital morphologies.

Chapter 3 - Tables

Table 6. Sampling sites for genomic analyses

Population (abbrev)	Species	N	Latitude	Longitude
Bull Lake, MT (BL)	*E. carunculatum*	13	48.226272	-115.84045
Eyraud Lakes, MT (EL)	*E. carunculatum*	13	48.014084	-111.97501
Flathead River, MT (FR)	*E. carunculatum*	14	47.367827	-114.57759
Muddy Creek, MT (MC)	*E. anna*	12	47.97961	-112.15654
Pondera Coulee, MT (PC)	*E. anna*	5	48.189244	-111.3268
Willow Creek, MT (WC)	*E. anna*	11	48.658064	-112.75906
Whitefish River, MT (WF)	*E. carunculatum*	40		
	E. anna	45	48.371231	-114.30252
	hybrids	30		
Lab-reared progeny from	*E. carunculatum*	18		
WF populations	*E. anna*	48	--	--
	hybrids	97		

N denotes the number of damselflies for which genomic sequence data were obtained.

Table 7. Pairwise population F_{ST} estimates

		E. anna			*E. carunculatum*				Hybrids
	Population	MC	PC	WC	WF	BL	EL	FR	WF
E. anna	WF	0.046	0.120	0.056	0.157	0.166	0.188	0.138	0.106
	MC		0.251	0.122	0.183	0.307	0.329	0.272	0.152
	PC			0.257	0.120	0.253	0.251	0.306	0.101
	WC				0.159	0.225	0.295	0.206	0.099
E. carunculatum	WF					0.080	0.083	0.093	0.102
	BL						0.176	0.255	0.113
	EL							0.273	0.152
	FR								0.147

Estimates are based on a set of 5 loci found in all populations. Only field-caught damselflies were included in the analysis. Population abbreviations are described in Table 6.

Chapter 3 - Figure captions

Figure 18. Sampling locations of *E. anna*, *E. carunculatum*, and admixed damselflies (gray triangle). Shading indicates regions where both species' ranges overlap (adapted from Johnson 2009; Paulson 2009, 2011).

Figure 19. Summary population genetic statistics for *E. anna*, *E. carunculatum* (car), and admixed populations. **(A)** Heterozygosity. **(B)** Nucleotide diversity. **(C)** Inbreeding coefficient F_{IS}). **(D-F)** Per-locus (corrected AMOVA) F_{ST} between *E. anna* and *E. carunculatum* **(D)**, females with extremes of mesostigmal plate shape **(E)**, and males with extremes in cercus shape **(F)**. In panels A-C, each point represents the population mean, and bars indicate standard error. Population abbreviations are described in Table 6. In panels D-F, shaded points indicate loci with significantly elevated F_{ST}. In D, points with hatches indicate outlier loci also identified in F_{ST} calculations between males with extremes of cercus shape (E), and black points indicate outlier loci also identified in F_{ST} calculations between females with extremes of mesostigmal plate shape (F).

Figure 20. Bayesian estimation of admixture proportions in the program *STRUCTURE* with the number of genetic clusters to assign samples to (*K*) = 2. Each vertical bar represents one individual. The y-axis values represent the assignment probability to either the *E. anna* (gray) or *E. carunculatum* (black) genetic cluster, respectively. **(A)**

Estimation from 272 damselflies from two generations from the Whitefish River site (generation 1 field-caught, generation 2 lab-reared). **(B)** Estimation from 127 field-caught damselflies from Whitefish River. **(C)** Estimation from 200 damselflies from 4 natural populations of each species, including Whitefish River. White lines separate each group: species (A and B) or species and site (C).

Figure 21. Bayesian estimation of admixture proportions in multiple *STRUCTURE* analyses with the number of genetic clusters to assign samples to (*K*) set between 3 and 9. The genotype data are the same as those in Figure 20C (2356 loci in 200 damselflies from 4 natural populations of each species). Each vertical bar represents one individual. The proportion of each color within a vertical bar represents the proportion of the genome assigned to 1of *K* clusters. Black lines separate each population.

Figure 22. Results of introgression analysis. **(A)** Genomic hybrid index estimates. Each gray bar represents the estimated proportion of alleles inherited from *E. anna* for a single individual. Blue bars represent 95% confidence limits of ancestry estimates. **(B)** Lack of agreement between ancestry estimates ancestry for each hybrid in *STRUCTURE* vs *introgress*.

Figure 23. Relationships between admixture estimates and morphology. Hybrid index is the proportion of the genome associated with the *E. anna* genetic cluster by *STRUCTURE*. PC1 values for male cerci and female mesostigmal plates come from Barnard et al. 2017. Each point represents one individual. Illustrations on the y-axes represent cercus and plate phenotypes associated with each parental species.

Figure 18. Sampling locations

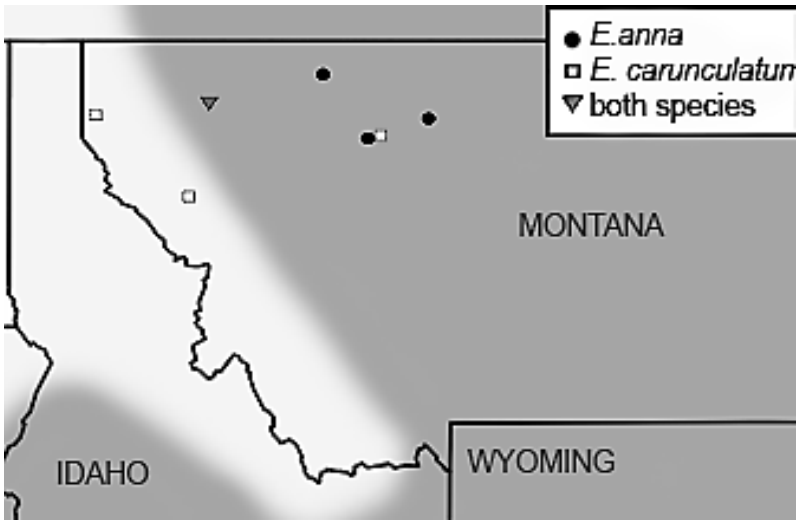

Figure 19. Summary population genetic statistics

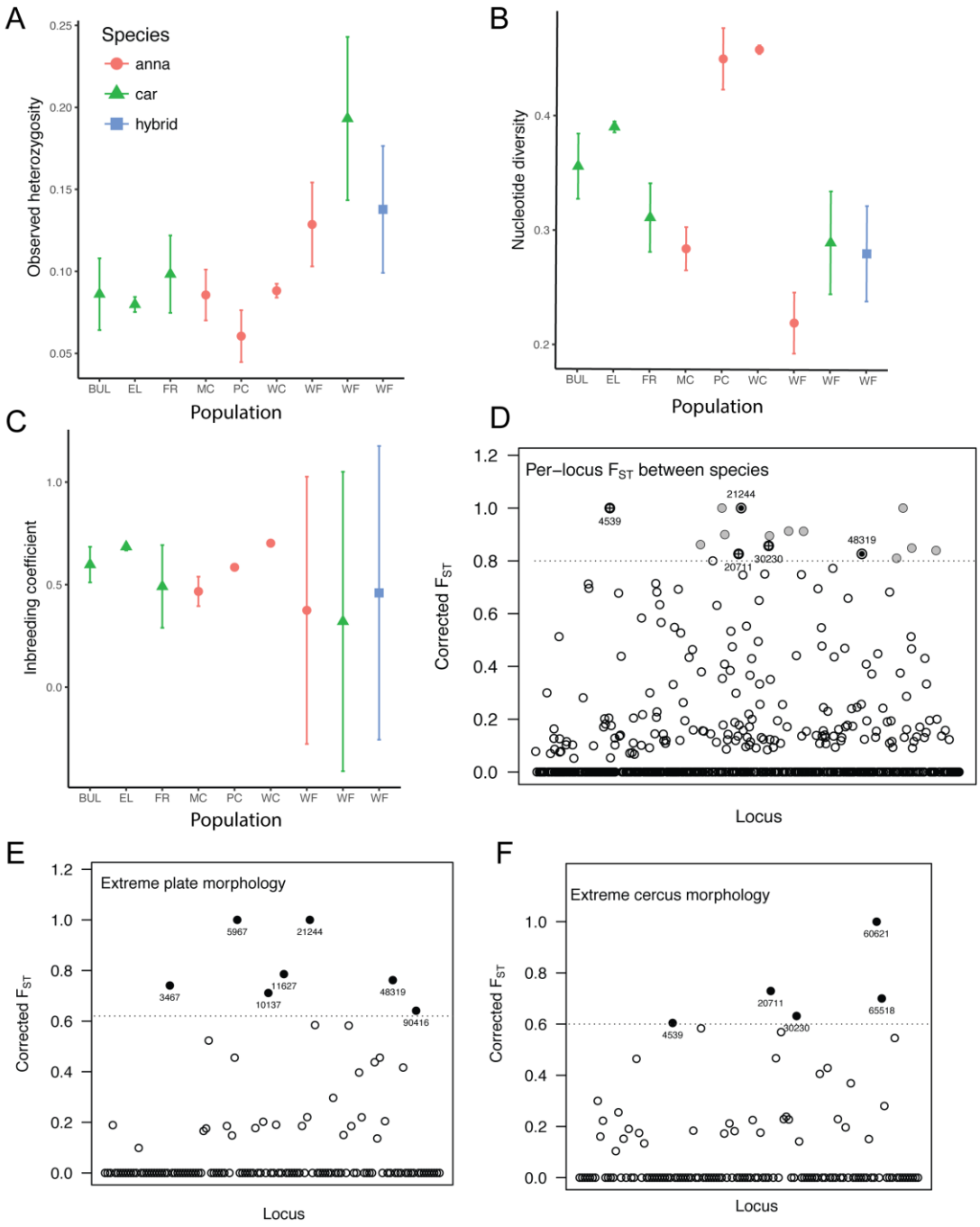

Figure 20. Bayesian estimation of admixture proportions in *STRUCTURE* (K = 2)

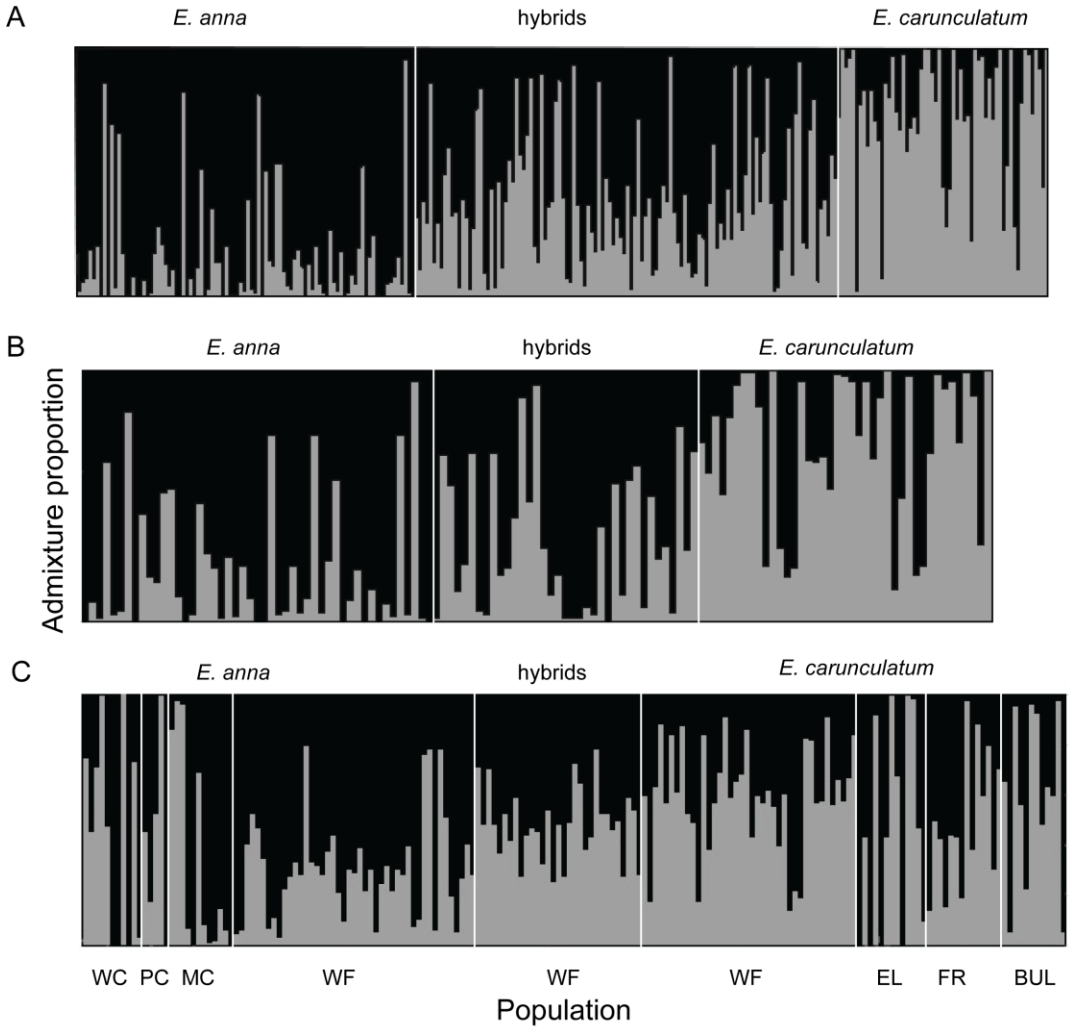

Figure 21. Bayesian estimation of admixture proportions in multiple *STRUCTURE* analyses with K set between 3 and 9

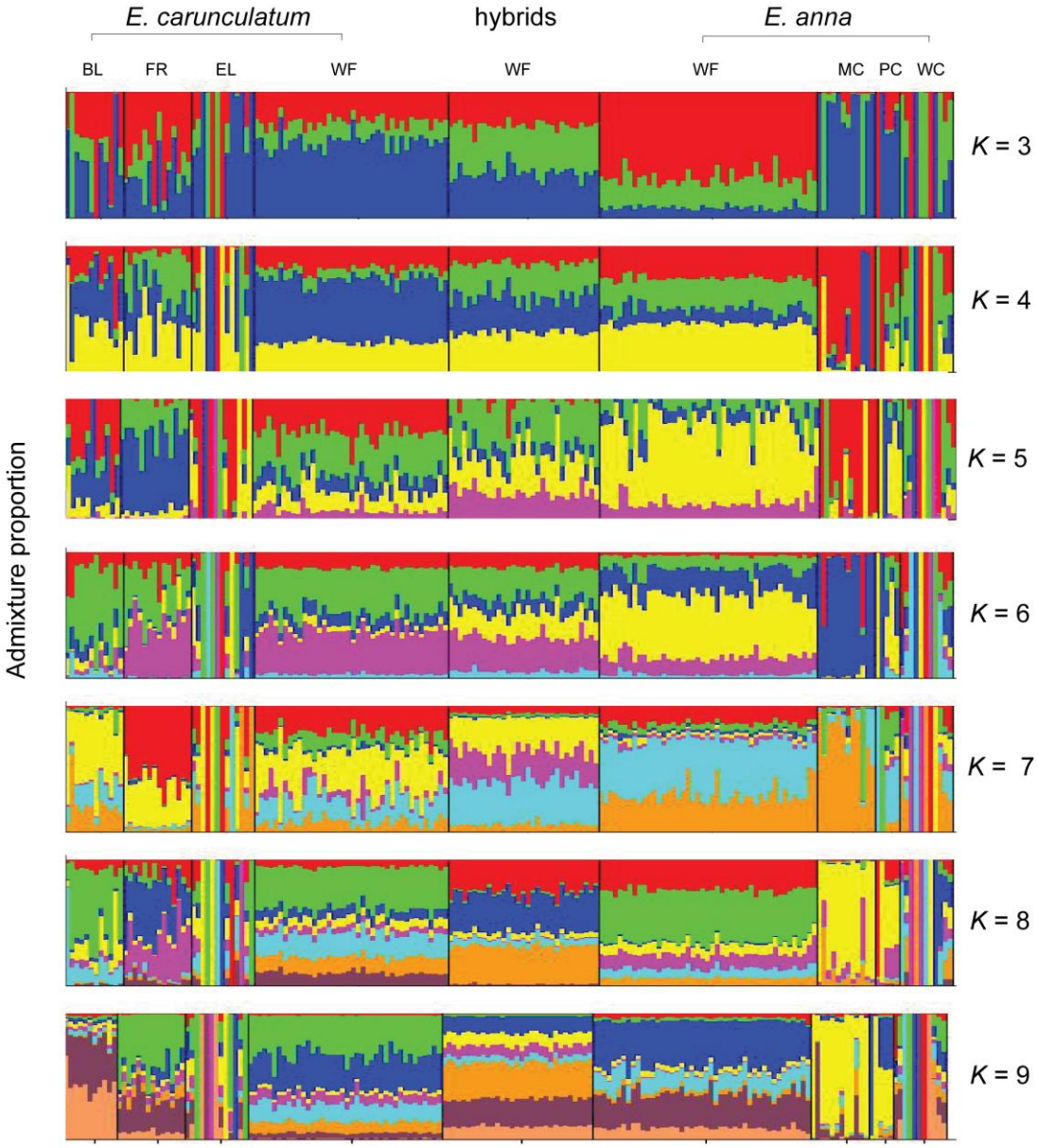

Figure 22. Results of introgression analysis

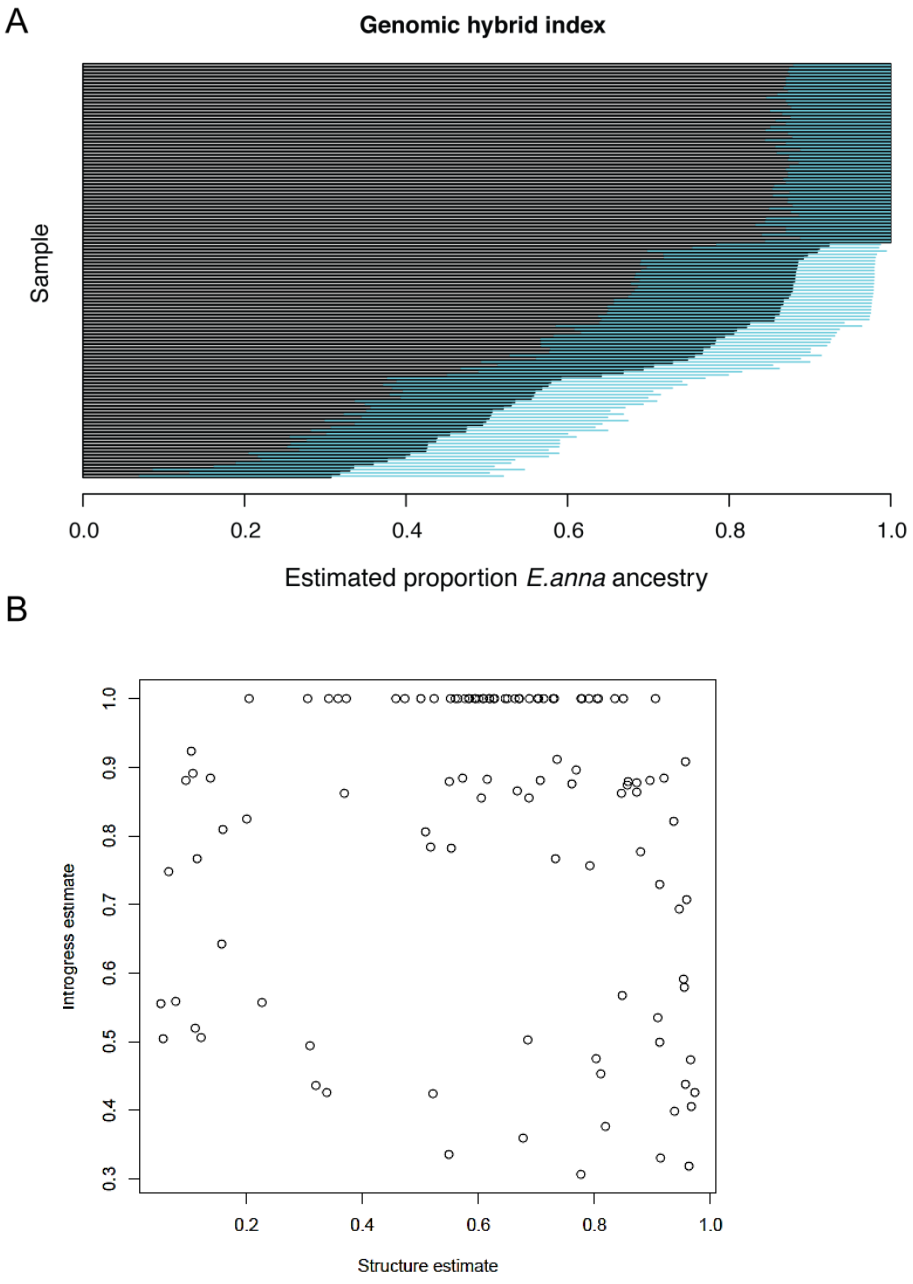

Figure 23. Relationships between admixture estimates and morphology

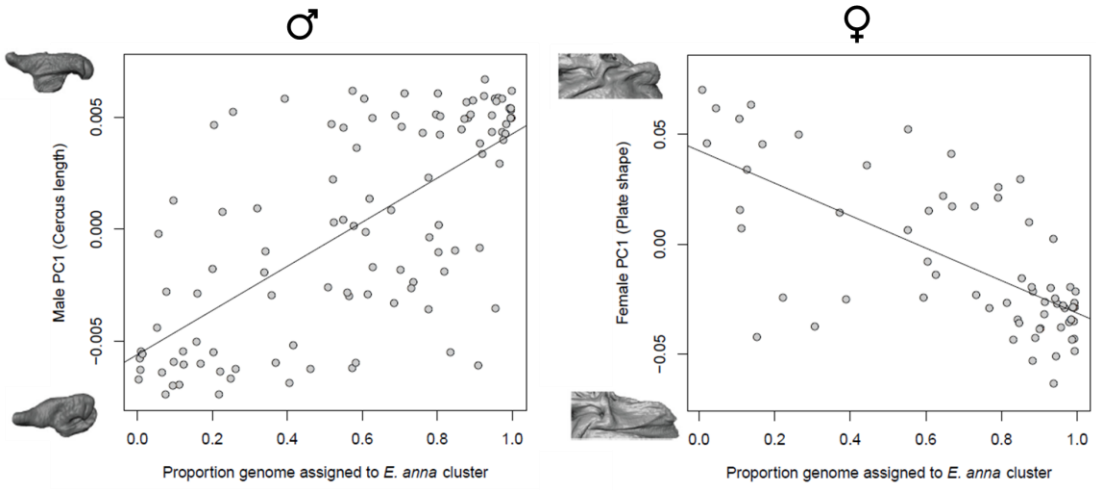

References

Abbott, R., D. Albach, S. Ansell, J. W. Arntzen, S. J. Baird, N. Bierne, J. Boughman, A. Brelsford, C. A. Buerkle, and R. Buggs. 2013. Hybridization and speciation. Journal of Evolutionary Biology 26:229-246.

Abramoff, M. D., P. J. Magalhaes, and S. J. Ram. 2004. Image processing with ImageJ. Biophotonics International 11:36-42.

Adams, D. C. and E. Otarola-Castillo. 2013. geomorph: an R package for the collection and analysis of geometric morphometric shape data. Methods in Ecology and Evolution 4:393-399.

Anderson, C. M. and R. B. Langerhans. 2015. Origins of female genital diversity: Predation risk and lock-and-key explain rapid divergence during an adaptive radiation. Evolution 69:2452-2467.

Arnqvist, G. 1989. Sexual selection in a water strider: the function, mechanism of selection and heritability of a male grasping apparatus. Oikos 56:344-350.

Arnqvist, G. and L. Rowe. 2005. Sexual conflict. Princeton University Press, Princeton, NJ.

Barnard, A. A., O. M. Fincke, M. A. McPeek, and J. P. Masly. 2017. Mechanical and tactile incompatibilities cause reproductive isolation between two young damselfly species. Evolution 71:2410–2427.

Barton, N. and B. O. Bengtsson. 1986. The barrier to genetic exchange between hybridising populations. Heredity 57:357.

Barton, N. and G. M. Hewitt. 1989. Adaptation, speciation and hybrid zones. Nature 341:497.

Bath, E., N. Tatarnic, and R. Bonduriansky. 2012. Asymmetric reproductive isolation and interference in neriid flies: the roles of genital morphology and behaviour. Animal Behaviour 84:1331-1339.

Battin, T. J. 1993. The odonate mating system, communication, and sexual selection: A review. Bulletin of Zoology 60:353-360.

Bergsten, J., A. Töyrä, and A. N. Nilsson. 2001. Intraspecific variation and intersexual correlation in secondary sexual characters of three diving beetles (Coleoptera: Dytiscidae). Biological Journal of the Linnean Society 73:221-232.

Bertin, A. and D. Fairbairn. 2005. One tool, many uses: precopulatory sexual selection on genital morphology in *Aquarius remigis*. Journal of Evolutionary Biology 18:949-961.

Bick, G. H. and J. C. Bick. 1981. Heterospecific pairing among Odonata. Odonatologica 10:259-270.

Bourret, A., M. A. McPeek, and J. Turgeon. 2012. Regional divergence and mosaic spatial distribution of two closely related damselfly species (*Enallagma hageni* and *Enallagma ebrium)*. Journal of Evolutionary Biology 25:196-209.

Brennan, P. L. 2016. Studying genital coevolution to understand intromittent organ morphology. Integrative and Comparative Biology 56:669-681.

Brideau, N. J., H. A. Flores, J. Wang, S. Maheshwari, X. Wang, and D. A. Barbash. 2006. Two Dobzhansky-Muller genes interact to cause hybrid lethality in *Drosophila*. Science 314:1292-1295.

Brown, W. L. and E. O. Wilson. 1956. Character displacement. Systematic Zoology 5:49-64.

Bussell, J. J., N. Yapici, S. X. Zhang, B. J. Dickson, and L. B. Vosshall. 2014. Abdominal-B neurons control *Drosophila* virgin female receptivity. Current Biology 24:1584-1595.

Butlin, R., A. Debelle, C. Kerth, R. R. Snook, L. W. Beukeboom, R. F. Castillo Cajas, W. Diao, M. E. Maan, S. Paolucci, F. J. Weissing, L. van de Zande, A. Hoikkala, E. Geuverink, J. Jennings, M. Kankare, K. E. Knott, V. I. Tyukmaeva, C. Zoumadakis, M. G. Ritchie, D. Barker, E. Immonen, M. Kirkpatrick, M. Noor, C. Macias Garcia, T. Schmitt, and M. Schilthuizen. 2012. What do we need to know about speciation? Trends in Ecology & Evolution 27:27-39.

Callahan, M. S. and M. A. McPeek. 2016. Multi-locus phylogeny and divergence time estimates of *Enallagma* damselflies (Odonata: Coenagrionidae). Molecular Phylogenetics and Evolution 94:182-195.

Carneiro, M., S. J. Baird, S. Afonso, E. Ramirez, P. Tarroso, H. Teotónio, R. Villafuerte, M. W. Nachman, and N. Ferrand. 2013. Steep clines within a highly permeable genome across a hybrid zone between two subspecies of the European rabbit. Molecular Ecology 22:2511-2525.

Castillo, D. M., M. K. Burger, C. M. Lively, and L. F. Delph. 2015. Experimental evolution: Assortative mating and sexual selection, independent of local

adaptation, lead to reproductive isolation in the nematode *Caenorhabditis remanei*. Evolution 69:3141-3155.

Catchen, J., P. A. Hohenlohe, S. Bassham, A. Amores, and W. A. Cresko. 2013. Stacks: an analysis tool set for population genomics. Molecular Ecology 22:3124-3140.

Catchen, J. M., A. Amores, P. Hohenlohe, W. Cresko, and J. H. Postlethwait. 2011. Stacks: building and genotyping Loci de novo from short-read sequences. G3: Genes, Genomes, Genetics 1:171-182.

Catling, P. M. 2001. Morphological evidence for the hybrid *Enallagma ebrium* x *hageni* (Zygoptera: Coenagrionidae) from Ontario. Proceedings of the Entomological Society of Ontario 132:99-101.

Chamberlain, N. L., R. I. Hill, D. D. Kapan, L. E. Gilbert, and M. R. Kronforst. 2009. Polymorphic butterfly reveals the missing link in ecological speciation. Science 326:847-850.

Coleman, S. W. 2008. Taxonomic and sensory biases in the mate-choice literature: there are far too few studies of chemical and multimodal communication. Acta Ethologica 12:45-48.

Corbet, P. S. 1999. Dragonflies: Behaviour and ecology of Odonata. Cornell University Press, Ithaca, NY.

Córdoba-Aguilar, A. 2008. Dragonflies and damselflies: Model organisms for ecological and evolutionary research. Oxford University Press, New York, NY.

Córdoba-Aguilar, A. and A. Cordero-Rivera. 2008. Cryptic female choice and sexual conflict. Pp. 189-202 *in* A. Córdoba-Aguilar, ed. Dragonflies and damselflies: Model organisms for ecological and evolutionary research. Oxford University Press, New York, NY.

Coyne, J. A. 1992. Genetics and speciation. Nature 355:511.

Coyne, J. A. 1993. The genetics of an isolating mechanism between two sibling species of *Drosophila*. Evolution 47:778-788.

Coyne, J. A. and H. A. Orr. 1989. Patterns of speciation in *Drosophila*. Evolution 43:362-381.

Coyne, J. A. and H. A. Orr. 1997. "Patterns of speciation in *Drosophila*" revisited. Evolution 51:195-303.

Coyne, J. A. and H. A. Orr. 1997. "Patterns of speciation in *Drosophila*" revisited. Evolution 51:195-303.

Coyne, J. A. and H. A. Orr. 2004. Speciation. Sinauer Associates, Sunderland, MA.

Danielsson, I. and C. Askenmo. 1999. Male genital traits and mating interval affect male fertilization success in the water strider *Gerris lacustris*. Behavioral Ecology and Sociobiology 46:149-156.

Darwin, C. 1859. On The Origin of Species by Means of Natural Selection, or Preservation of Favoured Races in the Struggle for Life. John Murray, London.

de Wilde, J. 1964. Reproduction. Pp. 9-58 *in* M. Rockstein, ed. The physiology of Insecta. Academic Press, New York, NY.

Delph, L. F. and J. P. Demuth. 2016. Haldane's rule: genetic bases and their empirical support. Journal of Heredity 107:383-391.

Donnelly, N. T. 2008. A Hybrid Complex in *Enallagma*. Argia 20:10-11.

Dopman, E. B., P. S. Robbins, and A. Seaman. 2010. Components of reproductive isolation between North American pheromone strains of the European corn borer. Evolution 64:881-902.

Dufour, L. 1844. Anatomie générale des diptéres. Annales des Sciences Naturelles 1:244-264.

Eberhard, W. G. 1985. Sexual Selection and Animal Genitalia. Harvard University Press, Cambridge, MA.

Eberhard, W. G. 1992. Species isolation, genital mechanics, and the evolution of species-specific genitalia in three species of *Macrodactylus* bseetles (Coleoptera, Scarabeidae, Melolonthinae). Evolution 46:1774-1783.

Eberhard, W. G. 2001. Species-specific genitalic copulatory courtship in Sepsid flies (Diptera, Sepsidae, Microsepsis) and theories of genitalic evolution. Evolution 55:93-102.

Eberhard, W. G. 2010. Evolution of genitalia: theories, evidence, and new directions. Genetica 138:5-18.

Ellison, C. K., C. Wiley, and K. L. Shaw. 2011. The genetics of speciation: genes of small effect underlie sexual isolation in the Hawaiian cricket *Laupala*. Journal of Evolutionary Biology 24:1110-1119.

Etter, P. D., S. Bassham, P. A. Hohenlohe, E. A. Johnson, and W. A. Cresko. 2012. SNP discovery and genotyping for evolutionary genetics using RAD sequencing. Pp. 157-178. Molecular Methods for Evolutionary Genetics. Humana Press.

Falush, D., M. Stephens, and J. K. Pritchard. 2003. Inference of population structure using multilocus genotype data: linked loci and correlated allele frequencies. Genetics 164:1567-1587.

Feder, J. L., R. Gejji, S. Yeaman, and P. Nosil. 2012. Establishment of new mutations under divergence and genome hitchhiking. Philosophical Transactions of the Royal Society B: Biological Sciences 367:461-474.

Federley, H. 1932. Die Bedeutung der Kreuzung für die Evolution. Jenische Zeitschrift für Naturwissenschaft 67:364-386.

Feng, K., M. T. Palfreyman, M. Häsemeyer, A. Talsma, and B. J. Dickson. 2014. Ascending SAG neurons control sexual receptivity of *Drosophila* females. Neuron 83:135-148.

Fincke, O. M. 2015. Trade-offs in female signal apparency to males offer alternative anti-harassment strategies for colour polymorphic females. Journal of Evolutionary Biology 28:931-943.

Fincke, O. M., A. Fargevieille, and T. D. Schultz. 2007. Lack of innate preference for morph and species identity in mate-searching *Enallagma* damselflies. Behavioral Ecology and Sociobiology 61:1121-1131.

Forbes, M. R. 1991. Female morphs of the damselfly E*nallagma boreale* Selys (Odonata: Coenagrionidae): a benefit for androchromatypes. Canadian Journal of Zoology 69:1969-1970.

Frazee, S. R. and J. P. Masly. 2015. Multiple sexual selection pressures drive the rapid evolution of complex morphology in a male secondary genital structure. Ecology and Evolution 5:4437-4450.

Garrigan, D., S. B. Kingan, A. J. Geneva, P. Andolfatto, A. G. Clark, K. R. Thornton, and D. C. Presgraves. 2012. Genome sequencing reveals complex speciation in the *Drosophila simulans* clade. Genome Research 22:1499-1511.

Gompert, Z. and C. Alex Buerkle. 2010. introgress: a software package for mapping components of isolation in hybrids. Molecular Ecology Resources 10:378-384.

Gompert, Z., E. G. Mandeville, and C. A. Buerkle. 2017. Analysis of population genomic data from hybrid zones. Annual Review of Ecology, Evolution, and Systematics 48:207-229.

Good, J. M., D. Vanderpool, S. Keeble, and K. Bi. 2015. Negligible nuclear introgression despite complete mitochondrial capture between two species of chipmunks. Evolution 69:1961-1972.

Grant, V. 1992. Floral isolation between orithophilous and spingophilous species of *Ipomospsis* and *Aquilegia*. Proceedings of the National Academy of Sciences USA 89:11828-11831.

Haldane, J. B. 1922. Sex ratio and unisexual sterility in hybrid animals. Journal of Genetics 12:101-109.

Harrison, R. G. 1990. Hybrid zones: Windows on evolutionary process. Oxford Surveys in Evolutionary Biology 7:69-128.

Harrison, R. G. 1993. Hybrid zones and the evolutionary process. Oxford University Press, Oxford. 364 pp.

Harrison, R. G. and E. L. Larson. 2016. Heterogeneous genome divergence, differential introgression, and the origin and structure of hybrid zones. Molecular Ecology 25:2454-2466.

Hilton, D. F. J. 1983. Mating isolation in two species of *Nehalennia*. Odonatologica 12:375-379.

Höbel, G., H. Carl Gerhardt, and M. Noor. 2003. Reproductive character displacement in the acoustic communication system of green tree frogs (*Hyla cinerea*). Evolution 57:894-904.

House, C. M. and L. W. Simmons. 2003. Genital morphology and fertilization success in the dung beetle *Onthophagus taurus*: An example of sexually selected male genitalia. Proceedings of the Royal Society of London B: Biological Sciences 270:447-455.

Howard, D. J. 1993. Reinforcement: origin, dynamics, and fate of an evolutionary hypothesis. Pp. 46–69 *in* R. G. Harrison, ed. Hybrid Zones and the Evolutionary Process. Oxford University Press, New York, NY.

Husband, B. C. and H. A. Sabara. 2004. Reproductive isolation between autotetraploids and their diploid progenitors in fireweed, *Chamerion angustifolium* (Onagraceae). New Phytologist 161:703-713.

Huxley, J. 1958. Introduction. Pp. 545. The Origin of Species. Signet Classics, New York, NY.

Janoušek, V., L. Wang, K. Luzynski, P. Dufková, M. M. Vyskočilová, M. W. Nachman, P. Munclinger, M. Macholán, J. Piálek, and P. K. Tucker. 2012. Genome-wide architecture of reproductive isolation in a naturally occurring hybrid zone between *Mus musculus musculus* and *M. m. domesticus*. Molecular Ecology 21:3032-3047.

Jiggins, C. D., R. E. Naisbit, R. L. Coe, and J. Mallet. 2001. Reproductive isolation caused by colour pattern mimicry. Nature 411:302–305.

Johansson, B. G. and T. M. Jones. 2007. The role of chemical communication in mate choice. Biological Reviews 82:265-289.

Johnson, J. 2009. Presumed *Enallagma anna* Williamson × *carunculatum* Morse hybrids from Oregon and California. Bulletin of American Odonatology 11:8-10.

Jordan, K. 1896. On mechanical selection and other problems. Novitates Zoologicae 3:426–525.

Kamimura, Y. and H. Mitsumoto. 2012. Lock-and-key structural isolation between sibling *Drosophila* species. Entomological Science 15:197-201.

Kay, K. M. 2006. Reproductive isolation between two closely related hummingbird pollinated neotropical gingers. Evolution 60:538-552.

Kennedy, C. H. 1919. A study of the phylogeny of the Zygoptera from evidence given from the genitalia (Doctoral dissertation). Cornell University, Ithaca, NY.

Kirkpatrick, M. and V. Ravigné. 2002. Speciation by natural and sexual selection: models and experiments. The American Naturalist 159:S22-S35.

Krieger, F. and E. Krieger-Loibl. 1958. Beiträge zum Verhalten von *Ischnura elegans* und *Ischnura pumilio* (Odonata) 1. Zeitschrift für Tierpsychologie 15:82-93.

Kronforst, M. R., M. E. Hansen, N. G. Crawford, J. R. Gallant, W. Zhang, R. J. Kulathinal, D. D. Kapan, and S. P. Mullen. 2013. Hybridization reveals the evolving genomic architecture of speciation. Cell Reports 5:666-677.

Kronforst, M. R., L. G. Young, D. D. Kapan, C. McNeely, R. J. O'Neill, and L. E. Gilbert. 2006. Linkage of butterfly mate preference and wing color preference

cue at the genomic location of wingless. Proceedings of the National Academy of Sciences USA 103:6575-6580.

Larson, E. L., T. A. White, C. L. Ross, and R. G. Harrison. 2014. Gene flow and the maintenance of species boundaries. Molecular Ecology 23:1668-1678.

LeVasseur-Viens, H., M. Polak, and A. J. Moehring. 2015. No evidence for external genital morphology affecting cryptic female choice and reproductive isolation in *Drosophila*. Evolution 69:1797-1807.

Loibl, E. 1958. Zur Ethologie und Biologie der deutschen Lestiden (Odonata) 1. Zeitschrift für Tierpsychologie 15:54-81.

Lorkovic, Z. 1953. L'accouplement artificiel chez les Lepidoptéres et son application dans les recherches sur la fonction de l'appareil génital des insectes. Physiologia Comparata et Oecologia 3:313-320.

Lorkovic, Z. 1958. Some peculiarities of spatially and sexually restricted gene exchange in the *Erebia tyndarus* group. Cold Spring Harbor Symposia on Quantitative Biology 23:319–325.

Macholán, M., P. Munclinger, M. Šugerková, P. Dufková, B. Bímová, E. Božíková, J. Zima, and J. Piálek. 2007. Genetic analysis of autosomal and X-linked markers across a mouse hybrid zone. Evolution 61:746-771.

Maroja, L. S., E. L. Larson, S. M. Bogdanowicz, and R. G. Harrison. 2015. Genes with restricted introgression in a field cricket (*Gryllus firmus*/*Gryllus pennsylvanicus*) hybrid zone are concentrated on the X chromosome and a single autosome. G3: Genes, Genomes, Genetics 5:2219-2227.

Martin, S. H., K. K. Dasmahapatra, N. J. Nadeau, C. Salazar, J. R. Walters, F. Simpson, M. Blaxter, A. Manica, J. Mallet, and C. D. Jiggins. 2013. Genome-wide evidence for speciation with gene flow in *Heliconius* butterflies. Genome Research 23:1817-1828.

Masly, J. P. 2012. 170 Years of "Lock-and-Key": Genital morphology and reproductive isolation. International Journal of Evolutionary Biology 2012:247352.

Masly, J. P., C. D. Jones, M. A. Noor, J. Locke, and H. A. Orr. 2006. Gene transposition as a cause of hybrid sterility in *Drosophila*. Science 313:1448-1450.

Masly, J. P. and D. C. Presgraves. 2007. High-resolution genome-wide dissection of the two rules of speciation in *Drosophila*. PLoS Biology 5:e243.

McMillan, W. O., C. Jiggins, and J. Mallet. 1997. What initiates speciation in passion-vine butterflies? Proceedings of the National Academy of Sciences USA 94:8628–8633.

Mason, N. A. and S. A. Taylor. 2015. Differentially expressed genes match bill morphology and plumage despite largely undifferentiated genomes in a Holarctic songbird. Molecular Ecology 24:3009-3025.

Matute, D. R. 2010. Reinforcement can overcome gene flow during speciation in *Drosophila*. Current Biology 20:2229-2233.

McMillan, W. O., C. Jiggins, and J. Mallet. 1997. What initiates speciation in passion-vine butterflies? Proceedings of the National Academy of Sciences USA 94:8628–8633.

McPeek, M. A., L. Shen, and H. Farid. 2009. The correlated evolution of three-dimensional reproductive structures between male and female damselflies. Evolution 63:73-83.

McPeek, M. A., L. Shen, J. Z. Torrey, and H. Farid. 2008. The tempo and mode of three-dimensional morphological evolution in male reproductive structures. The American Naturalist 171:E158-178.

McPeek, M. A., L. B. Symes, D. M. Zong, and C. L. McPeek. 2011. Species recognition and patterns of population variation in the reproductive structures of a damselfly genus. Evolution 65:419-428.

Mendelson, T. C. 2003. Sexual isolation evolves faster than hybrid inviability in a diverse and sexually dimorphic genus of fish (Percidae: *Etheostoma*). Evolution 57:317-327.

Mendelson, T. C. and G. Wallis. 2003. Sexual isolation evolves faster than hybrid inviability in a diverse and sexually dimorphic genus of fish (Percidae: *Etheostoma*). Evolution 57:317-327.

Miller, K. B. and M. A. Ivie. 1995. *Enallagma optimolocus*: A new species of damselfly from Montana (Odonata: Coenagrionidae). Proceedings of the Entomological Society of Washington 97:833-838.

Miller, M. N. and O. M. Fincke. 1999. Cues for mate recognition and the effect of prior experience on mate recognition in *Enallagma* damselflies. Journal of Insect Behavior 12:801-814.

Miller, M. N. and O. M. Fincke. 2004. Mistakes in sexual recognition among sympatric Zygoptera vary with time of day and color morphism (Odonata: Coenagrionidae). International Journal of Odonatology 7:471-491.

Myers, S. S., T. R. Buckley, and G. I. Holwell. 2016. Male genital claspers influence female mate acceptance in the stick in sect *Clitarchus hookeri*. Behavioral Ecology and Sociobiology 70:1547-1556.

Nadeau, N. J., A. Whibley, R. T. Jones, J. W. Davey, K. K. Dasmahapatra, S. W. Baxter, M. A. Quail, M. Joron, M. L. Blaxter, and J. Mallet. 2012. Genomic islands of divergence in hybridizing *Heliconius* butterflies identified by large-scale targeted sequencing. Philosophical Transactions of the Royal Society B: Biological Sciences 367:343-353.

Naisbit, R. E., C. D. Jiggins, and J. Mallet. 2001. Disruptive sexual selection against hybrids contributes to speciation between *Heliconius cydno* and *Heliconius melpomene*. Proceedings of the Royal Society of London B: Biological Sciences 268:1849-1854.

Naisbit, R. E., C. D. Jiggins, M. Linares, C. Salazar, and J. Mallet. 2002. Hybrid sterility, Haldane's rule and speciation in *Heliconius cydno* and *H. melpomene*. Genetics 161:1517-1526.

Nolte, A. W., Z. Gompert, and C. A. Buerkle. 2009. Variable patterns of introgression in two sculpin hybrid zones suggest that genomic isolation differs among populations. Molecular Ecology 18:2615-2627.

Noor, M. F. 1999. Reinforcement and other consequences of sympatry. Heredity 83:503-508.

Noor, M. and S. Bennett. 2010. Islands of speciation or mirages in the desert? Examining the role of restricted recombination in maintaining species. Heredity 104:418.

Nosil, P. and J. L. Feder. 2012. Genomic divergence during speciation: causes and consequences. Philosophical Transactions of the Royal Society of London B: Biological Sciences 367:332-342

Nosil, P., T. H. Vines, and D. J. Funk. 2005. Perspective: reproductive isolation caused by natural selection against immigrants from divergent habitats. Evolution 59:705-719.

Orr, H. A. 1995. The population genetics of speciation: the evolution of hybrid incompatibilities. Genetics 139:1805-1813.

Orr, H. A., J. P. Masly, and D. C. Presgraves. 2004. Speciation genes. Current Opinion in Genetics and Development 14:675-679.

Otronen, M. 1998. Male asymmetry and postcopulatory sexual selection in the fly *Dryomyza anilis*. Behavioral Ecology and Sociobiology 42:185-191.

Panhuis, T. M., R. Butlin, M. Zuk, and T. Tregenza. 2001. Sexual selection and speciation. Trends in Ecology & Evolution 16:364-371.

Paris, J. R., J. R. Stevens, and J. M. Catchen. 2017. Lost in parameter space: a road map for stacks. Methods in Ecology and Evolution 8:1360-1373.

Paulson, D. R. 1974. Reproductive isolation in damselflies. Systematic Zoology 23:40-49.

Paulson, D. R. 2009. Dragonflies and Damselflies of the West. Princeton University Press, Princeton, New Jersey.

Payseur, B. A. 2010. Using differential introgression in hybrid zones to identify genomic regions involved in speciation. Molecular Ecology 10:806-820.

Payseur, B. A., J. G. Krenz, and M. W. Nachman. 2004. Differential patterns of introgression across the X chromosome in a hybrid zone between two species of house mice. Evolution 58:2064-2078.

Payseur, B. A., J. G. Krenz, and M. W. Nachman. 2004. Differential patterns of introgression across the X chromosome in a hybrid zone between two species of house mice. Evolution 58:2064-2078.

Payseur, B. A. and L. H. Rieseberg. 2016. A genomic perspective on hybridization and speciation. Molecular ecology 25:2337-2360.

Pfennig, K. S., A. J. Chunco, and A. C. Lackey. 2007. Ecological selection and hybrid fitness: hybrids succeed on parental resources. Evolutionary Ecology Research 9:341-354.

Pfennig, D. W. and K. S. Pfennig. 2010. Character displacement and the origins of diversity. The American Naturalist 176:S26-S44.

Phadnis, N. and H. A. Orr. 2009. A single gene causes both male sterility and segregation distortion in *Drosophila* hybrids. Science 323:376-379.

Poelstra, J. W., N. Vijay, C. M. Bossu, H. Lantz, B. Ryll, I. Müller, V. Baglione, P. Unneberg, M. Wikelski, and M. G. Grabherr. 2014. The genomic landscape underlying phenotypic integrity in the face of gene flow in crows. Science 344:1410-1414.

Presgraves, D. C. 2002. Patterns of postzygotic isolation in Lepidoptera. Evolution 56:1168-1183.

Presgraves, D. C., L. Balagopalan, S. M. Abmayr, and H. A. Orr. 2003. Adaptive evolution drives divergence of a hybrid inviability gene between two species of *Drosophila*. Nature 423:715.

Price, C. S., C. H. Kim, C. J. Gronlund, and J. A. Coyne. 2001. Cryptic reproductive isolation in the *Drosophila simulans* species complex. Evolution 55:81-92.

Price, T. D. and M. M. Bouvier. 2002. The evolution of F1 postzygotic incompatibilities in birds. Evolution 56:2083-2089.

Pritchard, J. K., M. Stephens, and P. Donnelly. 2000. Inference of population structure using multilocus genotype data. Genetics 155:945-959.

R Core Team. 2015. R: A language and environment for statistical computing. R Foundation for Statistical Computing, Vienna, Austria.

Ramsey, J., H. D. J. Bradshaw, and D. W. Schemske. 2003. Components of reproductive isolation between the monkeyflowers *Mimulus lewisii* and *M. cardinalis* (Phrymaceae). Evolution 57:1520-1534.

Rand, D. M. and R. G. Harrison. 1989. Ecological genetics of a mosaic hybrid zone: mitochondrial, nuclear, and reproductive differentiation of crickets by soil type. Evolution 43:432-449.

Richards, O. W. and G. C. Robson. 1926. The species problem and evolution. Nature 117:345-347.

Ritchie, M. G. 1996. The shape of female mating preferences. Proceedings of the National Academy of Sciences USA 93:14628-14631.

Robertson, H. M. and H. E. H. Paterson. 1982. Mate recognition and mechanical isolation in *Enallagma* damselflies (Odonata: Coenagrionidae). Evolution 36:243-250.

Rochette, N. C. and J. M. Catchen. 2017. Deriving genotypes from RAD-seq short-read data using Stacks. Nature Protocols 12:2640.

Rodriguez, V., D. M. Windsor, and W. G. Eberhard. 2004. Tortoise beetle genitalia and demonstrations of a sexually selected advantage for flagellum length in *Chelymorpha alternans* (Chrysomelidae, Cassidini, Stolaini). Pp. 739-748. New Developments in the Biology of Chrysomelidae. SPB Academic Publishing, The Hague.

Rohlf, F. J. 1999. Shape statistics: Procrustes superimpositions and tangent spaces. Journal of Classification 16:197-223.

Roux, C., C. Fraisse, J. Romiguier, Y. Anciaux, N. Galtier, and N. Bierne. 2016. Shedding light on the grey zone of speciation along a continuum of genomic divergence. PLoS Biology 14:e2000234.

Russell, S. T. 2003. Evolution of intrinsic post-zygotic reproductive isolation in fish. Annales Zoologici Fennici 40:321-329.

Ryan, M. J. and W. Wilczynski. 1991. Evolution of intraspecific variation in the advertisement call of a cricket frog (*Acris crepitans*, Hylidae). Biological Journal of the Linnean Society 44:249-271.

Sánchez-Guillén, R. A., A. Cordoba-Aguilar, A. Cordero Rivera, and M. Wellenreuther. 2014. Rapid evolution of prezygotic barriers in non-territorial damselflies. Biological Journal of the Linnean Society 113:485-496.

Sánchez-Guillén, R. A., M. Wellenreuther, and A. Cordero Rivera. 2012. Strong asymmetry in the relative strengths of prezygotic and postzygotic barriers between two damselfly sister species. Evolution 66:690-707.

Presgraves, D. C., L. Balagopalan, S. M. Abmayr, and H. A. Orr. 2003. Adaptive evolution drives divergence of a hybrid inviability gene between two species of *Drosophila*. Nature 423:715.

Schick, R. X. 1965. The crab spiders of California (Araneida, Thomisidae). Bulletin of the American Museum of Natural History 129:1-180.

Shanku, A. G., M. A. McPeek, and A. D. Kern. 2013. Functional annotation and comparative analysis of a zygopteran transcriptome. G3: Genes, Genomes, Genetics 3:763-770.

Shapiro, A. M. and A. H. Porter. 1989. The lock-and-key hypothesis: Evolutionary and biosystematic interpretation of insect genitalia. Annual Review of Entomology 34:321-345.

Shaw, K. L. 1996. Polygenic inheritance of a behavioral phenotype: interspecific genetics of song in the Hawaiian cricket genus *Laupala*. Evolution 51:256-266.

Shaw, K. L. and S. C. Lesnick. 2009. Genomic linkage of male song and female acoustic preference QTL underlying a rapid species radiation. Proceedings of the National Academy of Sciences USA 106:9737-9742.

Shen, L., H. Farid, and M. A. McPeek. 2009. Modeling three-dimensional morphological structures using spherical harmonics. Evolution 63:1003-1016.

Siepielski, A. M., K.-L. Hung, E. E. B. Bein, and M. A. McPeek. 2010. Experimental evidence for neutral community dynamics governing an insect assemblage. Ecology 91:847-857.

Simmons, L. W. 2014. Sexual selection and genital evolution. Austral Entomology 53:1-17.

Simmons, L. W., C. M. House, J. Hunt, and F. Garcia-Gonzalez. 2009. Evolutionary response to sexual selection in male genital morphology. Current Biology 19:1442-1446.

Singer, T. L. 1998. Roles of hydrocarbons in the recognition systems of insects. American Zoologist 38:394-405.

Sobel, J. M. and Chen, G. F. 2014. Unification of methods for estimating the strength of reproductive isolation. Evolution, 68: 1511–1522.

Sota, T. and K. Kubota. 1998. Genital lock-and-key as a selective agent against hybridization. Evolution 52:1507-1513.

Standfuss, M. R. 1896. Handbuch der paläarktischen Gross-Schmetterlinge für Forscher und Sammler. Verlag von Gustav Fischer, Jena, Germany.

Stratton, G. E. and G. W. Uetz. 1986. The inheritance of courtship behavior and its role as a reproductive isolating mechanism in two species of *Schizocosa* wolf spiders (Araneae; Lycosidae). Evolution 40:129-141.

Svedin, N., C. Wiley, T. Veen, L. Gustafsson, and A. Qvarnström. 2008. Natural and sexual selection against hybrid flycatchers. Proceedings of the Royal Society of London B: Biological Sciences 275:735-744.

Szymura, J. M. and N. H. Barton. 1986. Genetic analysis of a hybrid zone between the fire-bellied toads, *Bombina bombina* and *B. variegata*, near Cracow in southern Poland. Evolution 40:1141-1159.

Tanabe, T. and T. Sota. 2008. Complex copulatory behavior and the proximate effect of genital and body size differences on mechanical reproductive isolation in the millipede genus *Parafontaria*. The American Naturalist 171:692-699.

Tennessen, K. J. 1975. Reproductive behavior and isolation of two sympatric coenagrionid damselflies in Florida (Doctoral dissertation). University of Florida, Gainesville, FL.

Tennessen, K. J. 1982. Review of reproductive isolating barriers in Odonata. Advances in Odonatology 1:251-265.

Ting, C.-T., S.-C. Tsaur, M.-L. Wu, and C.-I. Wu. 1998. A rapidly evolving homeobox at the site of a hybrid sterility gene. Science 282:1501-1504.

Toews, D. P., S. A. Taylor, R. Vallender, A. Brelsfod, B. G. Butcher, P. W. Messer, and I. J. Lovette. 2016. Plumage genes and little else distinguish the genomes of hybridizing warblers. Current Biology 26:2313-2318.

Tregenza, T. and N. Wedell. 1997. Definitive evidence for cuticular pheromones in a cricket. Animal Behaviour 54:979-984.

Turelli, M., N. H. Barton, and J. A. Coyne. 2001. Theory and speciation. Trends in Ecology & Evolution 16:330-343.

Turgeon, J., R. Stoks, R. A. Thum, J. A. Brown, and M. A. McPeek. 2005. Simultaneous quaternary radiations of three damselfly clades across the Holarctic. The American Naturalist 165:E78-E107.

Van Der Sluijs, I., T. J. Van Dooren, K. D. Hofker, J. J. van Alphen, R. B. Stelkens, and O. Seehausen. 2008. Female mating preference functions predict sexual selection against hybrids between sibling species of cichlid fish. Philosophical Transactions of the Royal Society of London B: Biological Sciences 363:2871-2877.

Via, S. 2009. Natural selection in action during speciation. Proceedings of the National Academy of Sciences USA 106:9939-9946.

Via, S. 2012. Divergence hitchhiking and the spread of genomic isolation during ecological speciation-with-gene-flow. Philosophical Transactions of the Royal Society B: Biological Sciences 367:451-460.

Via, S., A. C. Bouck, and S. Skillman. 2000. Reproductive isolation between divergent races of pea aphids on two hosts. II. Selection against migrants and hybrids in the parental environments. Evolution 54:1626-1637.

Wellenreuther, M. and R. A. Sánchez-Guillén. 2016. Nonadaptive radiation in damselflies. Evolutionary Applications 9:103-118.

Westfall, M. J. and M. L. May. 2006. Damselflies of North America, revised edition. Scientific Publishers, Inc., Gainesville, FL.

Wiley, D. F., N. Amenta, D. A. Alcantara, D. Ghosh, Y. J. Kil, E. Delson, W. Harcourt-Smith, F. J. Rohlf, K. St John, and B. Hamann. 2005. Evolutionary morphing. Pp. 431-438. VIS 05. IEEE Visualization, 2005. IEEE.

Wiley, C., C. K. Ellison, and K. L. Shaw. 2012. Widespread genetic linkage of mating signals and preferences in the Hawaiian cricket *Laupala*. Proceedings of the Royal Society of London B: Biological Sciences 279:1203-1209.

Williams, T. H. and T. C. Mendelson. 2014. Quantifying reproductive barriers in a sympatric pair of darter species. Evolutionary Biology 41:212-220.

Williamson, E. B. 1906. Copulation of Odonata. Entomological News 17:143-148.

Willkommen, J., J. Michels, and S. N. Gorb. 2015. Functional morphology of the male caudal appendages of the damselfly *Ischnura elegans* (Zygoptera: Coenagrionidae). Arthropod Structure and Development 44:289-300.

Wittbrodt, J., D. Adam, B. Malitschek, W. Mäueler, F. Raulf, A. Telling, S. M. Robertson, and M. Schartl. 1989. Novel putative receptor tyrosine kinase encoded by the melanoma-inducing Tu locus in *Xiphophorus*. Nature 341:415-421.

Wojcieszek, J. M. and L. W. Simmons. 2012. Evidence for stabilizing selection and slow divergent evolution of male genitalia in a millipede (*Antichiropus variabilis*). Evolution 66:1138–1153.

Wojcieszek, J. M. and L. W. Simmons. 2013. Divergence in genital morphology may contribute to mechanical reproductive isolation in a millipede. Ecology and Evolution 3:334-343.

Wu, C.-I. and A. W. Davis. 1993. Evolution of postmating reproductive isolation: the composite nature of Haldane's rule and its genetic bases. The American Naturalist 142:187-212.

Xu, M. and O. M. Fincke. 2011. Tests of the harassment-reduction function and frequency-dependent maintenance of a female-specific color polymorphism in a damselfly. Behavioral Ecology and Sociobiology 65:1215-1227.

Yeaman, S. and M. C. Whitlock. 2011. The genetic architecture of adaptation under migration–selection balance. Evolution 65:1897-1911.

Zhou, C., Y. Pan, C. C. Robinett, G. W. Meissner, and B. S. Baker. 2014. Central brain neurons expressing doublesex regulate female receptivity in *Drosophila*. Neuron 83:149-163.